



Hamza Furkan Alkan, MSc.

Aspartate metabolism in cancer

DOCTORAL THESIS

to obtain the university degree of

Doktor der Naturwissenschaften

submitted to

Graz University of Technology

Supervisor

Assoc.Prof. Mag.rer.nat. Dr.rer.nat. Juliane Bogner-Strauss

Institute of Biochemistry, Graz University of Technology

Graz, February 2020

STATUTORY DECLARATION

I declare that I have authored this thesis independently, that I have not used other than the declared sources / resources, and that I have explicitly marked all material which has been quoted either literally or by content from the used sources. I also declare that some passages within the methods section and the figure legends have been quoted from my own original research article as the description of those experiments are essentially identical. The text document uploaded to TUGRAZonline is identical to the present doctoral thesis.

date

(signature)

*This thesis is dedicated to **Tülin Alkan**, the kindest and the strongest woman I know,
who lost her battle with cancer during the writing of this dissertation.*

Acknowledgments

I would like to thank Juliane Bogner-Strauss, my supervisor and Matthew Vander Heiden, my mentor during my abroad stay for giving me the opportunity to be a part of their amazing projects and sharing their experiences with me to keep me in the tracks of becoming a better scientist.

I am grateful to all my thesis committee members; Gerald Höfler, Rudolf Zechner, Dagmar Kratky, and Hubert Hackl, for guiding me throughout my thesis work. I am thankful for all the fruitful discussions with Wolfgang Graier, Paul Vesely and Tobias Madl who also helped me by attending to some of my thesis committee meetings.

I also appreciate the helps of several scientists that contributed to the work in this thesis. Namely, Katharina Eva Walter and Alba Luengo for helping me with some *in vitro* and *in vivo* experiments when I was struggling with paper revisions, Sarah Streyck and Tobias Madl for NMR measurements, Corina Madreiter-Skolowski for oxygen consumption experiment, Wael Al-Zoughbi for analyzing immunohistochemistry stainings, Caroline Lewis and Bena Chan for liquid chromatography-mass spectrometry measurements, Paul Vesely, Silvia Schauer for the tail vein injections and preparing lung slides and Thomas Schreiner and Wolfgang Krispel for their technical helps in uncountable number of experiments.

I am grateful to Aaron Hosios, Lucas Sullivan, Zhaoqi Li, Dan Gui, Allison Lau, Laura Danai, Ariane Pessentheiner, Melina Amor, and Daniel Schmidt to constructive discussions and experimental advices. In addition, I want to thank all the scientists and staff working in the Doctoral School of Metabolic and Cardiovascular Disease (DK-MCD), the ZMB Building and Koch Institute of Integrative Cancer Research Building.

I want to thank my pets Summer, Simba and Nala for giving me joy; coffee and Redbull for giving me strength; and my siblings for giving me a reason to finish this thesis.

Last but not least, I am very grateful to all the scientists, dead or alive, who put their blood, sweat and tears to bring the cancer research so far that this was study possible. Their work allowed my mother with terminal breast cancer to stay with us for another four years and I sincerely hope that the outcomes of this thesis will one day help someone else cherish those extra moments with their loved ones.

Abstract

Despite prominent lactate fermentation, mitochondrial function and the TCA cycle activity remains relevant in proliferating cells. Because cancers display excessive glucose uptake and high rates of glycolysis, there is a debate on whether mitochondrial energy production is still needed for cell proliferation. In this thesis, we provide evidence that a major role of the TCA cycle is to supply aspartate and the TCA cycle is not required for cell survival or proliferation in the presence of exogenous aspartate. We also demonstrate that inhibiting aspartate export from the mitochondria to the cytosol via knockdown of aspartate-glutamate carrier 1 (gene name: SLC25A12, protein name: AGC1) impairs redox homeostasis and leads to slower proliferation. Consistently, when TCA cycle carbons were depleted through glutamine starvation and/or glutaminase inhibition, insufficient aspartate delivery cause apoptosis, which can again be prevented by exogenous aspartate supplementation. Our mechanistic work suggests that the most limiting function of cytosolic aspartate is to support nucleotide and protein synthesis. Furthermore, AGC1-depleted allograft tumors grow significantly slower *in vivo*. Loss of AGC1 sensitizes resistant-tumors to treatments with the glutaminase inhibitor CB-839. In summary, our work suggests that delivering aspartate to the cytosol maintains cell survival when glutamine is limiting and AGC1 inhibition can synergize with glutaminase inhibitors to block tumor growth.

Kurzfassung

In proliferierenden Zellen sind trotz der ausgeprägten Milchsäuregärung die Mitochondrienfunktion und die Citratzyklusaktivität von großer Bedeutung. Auf Grund der exzessiven Glukoseaufnahme und erhöhten Glykolyse in Krebs, wird oft diskutiert, ob die mitochondriale Energiegewinnung für die Zellproliferation noch benötigt wird. Diese Arbeit zeigt, dass die Aspartatversorgung eine der Hauptaufgaben des Citratzykluses ist und dass exogen zugeführtes Aspartat das Überleben und die Proliferation von Zellen unabhängig von der Citratzyklusaktivität unterstützt. Wir konnten ebenfalls zeigen, dass die Hemmung des Aspartatexports von den Mitochondrien zum Cytosol durch den Knockdown des Aspartat-glutamat-Carrier 1 (Gen: SLC25A12; Protein: AGC1) die Redoxhomöostase beeinträchtigt und zu einer langsameren Proliferation führt. Außerdem, wenn die Citratzyklus-Kohlenstoffe durch Glutaminmangel und/oder Glutaminase-Hemmung erschöpft sind, führt eine unzureichende Aspartatversorgung zu Apoptose, die wiederum durch exogene Aspartat-Supplementierung verhindert werden kann. Untersuchungen des Wirkmechanismus legen nahe, dass die größte limitierende Funktion von cytosolischen Aspartate die Unterstützung der Nukleotid- und Proteinsynthese ist. Darüber hinaus wachsen AGC1-deziierte allograft Tumore in lebenden Organismen signifikant langsamer. Des Weiteren sensibilisiert der Verlust von AGC1 resistente Tumore gegenüber Behandlungen mit dem Glutaminaseinhibitor CB-839. Zusammenfassend wird in dieser Arbeit gezeigt, dass der Transport von Aspartat ins Cytosol das Überleben der Zell unterstützt, wenn die Verfügbarkeit von Glutamin begrenzt ist und die Hemmung von AGC1 im Zusammenspiel mit Glutaminaseinhibitoren den Tumorwachstum blockieren.

Table of Contents

1. Introduction	2
1.1 Cancer metabolism.....	2
1.1.1 Warburg effect.....	3
1.1.2 Mitochondria in cancers.....	5
1.1.3 Glutamine anaplerosis	7
1.2 The malate-aspartate shuttle	8
1.2.1 Aspartate-glutamate carriers (AGCs).....	10
1.3 Aim of the study.....	12
2. Materials and Methods.....	14
2.1 Bioinformatics.....	14
2.2 Cell Culture.....	14
2.2.1 Basic Maintenance	14
2.2.2 Stable knock-down of the SLC25A12 gene.....	14
2.2.3 CRISPR/Cas9-mediated knock-out of Slc25a12 gene	15
2.2.4 Transient overexpression of mouse and human SLC25A12	15
2.2.5 siRNA-mediated knock-down of Got1/2	16
2.2.6 Cell Counting Experiments (Proliferation/Survival Rates).....	16
2.2.7 Cell Viability Assays.....	17
2.2.8 Annexin V/PI Staining (Apoptosis Assay).....	17
2.2.9 C2C12 differentiation experiment.....	18
2.2.10 Mitochondrial Respiration Measurement.....	18
2.2.11 NAD ⁺ /NADH measurement	18
2.2.12 ROS Measurement.....	19
2.2.13 Radioactive CO ₂ release.....	19
2.2.14 Extracellular Flux Analysis	19

2.3	Metabolic Profiling	20
2.3.1	NMR Spectroscopy.....	20
2.3.2	Isotope Tracing and GCMS Analysis	21
2.3.3	Metabolic profiling using LCMS	21
2.4	In vivo Tumor Experiments	22
2.4.1	Animal Care.....	22
2.4.2	Subcutaneous growth of LLC1 tumors.....	22
2.4.3	Allografts and in vivo CB-839 treatment.....	23
2.4.4	Tail vein injection of B16F10 cells.....	23
2.5	Immunohistochemistry	23
2.6	Quantitative Real-Time PCR.....	24
2.7	Western Blot.....	24
2.8	Statistical analysis	25
2.9	Reagents	25
Table 1: Key resources table.		25
3.	Results.....	31
3.1	Malate-aspartate shuttle components are highly expressed in proliferating cells	31
3.2	shRNA-mediated knockdown of AGC1 reduced the proliferation in mouse cell lines	32
3.3	AGC1 knock-down and overexpression altered the cellular metabolism	34
3.4	AGC1-knockdown increased cellular dependence on exogenous glutamine.....	38
3.5	Glutamine dependence in AGC1-KD cells is not due to change in anaplerosis source	40
3.6	AGC1-KD cells are unable to preserve cytosolic aspartate levels, causing cell death upon glutamine-deprivation.....	45
3.7	High mitochondrial aspartate levels are required for AGC1-KD cells to activate aspartate export and maintain cytosolic aspartate levels	49
3.8	Cytosolic aspartate is not crucial for non-essential amino acids in low-glutamine	51
3.9	Cytosolic aspartate is not crucial for feeding the TCA cycle in low-glutamine.....	55

3.10	Cytosolic aspartate is required for nucleotide biosynthesis.....	58
3.11	AGC1 knockdown limits tumor growth.....	60
3.12	AGC1 knockdown sensitizes tumors to CB-839 treatment.....	60
3.13	AGC1 expression is upregulated in Pancreatic Ductal Adenocarcinomas.....	63
3.14	High AGC1 expression may correlate with better prognosis in some cancers (Supplementary Findings 1).....	66
3.15	AGC1-KD increased the pulmonary metastatic capacity of LLC1 and B16F10 cells (Supplementary Findings 2).....	66
3.15	AGC1-KD impaired myogenic differentiation of C2C12 (Supplementary Findings 3).....	70
4.	Discussion.....	73
4.1	High mitochondrial export or exogenous aspartate supply maintain cell proliferation and survival when glutamine is limiting.....	73
4.2	Knockdown of AGC1 increased the pulmonary metastatic capacity of LLC1 and B16F10 cells 79	
5.	References.....	81
6.	Figure and Table Legends.....	91
6.1	Figure Legends.....	91
6.2	Table Legends.....	92
7.	Abbreviations.....	94
8.	Appendices.....	97
8.1	Published Original Article: Cytosolic Aspartate Availability Determines Cell Survival When Glutamine Is Limiting.....	97
8.2	Published Commentary: Maintaining cytosolic aspartate levels is a major function of the TCA cycle in proliferating cells.....	114

INTRODUCTION

1. Introduction

1.1 Cancer metabolism

Cancer is a very lethal chronic disease, leading to approximately 8.2 million deaths per year globally (Cancer Research UK, 2018). It is the second leading cause of death worldwide after the heart disease and the percent of deaths caused by cancer has been increasing over the last decades (Weir et al, 1969-2020). Therefore, understanding cancer and learning how to fight against it has been a major topic of interest for health sciences.

Cancer formation begins when a normal cell of multicellular organism obtains the ability to continuously grow, avoid cell death and evade immune response as a result of various genetic alterations. These genetic alterations usually lead to two possible changes within the target protein: gain-of-function, where a mutation causes either a constitutive activation of a protein or introduce a novel activity; and loss-of-function, where the protein is incapable of performing its main role. The genes of those gain-of-function mutations can lead to cancers are referred to as oncogenes while the loss of tumor suppressor genes makes cells vulnerable to becoming cancerous. Tumor suppressor genes are mainly responsible for the expression of proteins that regulate the cell cycle, DNA repair, and checkpoint control (Alberts et al., 2008).

Cancer cells require different metabolic reactions than healthy (non-cancer) cells. The main requirements of healthy cells are to produce energy to sustain cellular homeostasis which is satisfied by mostly catabolic reactions. However, cancer cells need to balance the catabolic and anabolic reactions to comply with the maintenance of cellular homeostasis as well as duplicating the cellular biomass which includes massive macromolecule biosynthesis. In order to meet this metabolic requirement, cancer formation must be accompanied by metabolic rewiring of the cancer cells to deviate from the healthy cells from the tissue (Gatenby and Gillies, 2004; Lunt and Vander Heiden et al., 2011).

The rapidly growing nature and therefore the demand for macromolecule biosynthesis are one of the most common features of cancer cells that differentiate them from most of the normal cells. This characteristic was exploited for inventing chemotherapeutic drugs such as aminopterin (folate analog, later developed into methotrexate) and 5-fluorouracil (5-FU, uridine analog) to target de novo nucleic acid synthesis pathways (Farber and Diamond, 1948; Heidelberger et al., 1957).

Another distinctive feature of cancer cells compared to healthy cells is increased glucose uptake and aerobic glycolysis which was first observed by Otto Warburg (Warburg, 1956) (Figure 1). Metabolic

advantages of aerobic glycolysis and its therapeutic and diagnostic use will be discussed in the following section.

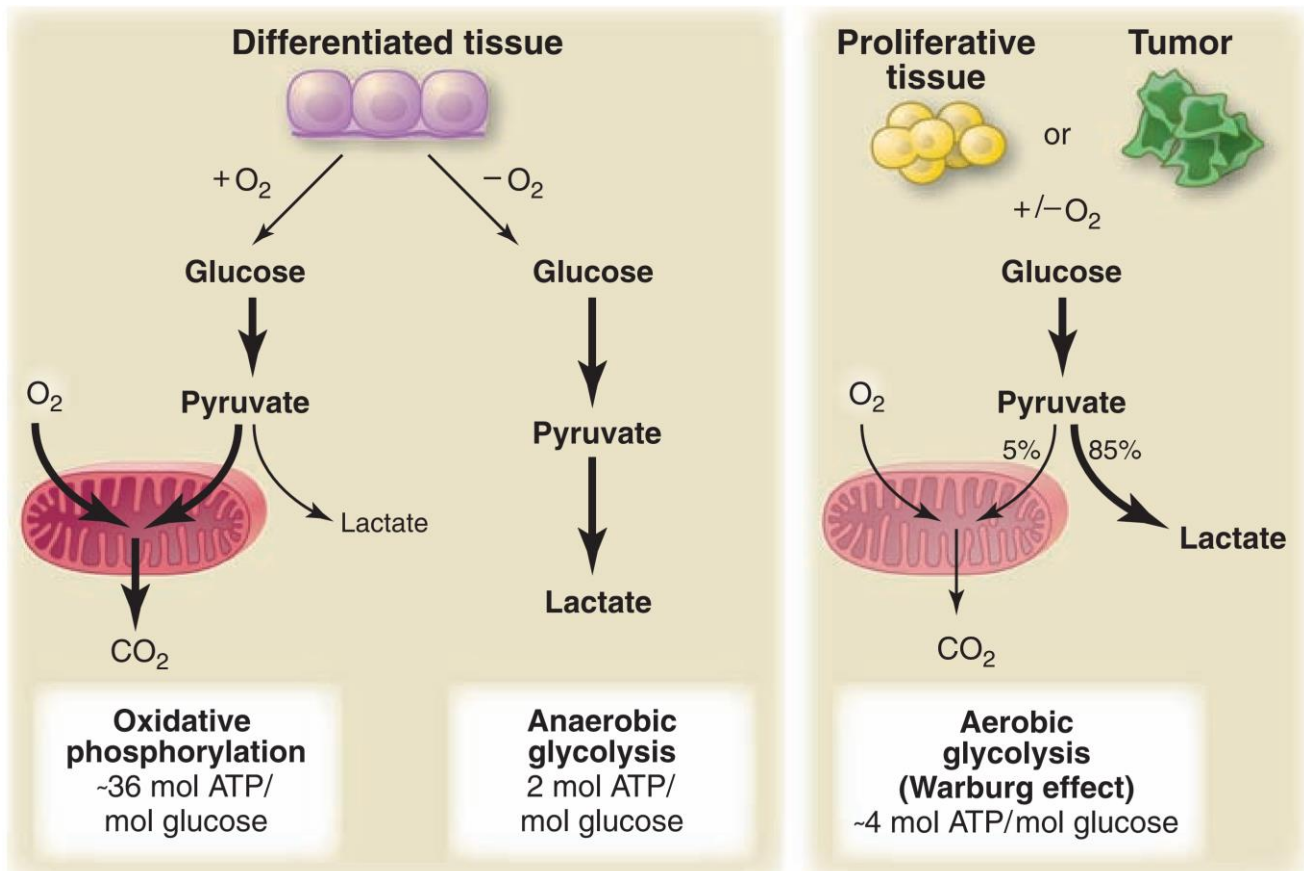


Figure 1: Aerobic and anaerobic glycolysis in proliferative and non-proliferative cells. Left: Non-cancerous (differentiated) cells mainly use oxidative phosphorylation to catabolize glucose in the presence of ample oxygen. When oxygen levels are insufficient to maintain oxidative phosphorylation, lactate fermentation occurs (anaerobic glycolysis). Right: In proliferative cells and cancer cells however, the majority of glucose is converted to lactate regardless of oxygen levels (aerobic glycolysis, also known as Warburg effect). (Vander Heiden et al., 2009)

1.1.1 Warburg effect

In order to keep up with increased energetic and biosynthetic needs of constant proliferation, cancer cells exhibit altered nutrient metabolism compared to non-proliferating healthy cells. (Vander Heiden and DeBerardinis, 2017; Cantor and Sabatini, 2012; Warburg, 1956). The most common carbon sources for cancer cells are glucose and glutamine. (Hosios et al., 2016). An almost universal characteristic of cancer cells is their increased glucose uptake. In addition, increased glucose uptake in cancer cells is very often accompanied by increased lactate production even under normoxic conditions (aerobic glycolysis) even though oxidative catabolism of glucose yields more energy per glucose. This phenomenon is also referred

INTRODUCTION

to as the Warburg effect to credit German biochemist Otto Warburg who first discovered it on tissue slides (Figure 1).

Because the Warburg effect is one of the most distinguishing metabolic differences between cancer cells and their tissue of origin, a significant amount of studies have been focusing on discovering potential vulnerabilities targeting increased glycolysis. For instance, 2-deoxyglucose (2-DG) can inhibit glucose metabolism by blocking the glycolysis following the hexokinase reaction. In fact, several studies reported that 2-DG could reduce proliferation and tumor growth (Zhang et al., 2014), however clinical studies so far demonstrated that more tolerable doses of 2-DG failed to cause regression in patients (Vander Heiden and DeBerardinis, 2017). Because inhibition of glucose metabolism in healthy tissues dependent on high glucose such as brain disrupts their regular activity, high enough doses of 2-DG to stop cancer progression are not viable. Despite its relative failure with cancer treatment, high glucose uptake of cancer cells has been successfully exploited for cancer diagnosis. Fluro-deoxyglucose positron-emission-tomography (FDG-PET) imaging is used to determine the stage of cancers and evaluate the responses to therapy (Figure 2).

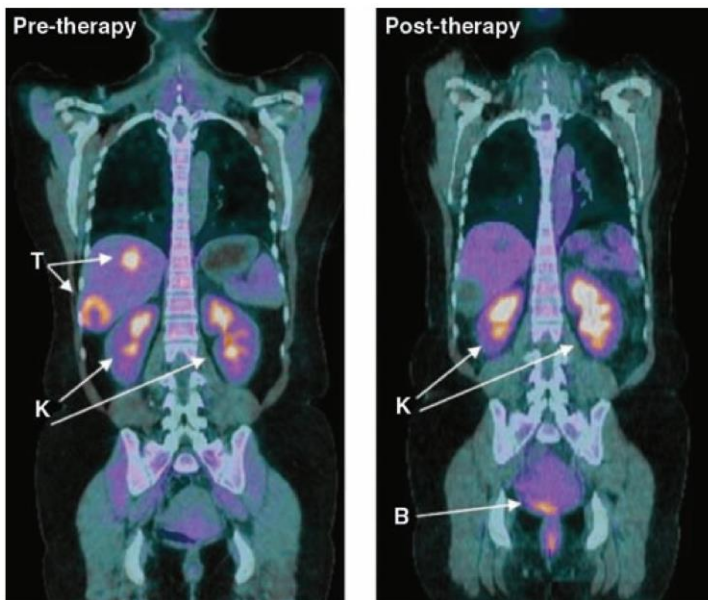


Figure 2: FDG-PET/CT imaging is used to monitor tumor regression. Malignant sarcoma tumors (T) were visualized by PET coupled with computerized tomography (CT) exploiting their increased uptake of glucose analog FDG. FDG uptake was reduced after 4 weeks of therapy hinting metabolic inactivity and tumor regression. Kidneys (K) and bladder (B) were also labeled with FDG due to excess FDG being excreted in the urine (Vander Heiden et al., 2009).

Due to increased lactate secretion, Otto Warburg initially hypothesized that cancer cells contain defective mitochondria and unable to perform oxidative phosphorylation. Since then, it has been a topic of debate whether mitochondrial dysfunction may be a factor or even the ultimate cause of cancer formation. However, discoveries in the last decades have made it clear that some level of mitochondrial activity is actually essential for the proliferation of cancer cells, which makes it rather confusing as to why they prefer such an energy-inefficient fate for glucose catabolism (Cantor and Sabatini, 2012; Vander Heiden et al., 2009). There is a number of working hypotheses aiming to explain this phenomenon, although

there is probably more research required to reach a concrete conclusion. Briefly, considering the high rate of glycolysis and excessive glucose uptake, rapidly generated 2ATP/glucose may surpass the potential energy yield of oxidative catabolism. In addition, for each pyruvate molecule that is dragged into the mitochondria for the TCA cycle instead of being reduced to lactate by lactate dehydrogenase cells would need to find another way to reoxidize one reducing equivalent (NADH) to maintain sufficient levels of cytosolic electron acceptors (NAD⁺). Because the rates of malate-aspartate shuttle or glycerol3-phosphate shuttle fail to even up with the rate of glycolysis, this would eventually lead to reduced NAD⁺/NADH ratio which could hamper many anabolic reactions or glycolysis itself. Therefore, cultured cancer cells exhibit almost perfect 1:2, glucose uptake: lactate production ratio, mimicking cells with mitochondria deficiency and/or under hypoxic stress.

1.1.2 Mitochondria in cancers

Contrary to Otto Warburg's assumptions, there are several reports highlighting the importance of mitochondrial function for cell proliferation (DeBerardinis and Chandel, 2016), particularly via supporting biosynthesis (Figure 3). In several cancers, mitochondrial one-carbon metabolism is highly active and essential for the production of purine and thymidine nucleotides (Vyas et al., 2016; Zong et al., 2016). It was reported that some portion of breast cancers depend on *de novo lipogenesis* for growth, which begins with citrate formation in mitochondria and its delivery to the cytosol (Catalina-Rodriguez et al., 2012; Jiang et al., 2017). Respiratory function of mitochondria is also important for proliferation as it allows oxidation of reducing equivalents, therefore, maintaining higher levels of NAD⁺/NADH ratio. Mitochondrial redox balance supports aspartate biosynthesis, a non-essential amino acid that is used to make protein as well as purine and pyrimidine nucleotides (Birsoy et al., 2015; Gui et al., 2016; Sullivan et al., 2015). In fact, intracellular aspartate production could be a major limitation of tumor growth *in vitro* or *in vivo* as aspartate is poorly taken up by many types of cancer cells due to lack of appropriate transport expression (Garcia-Bermudez et al., 2018; Sullivan et al., 2018). Due to these biosynthetic roles, carbon units are constantly taken away from the TCA cycle. In order for biosynthesis, and therefore proliferation to continue, the amount of TCA cycle carbons lost in biosynthesis needs to be replenished (also referred to as TCA cycle anaplerosis). Because a great amount of glucose molecule is converted to lactate in cancer cells, glutamine is the primary the anaplerotic carbon source for the TCA cycle, making those cells susceptible to glutamine starvation (Yuneva et al., 2007). This dependency on glutamine anaplerosis was considered

INTRODUCTION

as Achilles' hill of cancer cells which led to the development of inhibitors targeting glutamine metabolism, such as CB-839 (Gross et al., 2014).

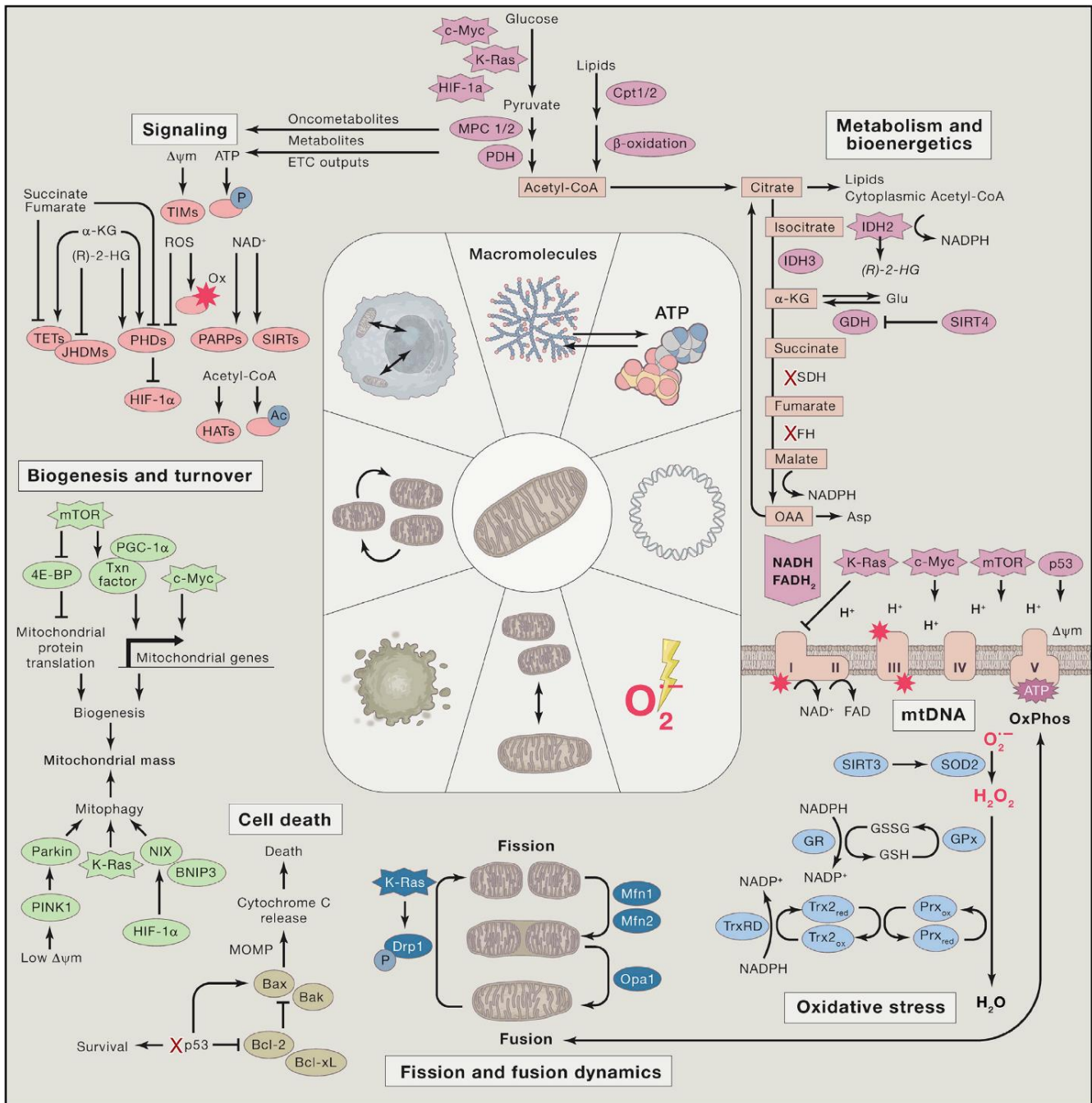


Figure 3: Mitochondria and cancers. Mitochondria play important roles in cancer cells by regulating cellular energetics, oxidative stress, biomass production, apoptosis, and signaling. (Vyas et al., 2016)

1.1.3 Glutamine anaplerosis

Several carbon tracing experiments over the last decade have clarified that many proliferating cells in culture convert almost every glucose molecule into lactate and feed the TCA cycle using glutamine carbons (Vander Heiden and DeBerardinis, 2017). Instead of following the traditional oxidative TCA pathway where assembly of oxaloacetate with glucose-derived Acetyl-CoA to form citrate initiates the cycle, the first step of this pathway in cancer cells is the subsequent deamination of glutamine to yield alpha-ketoglutarate (α -KG; also known as 2-oxoglutarate) (Figure 4). First, the amide nitrogen of glutamine is cleaved by glutaminase enzyme to make glutamate. Then, glutamate is converted to TCA cycle substrate α -KG by either transaminations or via glutamate dehydrogenase. This step is a central step for replenishing the TCA cycle and supporting *de novo lipogenesis* because α -KG could then be oxidized to Succinyl-CoA or reduced to isocitrate (Figure 4).

Three catalytically active isoforms of glutaminase enzyme have been identified in mammalian cells: liver isoform (LGA, also known as GLS2), kidney isoform (KGA, also known as GLS) and GAC (glutaminase C) which is a post-transcriptional splice variant of the kidney isoform (Cassago et al., 2012). GLS is recognized to be mitochondrial and involved in central carbon metabolism while GLS2 has been argued to localize in the nuclei and may have a role in co-regulating gene expressions (Matés, 2018). Gene expressing data from The Cancer Genome Atlas (TCGA) indicate that GLS levels are increased in several cancers including myeloid leukemia, adrenocortical cancer, triple-negative breast cancer, colorectal cancer, kidney clear or papillary cell carcinoma, lung adenocarcinoma, melanoma, mesothelioma, pancreatic cancer, sarcoma and thyroid cancer (Katt et al., 2017). A substantial amount of functional studies has made it clear that GLS, specifically GAC isoform, and glutamine metabolism are strongly associated with tumor growth and metastasis, suggesting that inhibiting glutaminase enzyme may open up new therapeutic windows for the treatment of various cancers.

A number of glutaminase inhibitors have been identified in the last two decades. BPTES (bis-2-(5-phenylacetamido-1,2,4-thiadiazol-2-yl)ethyl sulfide) was one of the first identified compounds that could potentially target glutamine metabolism in cancers (Robinson et al., 2007). Despite demonstrating the anti-tumor activity, the outcomes of several studies indicated that the clinical use of BPTES is challenging due to its low stability, poor solubility and weak efficiency (Gross et al., 2014). On the other hand, CB-839, a relatively newer orally bioavailable compound, selectively inhibits cancer-related GLS isoforms (GAC and KGA) with much higher potency and specificity (Gross et al., 2014). Glutaminase inhibition via CB-839 strongly impairs proliferation *in vitro* (Gross et al., 2014; Wise et al., 2008). However, the anti-proliferative effects of CB-839 appear to be much smaller or absent in tumors growing *in vivo* (Davidson

et al. 2015, Muir et al., 2018), indicating further research is required to understand different metabolic dependencies and adaptation mechanisms of cancer cells in different environments.

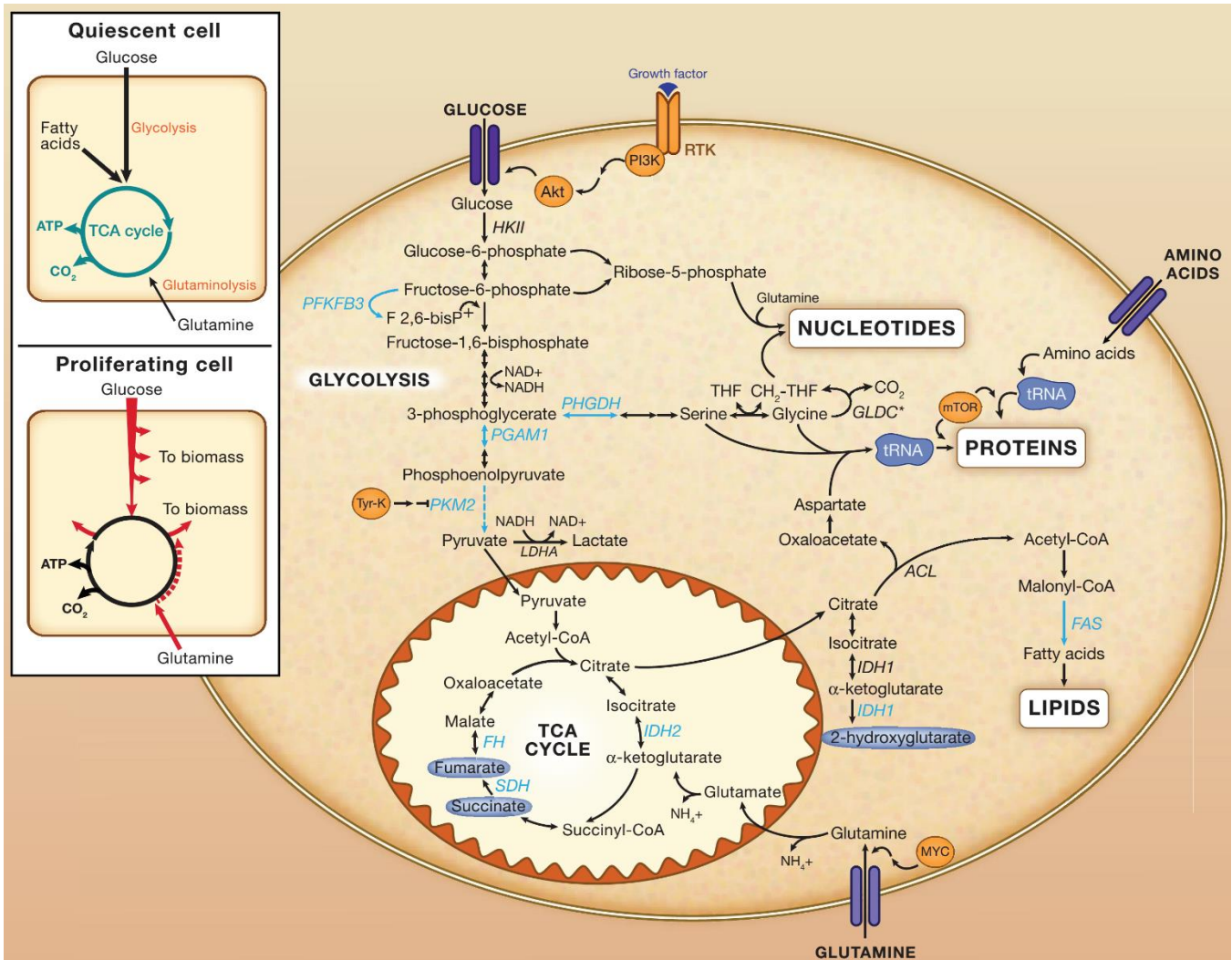


Figure 4: Central carbon metabolism in proliferating cells. Quiescent cells use carbon sources to maintain cellular homeostasis while proliferating cells require to generate biomass in addition to cellular homeostasis. In proliferating cells, several glycolysis and TCA cycle intermediates are converted to macromolecules through de novo synthesis of lipids, nucleotides and various amino acids. Therefore, proliferating cells are rewired to take up higher amounts of glucose and support the TCA cycle with increased glutaminolysis. Glutamine could provide the carbon backbone to non-essential amino acids and fatty acids (Finley et al., 2013).

1.2 The malate-aspartate shuttle

The mitochondrial membrane is impermeable for NAD⁺ and NADH. In order for glycolysis to continue, NAD⁺ needs to be regenerated from NADH that is produced during the oxidation of glyceraldehyde 3-phosphate in the cytosol. One simple solution to oxidize cytosolic NADH is through lactate fermentation,

INTRODUCTION

however, this would limit pyruvate availability for the TCA cycle. Therefore, several mitochondrial shuttle mechanisms exist to indirectly carry the electron from NADH into mitochondria instead of transferring NADH itself.

One of the most common ways of transferring electrons from NADH into the electron transport chain is called the glycerol 3-phosphate shuttle. In the cytosol, glycerol 3-phosphate dehydrogenase (GPDH) transfers a pair of electrons from NADH to dihydroxyacetone phosphate, to produce glycerol 3-phosphate (G3P) and oxidized NAD. G3P could then be used for glycerol synthesis in the cytosol or be converted back to dihydroxyacetone phosphate on the outer surface of the inner mitochondrial membrane by a second isoform of GPDH that is localized within the inner mitochondrial membrane. During the reaction, electrons from G3P were transferred to the FAD group to form FADH_2 which could later transfer its electrons to electron carrier Q to enter the electron transport chain. Unlike NADH, compound Q bypasses complex I in the electron transport chain, therefore energy yield of this shuttle is relatively lower (Mracek et al., 2013).

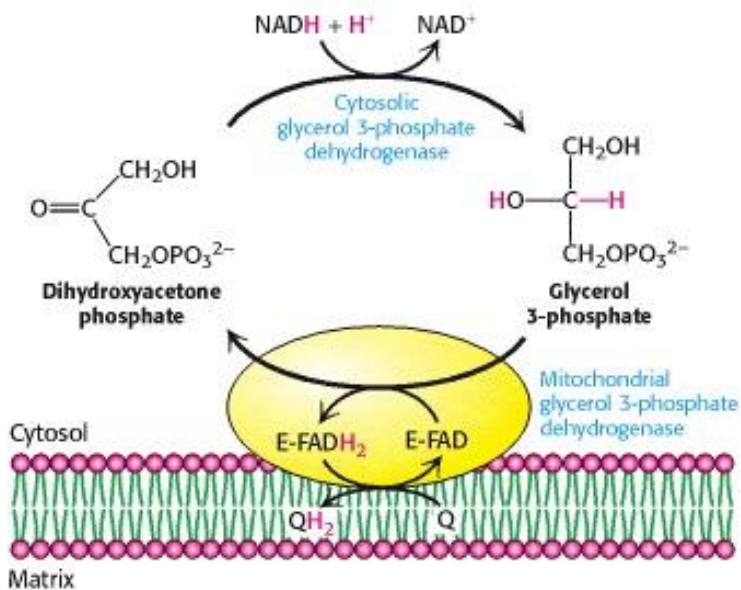


Figure 5: Glycerol 3-phosphate shuttle allows NADH electrons to enter the mitochondrial electron transport chain. (Berg et al., 2002)

Transferring electrons from cytosolic NADH via the malate-aspartate shuttle allows regeneration of one mitochondrial NADH per cytosolic NADH spent, making it energetically most conservative means to recycle cytosolic NADH. This shuttle consists of at least two mitochondrial transporters, two dehydrogenases and two aminotransferases (Figure 6). First, pair of electrons are transferred from cytosolic NADH to oxaloacetate to form malate which could pass through the inner mitochondrial membrane via a number of transporters. In the mitochondrial matrix, malate donates electrons to NAD⁺ to produce oxaloacetate and NADH that can readily be reoxidized in the electron transport chain to produce energy. These two redox reactions were catalyzed by cytosolic and mitochondrial isoforms of

malate dehydrogenase (MDH1 and MDH2), respectively. To complete the shuttle, oxaloacetate must be transferred back to the cytosol. However, oxaloacetate cannot cross the inner mitochondrial membrane, therefore it is required to form aspartate via transamination. Mitochondrial isoform of aspartate aminotransferase (GOT2) catalyzes the transfer of the amino group from mitochondrial glutamate to oxaloacetate, producing aspartate and alpha-ketoglutarate. Aspartate is then transported to the cytosol via aspartate-glutamate carrier (AGC1 or AGC2) in exchange for glutamate and proton. The shuttle is then completed with the formation of oxaloacetate in the cytosol via reverse transamination by cytosolic aspartate aminotransferase (GOT1). Notably, this shuttle also supports the movement of metabolic intermediates between the cytosol and the mitochondria (Berg et al., 2002).

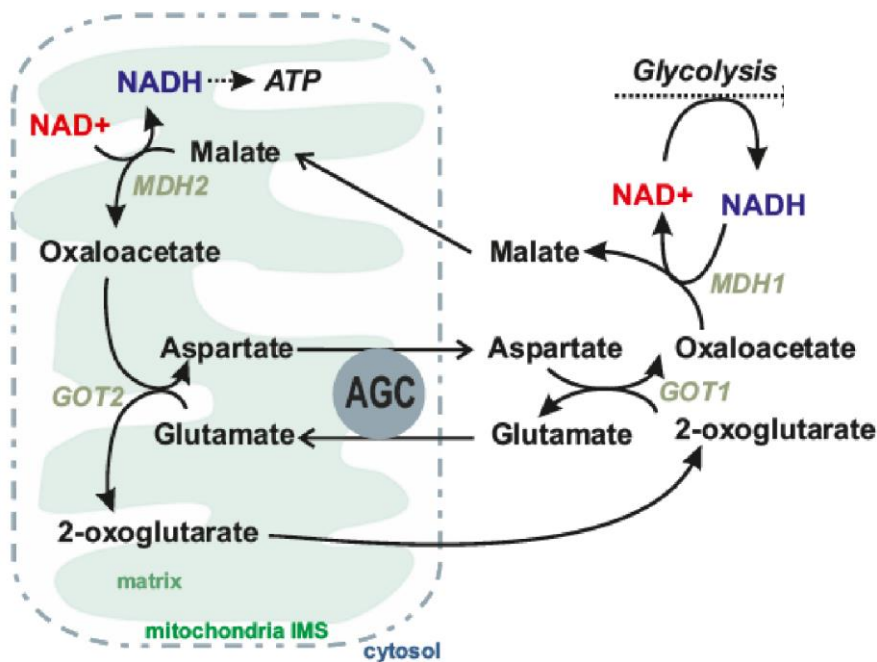


Figure 6: Malate-aspartate shuttle consists of two cytosolic and two mitochondrial isoforms of malate dehydrogenase (MDH) and aspartate aminotransferase (GOT) along with membrane transporters to move the intermediates. A pair of electrons from cytosolic NADH is carried into the mitochondrial matrix in the form of malate. After consecutive reactions, aspartate is produced in mitochondria and exported to the cytosol via aspartate-glutamate carrier (AGC) to complete the shuttle.

1.2.1 Aspartate-glutamate carriers (AGCs)

Export of mitochondrial aspartate in exchange for cytosolic glutamate and a proton is facilitated by the aspartate-glutamate carriers (AGCs) located on the inner mitochondrial membrane (Satrustegui et al., 2007a). This exchange is considered to be the only irreversible and the rate-limiting step of the malate-aspartate shuttle (del Arco et al., 2002). There are two functional AGC isoforms expressed via different genes: SLC25A12 (AGC1, Aralar) and SLC25A13 (AGC2, Citrin). These two genes have a very similar structure, both having 18 exons and 77% overlap. AGCs are members of the mitochondrial carrier family, show strong homology to other mitochondrial carriers with regard to having six transmembrane carrier

INTRODUCTION

domains (Satrustegui et al., 2007b). In addition, AGCs consist of eight EF-hand domains on the N-terminal and an extra transmembrane α -helix domain on the C-terminal (Figure 7) (Thangaratnarajah et al., 2014). Interestingly, only one of the EF-hand domains is responsible for calcium-binding while others are required for homodimer formation. AGCs are required to be dimerized in response to extra-mitochondrial calcium to be activated (Conteras et al., 2007).

Although AGC1 and AGC2 are, in principle, functionally identical, they are often associated with different pathways and diseases because many tissues selectively express one or the other isoform. AGC1 expression is highest in the brain, skeletal muscle, heart, and pancreatic beta cells and involved in the malate-aspartate shuttle (del Arco et al., 1998; Begum et al., 2002; del Arco et al., 2002). On the other hand, AGC2 is primarily found in the liver and kidney (Begum et al., 2002; Palmieri et al., 2001), and AGC2 deficiency leads to urea cycle disorder type2-citrullinemia (Hayasaka and Nakamura, 2018).

Previous works have repeatedly demonstrated that AGC1 is essential for neuronal development supports aspartate and N-acetylaspartate (NAA) production, and reduces lactate secretion. Mice lacking AGC1 had growth deficiencies, general tremoring, motor coordination defects and did not survive after 15 days of postnatal (Jalil et al., 2005). Two independent studies have also reported that children patients with dysfunctional AGC1 mutations demonstrate similar phenotypes to AGC1-knockout mice including developmental delay, myelination defects and epilepsy-like seizures (Wibom et al., 2009; Sakurai et al., 2010; Falk et al., 2013).

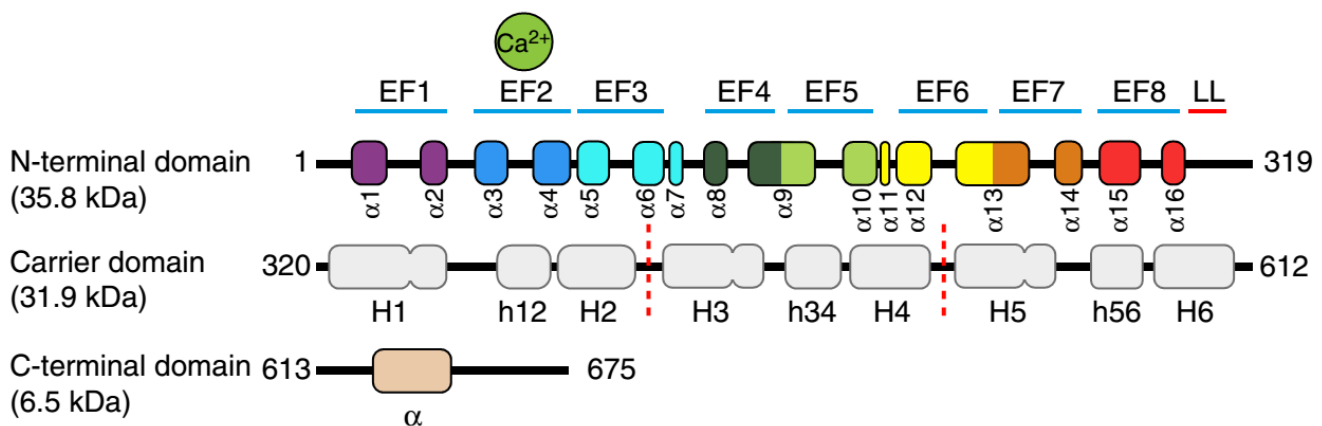


Figure 7: Aspartate-glutamate carriers. AGCs consist of three main structures: N-terminal (EF-hand) domain, carrier (transmembrane) domain and C-terminal domain. EF-hand 2 is the only calcium-binding component of AGCs, while other EF-hands were involved in dimerization. The carrier domain is homologous to other mitochondrial carrier proteins and essential for binding to the inner mitochondrial membrane. The c-terminal domain is predicted to be responsible for substrate recognition (Thangaratnarajah et al., 2014).

1.3 Aim of the study

Because proliferating cells are highly glycolytic, they may benefit from a mechanism such as malate-aspartate shuttle to reoxidize cytosolic NADH while preserving pyruvate carbons. We hypothesize that AGC, a critical member of the malate-aspartate shuttle, could also independently assist energy and biomass production via maintaining mitochondrial glutamate oxidation as well as boosting cytosolic aspartate pool which is essential for de novo synthesis of nucleotides. Although malate-aspartate shuttle activity in tumors has been reported long before (Greenhouse and Lehninger, 1976), and AGCs have been predicted to be involved in cancers (Amoedo et al., 2016), there has not been substantial work to describe functional role of mitochondrial-aspartate glutamate transport for proliferation. In this study, we focus on understanding the role of AGC1 (SLC25A12) in proliferation and tumor growth. we aim to knockdown AGC1 in different cell lines to investigate its effects on central carbon metabolism, cell proliferation, and tumor growth. Finally, we aspire to identify potential vulnerabilities of AGC1 inhibition in cancers that can be exploited for future therapeutic applications.

MATERIALS & METHODS

2. Materials and Methods

2.1 Bioinformatics

Screening of mRNA expressions of SLC25A12 (Aralar or AGC1) and SLC25A13 (Citrin or AGC2) was performed using “firebrowse.org” with the courtesy of Broad Institute of MIT & Harvard. Survival and disease-free survival rates are plotted via R Software. The cut-off for high or low gene expression was determined automatically for every plot to obtain the most significant spread between two groups. All results were based on RNA sequencing database generated by TCGA Research Network.

2.2 Cell Culture

2.2.1 Basic Maintenance

The following cell lines were used throughout this study: C2C12 (mouse proliferating myoblast), LLC1 (mouse lung carcinoma), B16F10 (mouse metastatic melanoma), AL1376 (mouse pancreas adenocarcinoma), HeLa (human cervical carcinoma), H1299 (human non-small cell carcinoma), A549 (human lung adenocarcinoma), PANC1 (human pancreas ductal carcinoma), CAPAN2 (human pancreas adenocarcinoma). All cells utilized tested negative for Mycoplasma. All cell lines maintained in DMEM (25mM Glucose, 4mM Glutamine, 1mM Sodium Pyruvate) supplemented with 10% Fetal Bovine Serum (FBS, Gibco) and 50units/mL Penicillin/Streptomycin (Gibco) in sterile incubators set to 37°C temperature and 5% CO₂ concentration. C2C12 cells were always maintained below 60% confluency (1:10 splitting ratio), cancer cells were often split (mouse cells 1:20 to 1:30; human cells 1:6 to 1:8) before or as soon as they grow confluent. For splitting, cells were first washed with PBS, detached using 1 volume of pre-heated Trypsin-EDTA for 1minute and neutralized with 4 volume DMEM (Gibco). C2C12 cells were induced for differentiation into myotubes by replacing 10% FBS DMEM with 2% Horse Serum (HS) DMEM once they grow confluent and incubated for 6 days by refreshing the media daily.

2.2.2 Stable knock-down of the SLC25A12 gene

SLC25A12 gene (AGC1 protein) was knocked-down in mouse (C2C12, B16F10, LLC1 and AL1376) and human (A549, PANC1, H1299, CAPAN2, HeLa) cell lines by using several independent lentiviral shRNA particles (3 for mouse and 2 for human cells) targeting mouse or human SLC25A12 mRNA, respectively (Sigma). For the control group, mammalian non-targeting lentiviral shRNA particles were used (Sigma). 5 000 to 25 000 cells/well were seeded into 8 well of 6-well plates from all cell lines mentioned above. Following day, media was refreshed with one containing 8µg/mL Polybrene and a different lentivirus for each well (Multiplicity of Infection: C2C12: 10; B16F10: 5; LLC1: 6; AL1376: 10; A549: 5; H1299: 5;

PANC1: 10; CAPAN2: 10). One well from each cell line was not transfected with lentivirus and used as death control for puromycin selection control. After 3-4 days, cells were moved to T25 flasks; and selection was performed using varying concentrations of puromycin (C2C12: 0.75µg/mL; B16F10: 0,6µg/mL; LLC1: 2,5µg/mL; AL1376: 3µg/mL; human cell lines: 1µg/mL) for 6-7 days until no cell remaining in selection control.

2.2.3 CRISPR/Cas9-mediated knock-out of Slc25a12 gene

In order to knock-out Slc25a12 from C2C12 and LLC1 cells, 7 different guide pairs targeting mouse Slc25a12 gene (sgAGC1, see Key resources table at section 2.9) were individually cloned into lentiCRISPRv2 vector (Sanjana et al., 2014; Shalem et al., 2014) that includes Cas9-expressing cassette.

These vectors, including the empty vector, are then used for lentivirus production. Specifically, vectors were delivered into HEK293T cells using X-tremeGENE siRNA Transfection Reagent (Roche, 04476093001) and media was collected and filtered (0,22µm) 48 hours following the transfection. Single-cell cloning could cause selection pressure that may lead to a phenotype independent from the knock-out of Slc25a12; therefore, the vectors containing different sgAGC1 guides were pooled during viral production. Then, viral supernatants are either stored in -80°C or immediately used to transduce C2C12 or LLC1 in a similar manner described in Section 2.2.1.

2.2.4 Transient overexpression of mouse and human SLC25A12

To investigate the effects of high Slc25a12 expression on proliferation rate, wild type C2C12 cells, 0,5x10⁵ cells were seeded into 1,5mL fresh media containing 6-well plates together with 1:1 mixture of 0.35µg pcDNA HisMax C vectors with or without AGC1 and 2µL Metafectane Pro (Biontex) -each diluted in 100µL serum-free DMEM-. The media was refreshed after 24 hours and cells were counted 60-64 hours after transfection. The proliferation rate was calculated as described below (Section 2.2.5).

Because mouse Slc25a12 targeting shRNAs used in this study will also inhibit the expression of exogenous Slc25a12 in HisMaxC vector, we used human SLC25A12 for shRNA-rescue experiments. To rescue AGC1-KD cells by expressing human SLC25A12, C2C12 cells were cultured in T-75 flasks until 60-70% confluent to be later sub-cultured into 6-well plates while transfecting pHLCX-flag vectors with or without human AGC1 (SLC25A12). 12hours later, 2,000 cells were seeded into 96-well plates for a cell viability assay. Once the cells attach to the plate surface (6-12 hours), cells were washed twice, reference measurements were obtained, relevant media conditions and treatments were applied. Final

measurements were obtained 48hours after the reference measurements, as described below (Section 2.2.6).

2.2.5 siRNA-mediated knock-down of Got1/2

Universal Negative Control siRNA (SIC001, Sigma) or MISSION esiRNA targeting mouse Got1 (EMU029631, Sigma) or mouse Got2 (EMU094111, Sigma) mRNAs were transfected into C2C12 cells using X-tremeGENE siRNA Transfection Reagent (Roche, 04476093001) following the manufacturer's instructions. Specifically, we gently mixed 100pmol control siRNA or combination of Got1/Got2 esiRNA (50pmol each) with 200 μ L transfection reagent and applied them onto C2C12 cells that were previously grown to 50-60% confluency in 6-well plates. 8 hours later, cells were split into new 6-well plates as described for proliferation assays and media conditions were applied 2-hours after all cell plating.

2.2.6 Cell Counting Experiments (Proliferation/Survival Rates)

In order to highlight the phenotypes and different cell numbers and experiment durations were used for assays where the loss of cell number is expected (survival assays; such as CB-839 treatment or starvation experiments) than the ones where cells grow rapidly (proliferation assays). Survival experiments were initiated with higher cell number and treatments were shorter compared to proliferation experiments that started with much lower cell number and took longer time. In cases where different conditions that causing cell death and supporting proliferation had to be examined within the same experimental setup, both cell number and duration were optimized for that specific experiment and indicated in the results section individually. For long-term proliferation experiments, approximately 15,000-25,000 cells/well or for short-term starvation or inhibitor treatment experiments 100,000-200,000 cells/well were seeded into 6-well plates. Cells were left to adhere overnight (or 6h), and at least two wells per biological group were washed twice with PBS (once in the case of LLC1 cells), trypsinized and initial cell numbers were determined. Then the experimental wells were washed in the same way as reference wells and media conditions were applied. Due to low-adherent nature of LLC1 cells, both PBS and fresh media was applied very carefully. Final cell numbers were counted 2 (short-term) or 3 (long-term) days for C2C12 and LLC1 cells and 4 (short-term) or 7 (long-term) days AL1376, A549, H1299, PANC1, CAPAN2, HeLa cells after the treatment for proliferation experiments. Minimum 3mL media was used per well, 4 or 5mL media was used for incubations longer than 3 days. Proliferation/survival rate was calculated by the following formula: Proliferation/Survival Rate = Log_2 (Final cell count / Initial cell count) / Days

2.2.7 Cell Viability Assays

For Cell Titer Glo Viability Assay (Promega), varying number of cells (500 for proliferation assays, 2000 for survival assays) were seeded in a flat-bottom adequate number of 96-well plates. One extra plate was assigned for reference. After allowing sufficient time for cells to attach (6-12hours); the cells were washed twice (once for LLC1) with PBS and experimental media was added in all wells (100µL-200µL) in all plates. Experimental plates were placed back into the incubators while the initial luminescent signals of at least 3 wells per biological group were measured from the reference plate using 40µL (for survival) or 100µL (for proliferation) of Cell Titer Glo Reagent. Manufacturer's recommendations were followed to determine luminescent signals. Specifically, plates were shaken for 2-3 minutes, incubated for 10minutes at room temperature and luminescence signals were measured using Orion II Microplate Reader Luminometer (Berthold). The following plates were also measured the same way at the endpoint of experiments. For survival studies, the final measurement was obtained after two or three days. For proliferation assays, media was refreshed every second day and final measurements were made at day four or five and the growth rate was calculated by the following formula:

Proliferation/Survival Rate = Log_2 (Final measurement / Initial measurement) / Days

2.2.8 Annexin V/PI Staining (Apoptosis Assay)

150,000-200,000 cells with or without AGC1 knockdown were seeded into 6-well plates using full DMEM media. After adhering overnight, cells were carefully washed twice with PBS and media conditions including CB-839 or low glutamine (0.1mM) treatments were applied in a similar manner as described for proliferation/survival experiments. The cells were treated with applied media conditions for 24 hours, then the cells were collected via trypsinization and washed three times. Thermo Fischer Dead Cell Apoptosis Kit with Annexin V Alexa Fluor™ 488 & Propidium Iodide (PI) (V13241) was used for staining dead and apoptotic cells that later was detected using a flow cytometer. According to the manufacturer's recommendations, up to 1,000,000/mL cells were resuspended with provided annexin binding buffer. 5µL Alexa Fluor 488-Annexin and 1µL 100µg/mL PI solutions were added onto each 100µL cell suspensions. After 15 minutes of incubation at room temperature, 400µL annexin binding buffer was added onto the solution and gently mixed. Within the next hour, fluorescence emissions were measured in FITC (for Alexa Fluor 488-Annexin) and Texas Red (for propidium iodide) channels using a flow cytometer (BD. FACS Diva). The rates of cells that were positively stained for either of these dyes were analyzed and calculated using FlowJo software.

2.2.9 C2C12 differentiation experiment

C2C12 cells were induced for differentiation into myotubes by replacing 10% FBS DMEM with 2% Horse Serum (HS) DMEM once they grow confluent and incubated for 6 days by refreshing the media daily. Ideally, 200,000 C2C12 NTC and 230,000 C2C12 AGC1-KD cells were seeded 3 days prior to the induction to make sure both cells grow confluent around the same time.

2.2.10 Mitochondrial Respiration Measurement

C2C12 cells with or without stable knockdown of AGC1 were seeded in XF96 polystyrene cell culture microplates (Seahorse Bioscience®) at a density of 30,000 cells per well. 24 h after plating, cells were washed and preincubated for 30 min in XF assay medium supplemented with D-glucose (25 mM), sodium pyruvate (1 mM) and glutamine (2 mM) at 37°C in a non-CO₂ environment. Oxygen consumption rate (OCR) was subsequently measured every 7 min using an XF96 extracellular flux analyzer (Seahorse Bioscience®). A standard protocol with 2 µM oligomycin, 0.5 µM carbonyl cyanide *p*-trifluoromethoxyphenylhydrazone (FCCP), and 2.5 µM antimycin A was performed. Oxygen consumption was normalized to the number of cells (pmol O₂/(min x cells per well)) and presented as basal and maximal mitochondrial respiration.

For CB-839 treatment, 60,000 C2C12 cells were seeded in XF24-well plates and allowed to adhere overnight. The next day, wells were washed twice with PBS and serum-free, pyruvate-free DMEM, in the presence or absence of 1 µM CB-839 (or 0.01% DMSO). 6 hours after treatment, OCRs were measured as described above and subsequently normalized to cell counts and OCRs of individual genotype (control vs AGC1-KD) in DMSO treated conditions.

2.2.11 NAD⁺/NADH measurement

For measuring the NAD⁺/NADH ratio; around 25k cells were seeded into 6-well plates; lysed in 120 µL 1:1 0.2N NaOH:PBS solution and 50 µL each was collected for NAD⁺ and NADH measurements. That point on, the protocol from NAD/NADH Glo Assay Kit (Promega) was followed precisely and luminescence signals from NAD⁺ and NADH samples were measured independently as described above. The ratio was determined following normalization to blanks.

NAD⁺/NADH ratio measurement method was adopted (Sullivan et al., 2015). 25,000 cells per well were seeded into 6-well plates using pyruvate-free DMEM, extracted in 120 µL 1:1 0.2N NaOH:PBS solution after 24 hours and frozen at -80°C immediately. For NADH measurement, 20 µL lysate was incubated at

MATERIALS & METHODS

75°C for 30 min, during which oxidized NAD is degraded. For NAD⁺, 20µL lysate was diluted 1:1 with lysis buffer and 20µL 0.4N HCl was added. Later, NAD⁺ samples were incubated at 60°C for 15min to selectively degrade the reduced form of NAD. After individual incubations, samples were cooled down to room temperature for 8 minutes and the degradation reactions were stopped by 20µL 0.25mM Tris in 0.2N HCl (NADH) and 0.5mM Tris base (NAD⁺). The manufacturer's instruction was followed after sample preparation using the NAD/NADH Glo Assay (Promega).

2.2.12 ROS Measurement

Sub-confluent C2C12 cells were incubated with 1µM CellRox (RED2 Channel, Invitrogen) solution for 1hour, washed twice with PBS, trypsinized and resuspended with media by pipetting long enough to obtain single cells. After centrifugation, cells were mixed well with 100µL PBS and incubated with 1:0000 Ghost Dye (NIR2 Channel, Tonbobio) for half an hour. Ghost Dye was washed away and cells were resuspended in PBS. Fluorescent signals were obtained via Guave Easy Cyte 8 (Millipore) and data were analyzed using InCyte Software (Millipore).

2.2.13 Radioactive CO₂ release

The day before measurements, 250,000 cells/well were plated into 6-well plates. 1.1µCi [U-14C]-glutamine (ARC 0196) was added into each well and wells were covered with Whatman paper soaked with 5M KOH. After incubating for 1h, wells were treated with 200µL of 2.6N HClO₄ for another 2h. Later, papers covering individual wells were cut gently and transferred into vials containing 20mL scintillation cocktail. Following rigorous shaking, radioactive carbon units were measured.

2.2.14 Extracellular Flux Analysis

150,000-200,000 cells were seeded into 6-well plates and let adhere overnight. After 2 washes, media conditions were applied (2ml/well) and cell counts were obtained from reference wells. 48 hours later, media samples were collected, centrifuged at top speed and stored at -80°C and final cell count was obtained from respective wells. Glucose, glutamine, lactate and glutamate concentrations were quantified using Metabolic Flux Analyzer (YSI 2900, YSI Life Sciences) in 96-well format.

2.3 Metabolic Profiling

2.3.1 NMR Spectroscopy

Methanol, sodium phosphate, dibasic (Na_2HPO_4), sodium hydroxide, hydrochloric acid (32 % m/v), and sodium azide (NaN_3) were obtained from VWR International (Darmstadt, Germany). 3(trimethylsilyl)propionic acid-2,2,3,3-d₄ sodium salt (TSP) was obtained from Alfa Aesar (Karlsruhe, Germany). Deuterium oxide (D_2O) was obtained from Cambridge Isotope Laboratories, Inc. (Tewksbury, MA). Deionized water was purified using an in-house Milli-Q® Advantage Water Purification System from Millipore (Schwalbach, Germany). All chemicals were used with no further purification. The phosphate buffer solution was prepared by dissolving 5.56 g of anhydrous NaH_2PO_4 , 0.4 g of TSP, and 0.2 g NaN_3 , in 400 ml of deionized water and adjusted to pH 7.4 with 1M NaOH and HCl. Upon the addition of deionized water to a final volume of 500 ml, the pH was readjusted to pH 7.4 with 1M NaOH and HCl. The buffer was lyophilized and taken up in 500 ml D_2O to obtain NMR buffer in D_2O .

For sample preparation; confluent cells from 150cm dishes or 20-150mg tissues collected in PBS. Tissues were lysed using 1.0mm diameter zirconia beads (Carl Roth) by vigorous shaking in Precellys 24 (Bertin Technologies) for 2x20seconds and by sonication 3x10seconds. Cell lysates were lysed solely via sonication. For quenching the metabolites; one volume of cell lysate, cell media, tissue lysate or plasma is mixed with two-volume of cold methanol, incubated at $-20\text{ }^\circ\text{C}$ for at least 1 hour, and centrifuged at 13000 rpm for 30 min to pellet proteins. Supernatants were transferred to fresh vials and dried for 4 hours at room temperature. 500 μL of NMR buffer in D_2O were added to the samples, re-dissolved and transferred to 5 mm NMR tubes.

All NMR experiments were performed at 310 K on a Bruker Avance III 500 MHz spectrometer equipped with a TXI probe head. The 1D CPMG (Carr–Purcell–Meiboom–Gill) pulse sequence (cpmgpr1d, 73728 points in F1, 12019.230 Hz spectral width, 1024 transients, recycle delay 4 s), with water suppression using pre-saturation, was used for ^1H 1D NMR experiments. Bruker Topspin version 3.1 was used for NMR data acquisition. The spectra for all samples were automatically processed (exponential line broadening of 0.3 Hz), phased, and referenced to TSP at 0.0 ppm using Bruker Topspin 3.1 software (Bruker GmbH, Rheinstetten, Germany). Preprocessed 1D NMR spectra were transferred into Matlab R2014a (The Mathworks, Inc., USA) and processed using lab-written scripts. 1D NMR spectra were referenced to the TSP peak at 0 ppm, before peak alignment by recursive segment-wise peak alignment (RSPA). The spectrum with the highest correlation to the other spectra was used as the alignment reference. The spectral data between 0.5 and 10.0 ppm were extracted for multivariate analysis, after

removal of the residual water (4.5–5.0 ppm) and TSP (-0.5 – 0.5 ppm) regions. Prior to multivariate analysis, the spectra were normalized by probabilistic quotient normalization (PQN). Multivariate analysis was performed on mean-centered data by orthogonalized partial least squares discriminant analysis (OPLS-DA) validated by leave-one-subject-out cross-validation and permutation testing ($n = 1000$, significance for $p_{\text{perm}} \leq 0.05$). Metabolite reference chemical shifts were taken from the Madison-Qingdao Metabolomics Consortium Database (<http://mmcd.nmrfa.wisc.edu/>) database and metabolites were cross-checked using reference compounds if necessary.

2.3.2 Isotope Tracing and GCMS Analysis

For metabolic tracing studies 150,000-200,000 cells/well were seeded in 6-well plates overnight. Cells were washed three times and 5mM [U-13C]glucose or 4mM [U-13C]glutamine (Cambridge Isotopes Laboratories) containing DMEM (10% dialyzed serum, no pyruvate) was applied. After 24h of culture, metabolites were extracted from cells or media (10 μ L) in 80% methanol in water containing 1 μ g/sample norvaline and dried under nitrogen gas. Polar metabolites were derivatized and measured as described previously (Lewis et al., 2014). Relative metabolite abundances were calculated by integrating ion peak area and normalized to norvaline and later to the cell numbers from identical plates. Mass isotopomer distributions of each ion peak were determined after natural abundance corrections adapted from (Fernandez et al., 1996).

2.3.3 Metabolic profiling using LCMS

For cells: 200,000 (in 6-well plate, for TCA intermediates and amino acids) (Corning) C2C12 cells were starved for glutamine in the absence or presence of 5mM Aspartate for 24hours. Samples were prepared the same way as described in the above GCMS section. For tumors: each tumor was snap-frozen in liquid nitrogen immediately after harvesting and stored at -80°C. 6 tumors per group were selected randomly and ~10-20mg from each tumor was sampled and extracted in 80% methanol following the abovementioned procedure. Metabolites were quantified as detailed previously (Sullivan et al., 2015, Davidson et al., 2016). Briefly, dried polar samples were resuspended in 50 μ L water and 2 μ L were injected into a ZIC-pHILIC 150 x 2.1 mm (5 μ m particle size) column (EMD Millipore). The analysis was conducted on a QExactive benchtop orbitrap mass spectrometer equipped with an Ion Max source and a HESI II probe, which was coupled to a Dionex UltiMate 3000 UPLC system (Thermo Fisher Scientific, San Jose, CA). External mass calibration was performed using the standard calibration mixture every 7 days. Chromatographic separation was achieved using the following conditions: Buffer A was 20 mM ammonium carbonate, 0.1% ammonium hydroxide; buffer B was acetonitrile. The column oven and

autosampler tray were held at 25°C and 4°C, respectively. The chromatographic gradient was run at a flow rate of 0.150 ml/min as follows: 0–20 min.: linear gradient from 80% to 20% B; 20–20.5 min.: linear gradient from 20% to 80% B; 20.5–28 min.: hold at 80% B. The mass spectrometer was operated in full-scan, polarity switching mode with the spray voltage set to 3.0 kV, the heated capillary held at 275°C, and the HESI probe held at 350°C. The sheath gas flow was set to 40 units, the auxiliary gas flow was set to 15 units, and the sweep gas flow was set to 1 unit. MS data acquisition was performed in a range of 70–1000 m/z, with the resolution set at 70,000, the AGC target at 10e6, and the maximum injection time at 20 msec. Relative quantitation of polar metabolites was performed with XCalibur QuanBrowser 2.2 (Thermo Fisher Scientific) using a 5 ppm mass tolerance and referencing an in-house library of chemical standards.

2.4 In vivo Tumor Experiments

2.4.1 Animal Care

Wild-type C57Bl/6J mice were kept in a standard temperature (23 – 25 °C) and humidity-controlled environment with a 12: 12 hour light-dark cycle. Mice had nesting material and *ad libitum* access to water and commercial chow diet (ssniff® #V1126 – Austria).

All animal experiments were carried out according to the EU ethical guidelines and approved the Austrian Federal Ministry of Science, Research, and Economy, respectively.

2.4.2 Subcutaneous growth of LLC1 tumors.

LLC1 cells were cultured in T175 flasks about a week prior to the day of injection. For getting ready with the injections, cells were grown to 50-60% confluency, washed with PBS, mixed with 5mL trypsin and resuspended with 25mL media as soon as they detach from the plate. Cells were flown through 0.45mm x 25mm needles to avoid clumps; and centrifuged for 5min at 1000rpm. Media was aspirated, the pellet was resuspended with 3mL ice-cold HBSS, viable cells were counted using a hemocytometer and diluted to 2.5×10^6 cells/mL in HBSS. Cell was kept at for 4°C and used for injection within less than 2 hours. 0.5×10^6 cells (200µL) were injected over the right flanks of 8-week-old female C57BL/6 mice (8 mice per group) using 0.6mm x 30mm needles. Solid tumor lengths and widths were measured from outside using calipers until day16 and estimated tumor volumes were calculated as follows: length x width². Survivability of mice was monitored every day in standard housing conditions ensuring their access to water and food supply.

2.4.3 Allografts and *in vivo* CB-839 treatment

The animal study was approved by the institutional ethics committee and experiments were performed according to the guidelines of the Austrian Federal Ministry of Science and Research. Experiment licenses were granted under BMWF-66.007/0026-WF/V/3b/2015 and BMWF-66.007/0008-WF/V/3b/2016. *In vivo*, CB-839 experiments were approved by the MIT Committee on Animal Care (IACUC). 500,000 LLC1 or 100,000 AL1376 cells were injected into flanks of 7-8 weeks old female C57BL/6 mice (Janvier and Jackson Laboratories). Tumor sizes were measured using calipers throughout the study and estimated volumes were calculated by using the formula $V = (\pi/6) * (\text{length} * \text{width}^2)$ (Gui et al., 2016). For CB-839 treatment studies, tumors were grown for 12 or 17 days followed by administration of 200mg/kg CB-839 or vehicle twice daily as previously described (Gross et al., 2014). Tumors were harvested 4 hours after the final drug dose and metabolites were quantified using LCMS.

2.4.4 Tail vein injection of B16F10 cells

B16F10 cells were cultured and prepared for injection as it is described above for LLC1 cells. Cells were diluted to 3×10^6 cells/mL in cold HBSS. 8-10week-old female C57BL/6 mice were restrained leaving only their tail outside, providing access to open-air through small holes near face area and $0,3 \times 10^6$ cells (100 μ L) were injected into the tail vein using 0.3mm x 12mm needles (Omnican). The mice were harvested at day16 and lungs were collected, rinsed and fixed in 10%Formalin for at least 48hours. Each lung was sliced into 12-15 pieces, embedded in paraffin, stained with H&E and total area as well as tumor area was measured for every piece using NisElements Software. Tumors were determined at 10X magnification; areas were measured at 2X. Mean “tumor percent in total lung area” of shAGC1 group mice was normalized to shControl group within the same experiment to avoid misleading variations among independent experiments.

2.5 Immunohistochemistry

Immunohistochemistry using Aralar B-2 Antibody (Santa Cruz, sc-271056) was performed on cancerous or non-cancerous human tissues: cancer tissue arrays, pancreatic cancer, and breast cancer sections. Paraffin sections were cut onto charged slides and allowed to be dried overnight at 37°C. Sections were dewaxed with xylene treatment for 2x10 minutes, dehydrated with descending concentrations of ethanol (100%, 96%, 70%) and washed with water for 5 minutes each. Samples were cooked using a microwave at 270watt for 40minutes in pH6 Sodium Citrate Buffer to unmask the antigen and then cooled down for

MATERIALS & METHODS

20 more minutes. After three times washing with PBS (3x3 minutes unless indicated otherwise), endogenous peroxidase was blocked by treating slides with 3% H_2O_2 in Methanol solution for 10minutes which was followed by another PBS washing step. Aralar antibody was diluted 1:50 in Antibody Diluent Solution (Dako, S2022); 100 μ L of the mixture was applied on each sample and incubated at room temperature for 60minutes. After washing, Rabbit/Mouse Detection Solution (Dako 5007) was applied for 30minutes. Slides were again washed and incubated for 5-10 minutes with sufficient volume of AEC Substrate Chromogen (Dako, K3464) to cover the sections. Following another washing step, nuclei were counterstained with Mayer's Haematoxylin for 1 minute and slides were washed under tap water for at least 3 minutes. Sections were mounted in Aquatex (Merck) and imaged using a standard light microscope(s).

2.6 Quantitative Real-Time PCR

Total RNA from cells was isolated using the PeqGOLD total RNA isolation kit (Peqlab). Tissue RNA was isolated with TRIzol reagent (Life Technologies). cDNA was generated using the Qiagen QuantiTect RT kit. mRNA expression was assessed using SYBR green real-time PCR on an ABI 7000 instrument as described. Ct values of every gene first subtracted from the ones of Tffl β and/or β -Actin (unless stated otherwise) within every cDNA sample, then normalized to the mean δ Ct of the control group for every gene. Fold changes were calculated by taking the $\delta\delta$ Ct power of ($\frac{1}{2}$).

2.7 Western Blot

Cells were harvested for protein analysis by scraping with SDS-lysis buffer (50 mM Tris-HCl, pH 6.8, 10 % glycerol, 2.5 % SDS, cOmplete™ protease inhibitor cocktail) and samples were digested by benzonase (Merck Millipore, Darmstadt, GER).

Tissues on ice were homogenized in RIPA buffer (150 mM Tris-HCl pH 8.0, 50 mM NaCl, 1 % TritonX-100, 0.5 % Na-Deoxycholate, 0.1 % SDS) and incubated on ice for 20 minutes. After centrifugation at 16000 g / 10 min / 4 °C, the intermediate phase was carefully collected into a new Eppendorf tube by puncture of the tube wall with a hot needle.

Protein concentrations were determined with the Pierce™ BCA Protein Assay Kit (ThermoFisher Scientific, Waltham, MA, US). 15-250 μ g of the sample was loaded into a 10% or 4-12% BisTris gel (NuPAGE, Invitrogen™, ThermoFisher Scientific, Waltham, MA, US), and gels were blotted to nitrocellulose membranes.

MATERIALS & METHODS

The following antibodies were used: anti-Aralar (1:1000) (sc271056, Santa Cruz) and anti- β -Actin (1:250000 for cells)(A5316, Sigma-Aldrich, St. Louis, MO, US). For chemiluminescent detection, horseradish peroxidase-conjugated secondary antibodies were used (anti-rabbit 1:3000-5000 and anti-mouse 1:3000-5000) (Dako Österreich GmbH, Vienna, AUT).

SuperSignal™ West Pico Chemiluminescent Substrate (ThermoFisher Scientific, Waltham, MA, US) and ECL prime substrate (RPN2232, GE Healthcare, Little Chalfont, GB) served as substrates. Before re-probing, blots were stripped with Restore™ Western Blot Stripping Buffer (ThermoFisher Scientific, Waltham, MA, US) for 15 – 20 minutes.

2.8 Statistical analysis

All experiments were performed using at least three independent replicates (different passages and mice for *in vitro* and *in vivo* experiments, respectively). Data are shown as mean \pm SD unless indicated otherwise. Single comparison between two groups, depending on the sample number, data distribution and the nature of the experiment, is calculated via two-tailed, parametric or non-parametric, paired or unpaired student's t-test, as will be explained in figure legends. Significance levels: * $p \leq 0.05$, ** $p \leq 0.01$, *** $p \leq 0.001$. non-significant tendencies were sometimes labeled with § ($p < 0,1$).

2.9 Reagents

Table 1: Key resources table.

REAGENT or RESOURCE	SOURCE	IDENTIFIER
Antibodies		
Mouse monoclonal α -Aralar (AGC1) antibody B2	Santa Cruz Biotechnology	Cat#: sc-271056
Mouse monoclonal α -Beta-actin antibody	Sigma-Aldrich	Cat#: A5316
Anti-mouse secondary antibody	Dako Österreich GmbH	Cat#: P0260
Chemicals, Peptides, and Recombinant Proteins		
2-deoxyglucose	Sigma-Aldrich	Cat#: D8375-1G
D-Glucose >99,5%, CELLPURE	Carl Roth GmbH	Art.-Nr. HN06.3
L-Glutamine	Sigma-Aldrich	Cat#: G6392-10VL
MEM 50X Amino Acid Solution	Sigma-Aldrich	Cat#: M5550
100X Non-essential Amino Acid Solution	Sigma-Aldrich	Cat#: M7145-100mL

MATERIALS & METHODS

Metformin	Sigma-Aldrich	Cat#: PHR1084-500MG
Sodium pyruvate	Sigma-Aldrich	Cat#: P2256-5G
dimethylalpha-ketoglutarate	Sigma-Aldrich	Cat#: 349631-5G
dimethylmalate	Sigma-Aldrich	Cat#: 238198-100G
L-Aspartate	Sigma-Aldrich	Cat#: A7219-100G
L-Asparagine monohydrate	Sigma-Aldrich	Cat#: A8381-100G
L-Glutamate	Sigma-Aldrich	Cat#: G1251-100G
L-Serine	Sigma-Aldrich	Cat#: S54500-1G
L-Glycine	Sigma-Aldrich	Cat#: G8790-100G
L-Alanine	Sigma-Aldrich	Cat#: A7627-1G
L-Proline	Sigma-Aldrich	Cat#: P5607
[¹³ C-U]-D-Glucose	Cambridge Laboratories	Isotopes Cat#: CLM-1396
[¹³ C-U]-L-Glutamine	Cambridge Laboratories	Isotopes Cat#: CLM-1822-H
[¹³ C-U]-L-Aspartate	Cambridge Laboratories	Isotopes Cat#: CLM-1801-H
[¹³ C-U]-L-Glutamate	Cambridge Laboratories	Isotopes Cat#: CLM-3949-PK
[U-14C]-glutamine	American Chemicals	Radiolabeled Cat#: ARC 0196
Adenine	Sigma-Aldrich	Cat#: A8626-5G
Guanine	Sigma-Aldrich	Cat#: G11950-10G
Hypoxanthine	Sigma-Aldrich	Cat#: H9377-5G
Thymine	Sigma-Aldrich	Cat#: T0376-5G
Uridine	Sigma-Aldrich	Cat#: U6381-5G
O-(Carboxymethyl)hydroxylamine hemihydrochloride (AOA)		Cat#: C13408-1G
Critical Commercial Assays		
Cell Titer Glo	Promega	Cat #: G7570
NAD/NADH Glo	Promega	Cat #: G9071
Dead Cell Apoptosis Kit	Thermo Fischer	Cat #: V13242
Deposited Data		
Cancer Cell Line Encyclopedia	Broad Institute	https://portals.broadinstitute.org/ccle
Experimental Models: Cell Lines		
Mouse: C2C12	ATCC	CRL-1772
Muse: LLC1	ATCC	CRL-1642

MATERIALS & METHODS

Mouse: AI1376	Our laboratory	N/A
Human: HeLa	ATCC	CCL-2
Human: A549	ATCC	CCL-185
Human: NCI-H1299	ATCC	CRL-5803
Human: PANC1	ATCC	CRL-1469
Human: CAPAN2	ATCC	HTB-80
Experimental Models: Organisms/Strains		
C57BL/6	Jackson Laboratories & Janvier	Stock No: 000664
Oligonucleotides		
mSlc25a12_guide 1:GCCATGCTGTGCTCGGAAGC	IDT DNA	custom oligo
mSlc25a12_guide 2:CCATGCTGTGCTCGGAAGCC	IDT DNA	custom oligo
mSlc25a12_guide 3:CTCATGAGGATCACCTCGTT	IDT DNA	custom oligo
mSlc25a12_guide 4:CAGGTGCATACAACCAAACG	IDT DNA	custom oligo
mSlc25a12_guide 5:GGCTTCCGAGCACAGCATGG	IDT DNA	custom oligo
mSlc25a12_guide 6:ACTCGCAGTCCCAGTTAAAA	IDT DNA	custom oligo
mSlc25a12_guide 7:ACTCGCAGTCCCAGTTAAAA	IDT DNA	custom oligo
Recombinant DNA		
pLKO.1:TRCN0000069911 mouse shRNA targetting AGC1 (KD1)	Sigma-Aldrich	Clone ID: NM_172436.2-691s1c1

MATERIALS & METHODS

pLKO.1:TRCN0000069908 mouse shRNA targetting AGC1 (KD2)	Sigma-Aldrich	Clone ID: NM_172436.2- 1241s1c1
pLKO.1:TRCN0000069912 mouse shRNA targetting AGC1 (KD3)	Sigma-Aldrich	Clone ID: NM_172436.2- 460s1c1
pLKO.1:TRCN0000044591 human shRNA targetting AGC1 (KDa)	Sigma-Aldrich	Clone ID: NM_003705.2- 132s1c1
pLKO.1:TRCN0000310089 human shRNA targetting AGC1 (KDb)	Sigma-Aldrich	Clone ID: NM_003705.3- 212s21c1
pLKO.1-puro Non-Target shRNA Control	Sigma-Aldrich	Cat #: SHC016V
pLentiCRISPRv2 (lentiviral Cas9 expressing vector)	Laboratory of Dr. Feng Zhang	Addgene Cat #52961
pcDNA4 HisMaxC-mouseAGC1	subcloned into pcDNA4 HisMaxC	N/A
PMXS-SLC1A3	Laboratory of Dr. Kivanc Birsoy	Addgene Cat #72873
Software and Algorithms		
GraphPad Prism 7 for Graphs and statistics	GraphPad Software	https://www.graphpad.com/
Amdis GCMS Data Analysis Software	NIST	N/A
xCalibur Software for LCSM Analysis	Thermo Fischer Scientific	N/A
MATLAB	The MathWorks, Inc	https://www.mathworks.com/
FlowJo v10 for Flow Cytometry Data Analysis	FlowJo, LLC	https://www.flowjo.com/
Corel Draw x7 for Figure Preparation	Corel Corporation	https://www.coreldraw.com/
Other		
DMEM, High Glucose, Pyruvate	Gibco	Cat #: 11995065
DMEM W/L-Glutamine and 4.5g/L Glucose; w/ot Sodium Pyruvate	Corning	Cat #: MT10017CV
DMEM, High Glucose, No Glutamine	Gibco	Cat #: 11960044

MATERIALS & METHODS

DMEM, No Glucose, No Glutamine No Sodium Pyruvate	Corning	Cat #: 17-207-CV
Hank's Balanced Salt Solution	Sigma	Cat #: H8264
Phosphate Buffered Saline (Calcium/Magnesium free)	Gibco	Ref # 10010-015 500mL

RESULTS



3. Results

3.1 Malate-aspartate shuttle components are highly expressed in proliferating cells

Bioinformatics data from Cancer Cell Line Encyclopaedia (CCLE) showed that mRNAs of malate-aspartate shuttle (MAS) components are abundantly expressed in a broad spectrum of human cell lines (Figure 7, left). Next, we tested in-house proliferating mouse and recognized similar patterns with regard to mRNA expression of the same MAS-related genes (Figure 7, right). Interestingly, SLC25A13 (AGC2) showed the highest variation among different cell lines from both species.

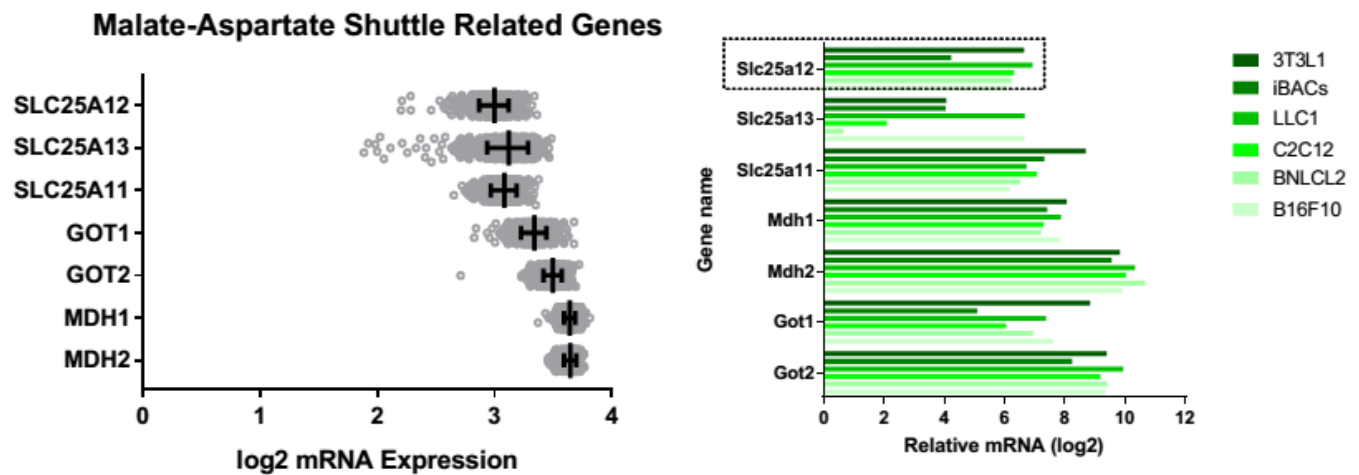


Figure 8: mRNA expression of MAS components. (left) Human cell lines from the or (right) in proliferating transformed or non-transformed mouse cell lines determined using qPCR (compared to Tfl1b) (n=1).

TCGA mRNA_seq database showed AGC1 (ARALAR, SLC25A12) is asymmetrically regulated in several tumors comparing to corresponding healthy (non-cancer) tissues (Figure 9, adapted from firebrowse.org). AGC1 mRNA expression is downregulated in glioblastoma (GBM), low-grade glioma (LGG), sarcoma (SARC), breast (BRCA), uterine (UCEC) and prostate (PRAD) cancers while is upregulated in lung squamous cell (LUSC) and adenocarcinoma (LUAD), pancreas adenocarcinoma (PAAD), cholangiocarcinoma (CHOL), pheochromocytoma and paraganglioma (PCPG) and liver hepatocellular carcinoma (LIHC) tumors (Figure 9).

RESULTS

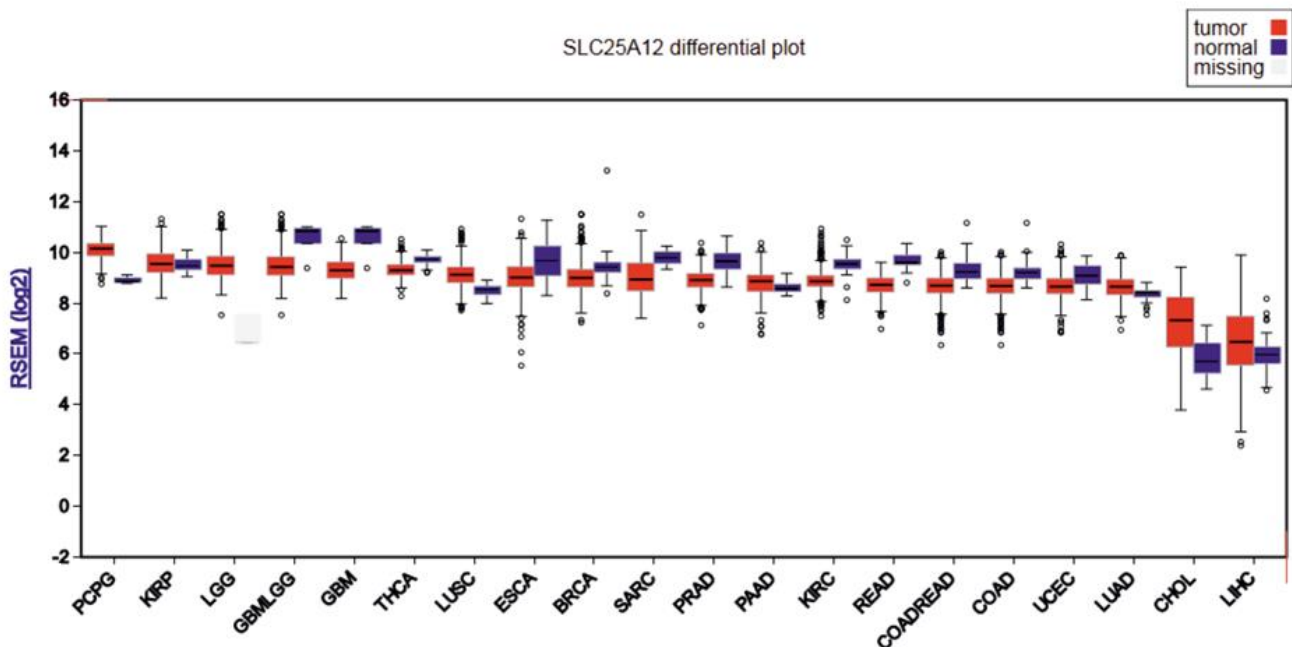


Figure 9: AGC1 expression in tumor vs healthy tissues. TCGA data comparing mRNA expression of AGC1 (SLC25A12) in various tumors (red bars) and their corresponding tissue of origin (blue bars). This plot is adapted from firebrowse.org. Standard deviations are shown.

3.2 shRNA-mediated knockdown of AGC1 reduced the proliferation in mouse cell lines

We created stable knockdown of AGC1 in C2C12, B16F10 and LLC1 cell lines using 5 independent shRNA constructs and compared with non-targeting controls (ntc). We selected the most efficient silencing (shAralar911 named AGC1-KD1) for phenotype characterization and, in most crucial experiments we also included a second (shAralar908, KD2) and third (shAralar912, KD3) knockdown in order to rule out off-target effects (Figure 10). Because C2C12 cells in proliferating state had the highest AGC1 and the lowest AGC2 ratio (8-fold) among the mouse cell lines we testes, we decided to use C2C12 cells for most of our mechanistic experiments to minimize the compensatory effects of AGC2.

Our first observation from the AGC1 knockdowns was that their doubling time in standard DMEM media was slightly increased (about 8-15% for KD1) in all three cell lines, measured by conventional cell counting method (Figure 10) in 6-well plates. The proliferation defect was consistent across other AGC1 knockdowns (Figure 11). However, it is important to note that cells with stable AGC1-knockdown appeared healthy and proliferated steadily -though relatively slowly- in standard culture conditions for many generations without showing signs of distress.

RESULTS

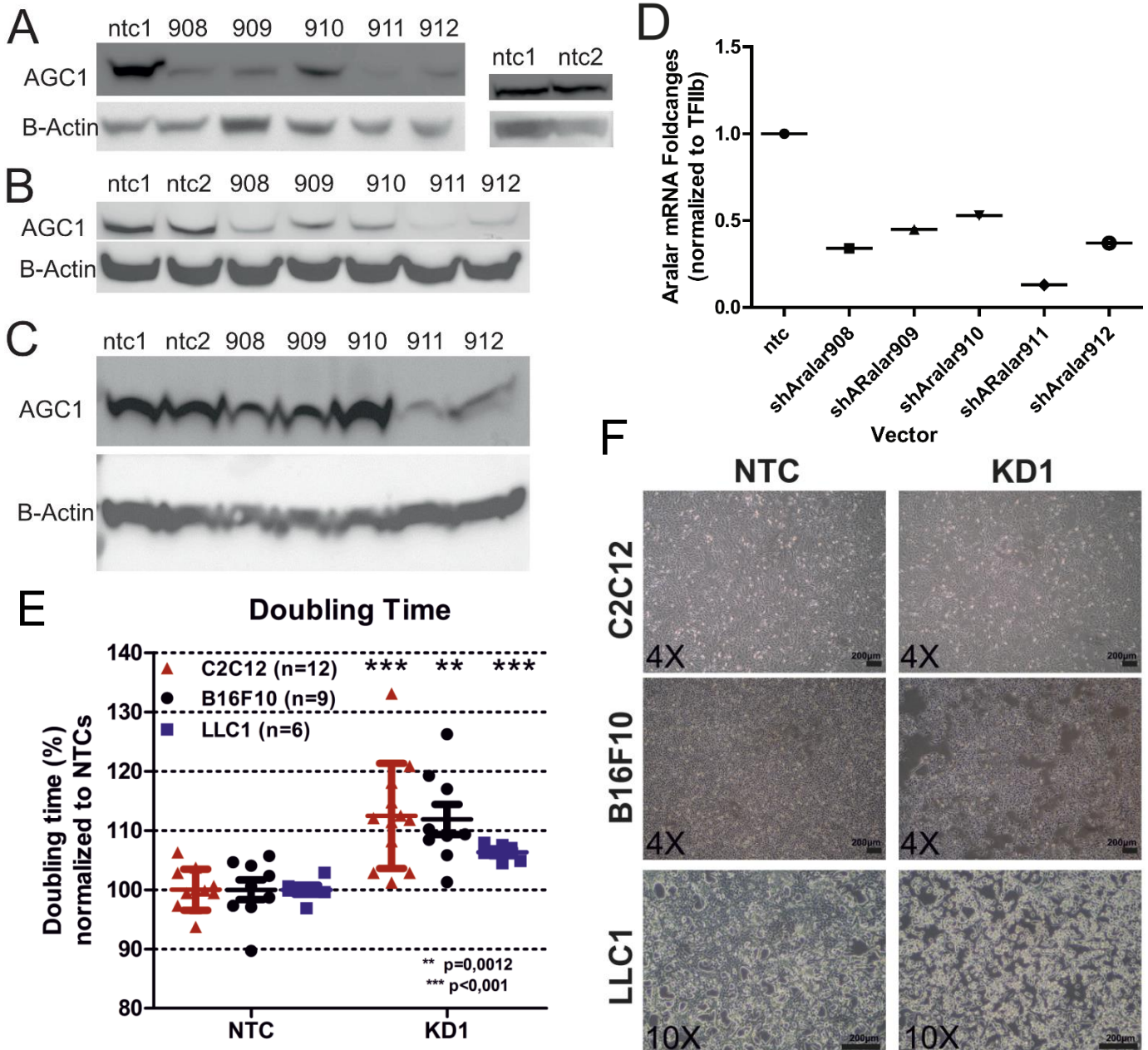


Figure 10: Knockdown of AGC1 decreases proliferation in C2C12, B16F10 and LLC1 cell lines. Western blotting analysis of AGC1 (Aralar expression following stable knockdown using lentiviral shRNA constructs. AGC1 knocked-down was most efficient via shRNA construct sh911 (AGC1-KD1) in A) C2C12, B) B16F10, C) LLC1 cell lines. In addition, sh908 and sh912 are also used as KD2 and KD3, respectively when required. D) mRNA levels of Aralar (AGC1) in C2C12 cells following AGC1-knockdown using the corresponding shRNAs. E) Percent change in doubling time following AGC1-KD in comparison to non-targeting controls (NTC). E) Representative showing of slower proliferation in AGC1-KD cells. Standard deviations are shown.

RESULTS

Extracellular pyruvate can serve as an electron acceptor to recycle NADH to oxidized NAD⁺ through lactate dehydrogenase (Figure 11). Therefore, we removed pyruvate from the media for subsequent experiments unless otherwise specified. After removal of pyruvate, the impact of AGC1-KD on cell proliferation becomes more evident and this shift is rescued by pyruvate or aspartate supplementation, as previously reported for mitochondrial dysfunction cells (Birsoy et al., 2015; Sullivan et al., 2015). Yet, AGC1-KD cells continue to remain viable and gradually proliferate in pyruvate-free media to (Figure 11C).

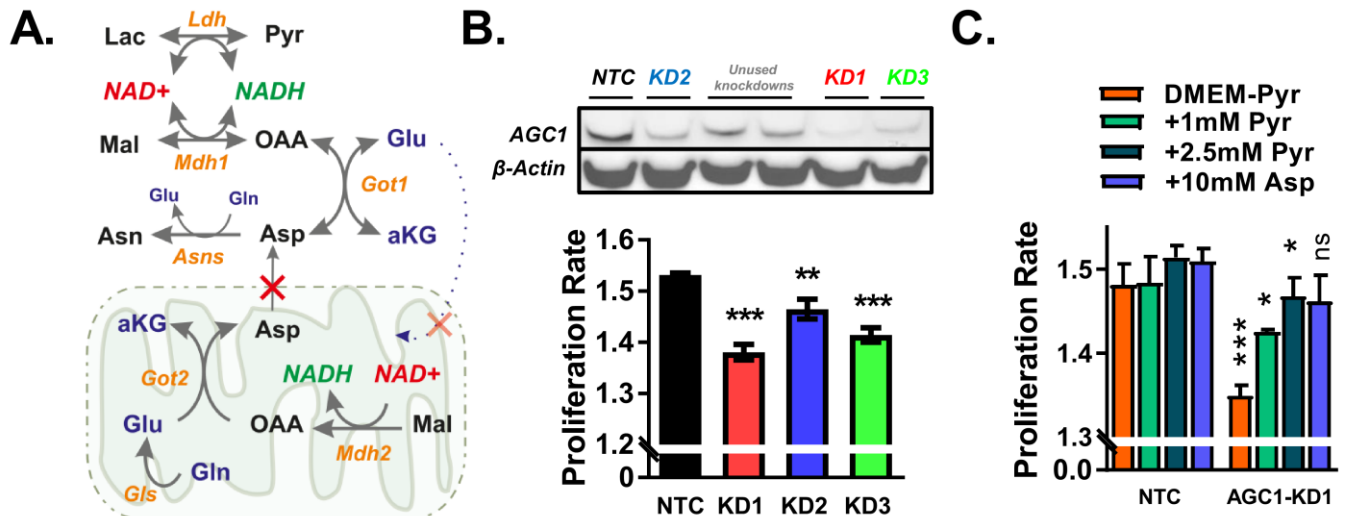


Figure 11: AGC1 knockdown reduced the proliferation rate. (A) Schematic demonstration of how malate-aspartate shuttle and lactate dehydrogenase can regenerate NAD⁺ in the cytosol (B) AGC1 knockdown in C2C12 cells using three different shRNA hairpins all reduced proliferation. The proliferation rate of control (NTC) and cells with AGC1-KD (KD1, KD2, and KD3) is shown as doublings/day (n=3). (C) The proliferation rate of control (NTC) and AGC1-KD1 C2C12 cells in the presence and absence of the indicated concentrations of pyruvate (Pyr) and aspartate (Asp) (n=3). Standard deviations are shown.

3.3 AGC1 knock-down and overexpression altered the cellular metabolism

Next, we wanted to characterize the metabolic changes that occur following AGC1 knockdown. It is expected that MAS disruption upon AGC1-loss will decrease the cytosol NAD⁺/NADH ratio and increase the mitochondrial NAD⁺/NADH ratio (del Arco et al., 2002). We observed that, in AGC1-KD C2C12 cells, the entire cellular NAD⁺/NADH ratio is lower than in non-targeting control (NTC) cells (Figure 12A). Because the lactate dehydrogenase reaction is regulated by cytosolic NAD⁺/NADH ratio, the pyruvate/lactate ratio is sometimes used as a proxy for this ratio (Christensen et al., 2014; Williamson et al., 1967). We observed that the pyruvate/lactate ratio of AGC1-KD C2C12 cells is lower than controls, suggesting that MAS is indeed disrupted in these cells and effectively impaired cytosolic NAD⁺/NADH ratio. In order to verify that AGC1-KD leads to similar metabolic changes in transformed cells, we measured NAD⁺/NADH

RESULTS

and Pyruvate/Lactate ratios in mouse Lewis lung carcinoma (LLC1) cells. In consistence with the observations from C2C12 cells, AGC1-KD LLC1 cells have reduced NAD⁺/NADH and pyruvate/lactate ratios compared to controls (Figure 12C-D). This suggests that AGC1 regulates cellular and cytosolic NAD⁺/NADH ratio of proliferating cells. In addition, knockdown AGC1-KD also lowered the basal mitochondrial oxygen consumption rate without having a significant impact on the mitochondrial number, surface area or volume (Figure 13). Reduced mitochondrial respiration is consistent with the expected increase in mitochondrial NAD⁺/NADH ratio following MAS inhibition. GC-MS analysis showed that in both C2C12 and LLC1 AGC1-KD cells, aspartate levels were reduced compared to control cells in consistence with impaired cytosolic NAD⁺/NADH ratio (Figure 14) (Birsoy et al., 2015). In addition, asparagine levels were also significantly lower in AGC1-KD cells. Because asparagine is not found in DMEM and conversion of aspartate to asparagine is mediated by the cytosolic enzyme asparagine synthetase (Asns) (Ahn and Metallo, 2015), this finding suggests that cytosolic aspartate levels are also lower in AGC1-KD cells.

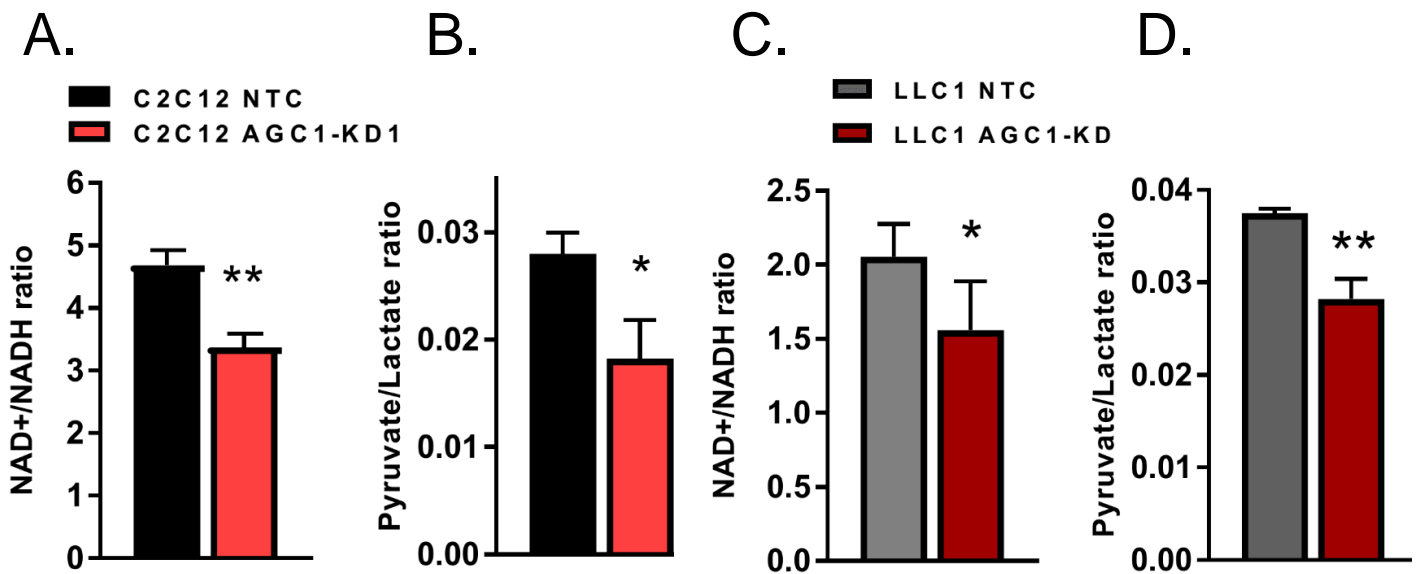


Figure 12: AGC1 knockdown decreases cellular and cytosolic NAD⁺/NADH ratio (A) NAD⁺/NADH ratio of control (NTC) and AGC1-KD1 C2C12 cells cultured in pyruvate free DMEM (n=5), Mean ± SEMs are shown. (B) Pyruvate to lactate ratio of control (NTC) and AGC1-KD1 C2C12 cells cultured in pyruvate-free media (n=3). C) (A) NAD⁺/NADH ratio of control (NTC) and AGC1-KD1 LLC1 cells cultured in pyruvate free DMEM (n=5) D) Pyruvate to lactate ratio of control (NTC) and AGC1-KD1 LLC1 cells cultured in pyruvate-free media (n=3). SDs and SEMs are shown for Pyruvate/Lactate and NAD⁺/NADH ratios, respectively.

RESULTS

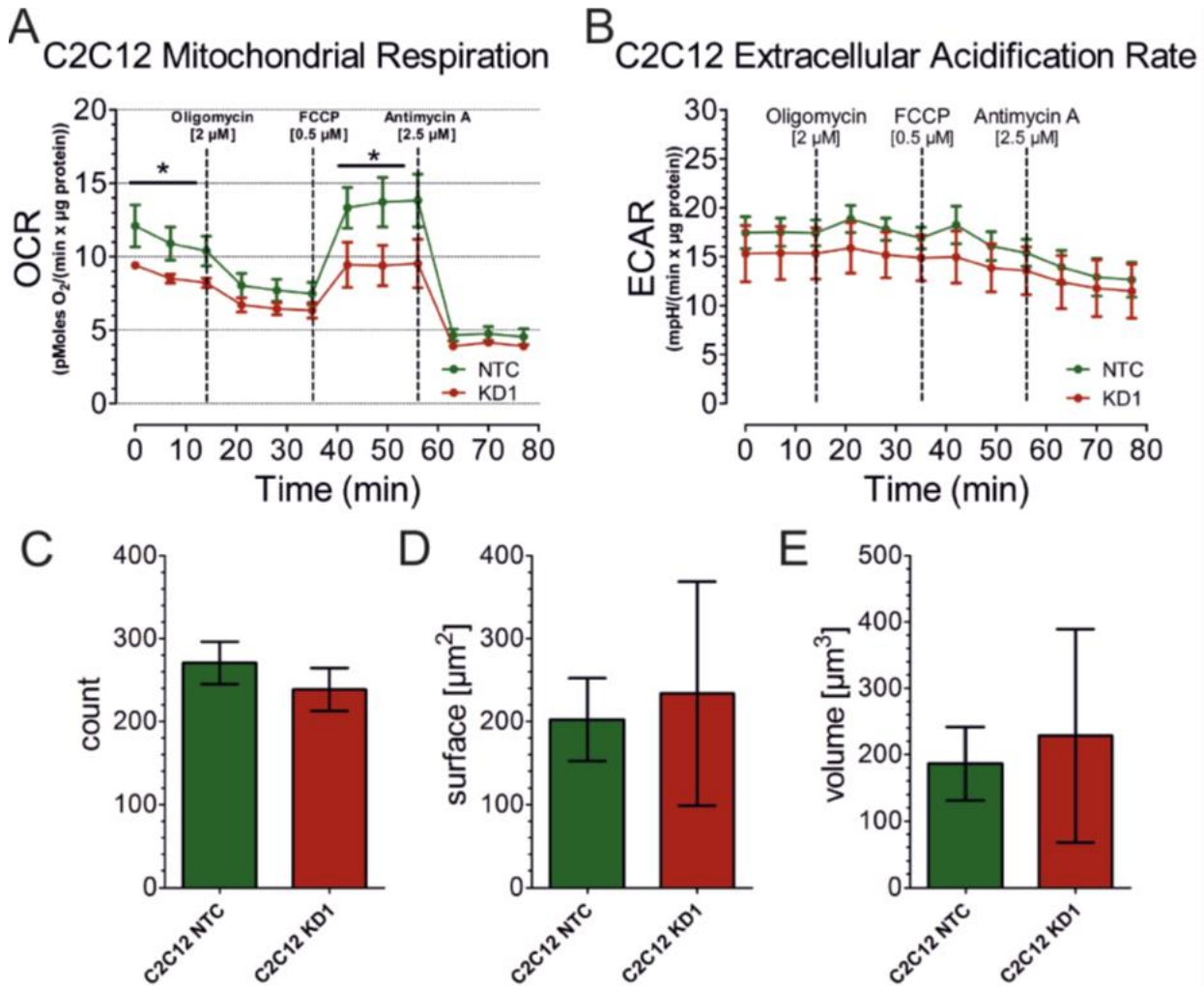


Figure 13: AGC1 knockdown decreases basal mitochondrial oxygen consumption rate (A) Basal and maximal oxygen consumption rate was reduced in AGC1 KD C2C12 cells (n=3) while (B) there was no difference in extracellular acidification rate. (C, D, E) Mitochondrial number, surface area, and volume was not altered in AGC1 KD C2C12 cells (n=3). Standard deviations are shown.

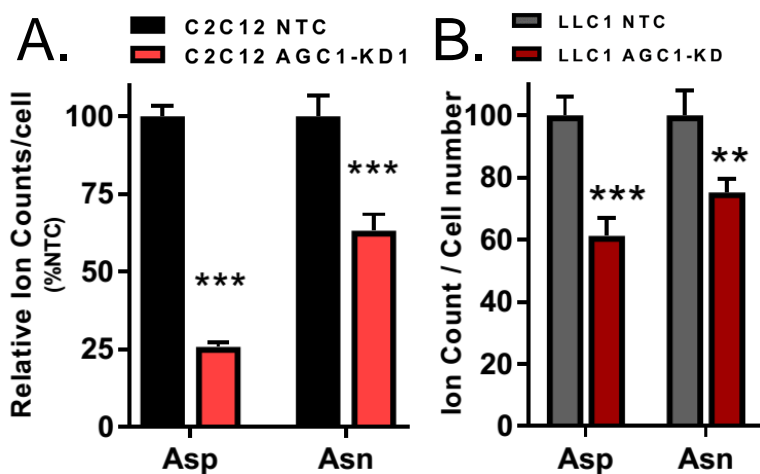


Figure 14: AGC1-KD reduced aspartate and asparagine levels. Relative cellular aspartate and asparagine levels of control (NTC) and AGC1-KD1 C2C12 and LLC1 cells cultured in standard DMEM without pyruvate (n=3). Standard deviations are shown.

RESULTS

Next, we verified that the metabolic changes upon AGC1-KD via sh911 construct are not due to off-target effects by analyzing knockdowns mediated by two other shRNAs and also via transiently overexpressing mouse AGC1. Opposite to what was observed in AGC1-KD, increased AGC1 expression in C2C12 cells slightly promoted cell proliferation and increased the cellular NAD⁺/NADH ratio and aspartate levels (Figure 15). In addition, NMR analysis from two other AGC1-knockdowns and one other non-targeting controls showed a comparable reduction in aspartate and asparagine levels (Figure 16), suggesting that off-target effects of shRNA-mediated knockdown of AGC1 could be neglected with regard to metabolic changes.

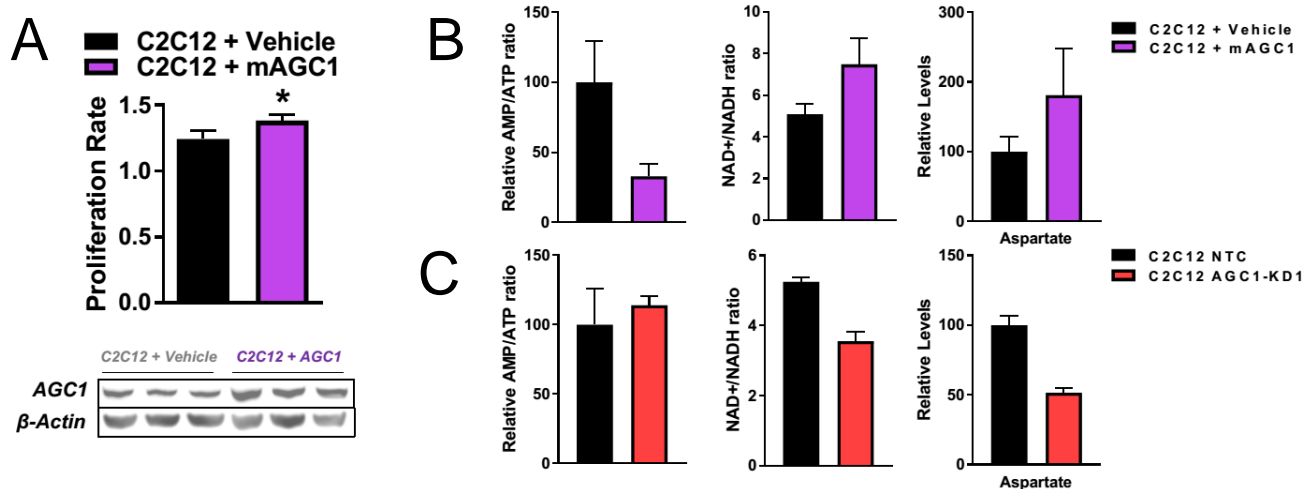


Figure 15: AGC1 overexpression increased proliferation rate, NAD⁺/NADH ratio and aspartate levels in C2C12 cells (A) (Top) Proliferation rate of control (C2C12 + Vehicle) and AGC1-overexpressing (C2C12 + mAGC1) C2C12 cells in pyruvate-free media. Final cell counts were normalized to the initial cell number before transfection (n=3). (Bottom) AGC1 protein expression by Western blot with beta-actin expression shown as a loading control. (B-C) NMR measurements of AMP/ATP ratio, NAD⁺/NADH ratio and Aspartate levels in C2C12 cells that (H) transiently overexpressed mouse AGC1 (as in A) or (C) had stable knockdown of AGC1 (n=3). Error bars represent standard deviations.

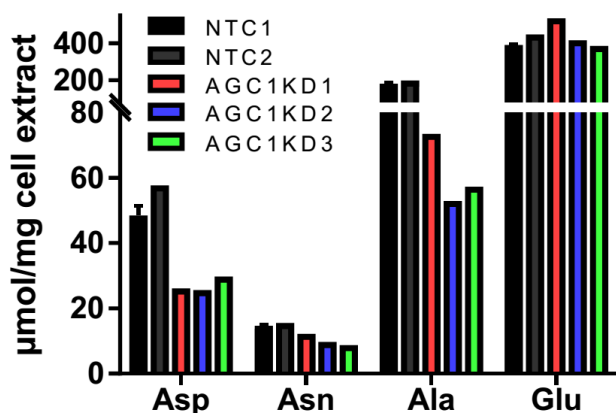


Figure 16: AGC1-knockdown reduced cellular aspartate levels. NMR measurements of aspartate (Asp), asparagine (Asn), alanine (Ala), and glutamate (Glu) levels in C2C12 cells that individually express 2 independent non-targeting shRNA controls (NTC1 and NTC2) or 3 independent shRNAs targeting mouse AGC1 (KD1, KD2 or KD3). n=2 for NTC1, n=1 for all other conditions.

3.4 AGC1-knockdown increased cellular dependence on exogenous glutamine

Because anti-proliferative effects of AGC1-knockdown is more negligible than we initially expected, we hypothesized that cells lacking AGC1 might be sustaining proliferation by rewiring metabolism and by obtaining cytosolic aspartate using a different source. In order to investigate this idea, we systematically depleted the media from glucose and select amino-acids and evaluated how these changes influenced cell proliferation in AGC1-knockdown cells. Low glucose conditions (0.5mM, instead of 25mM contained in regular DMEM) or treatment with glycolysis inhibitor 2-deoxyglucose (2-DG) did not affect proliferation or survival of AGC1-KD cells substantially differently than control cells (Figure 17A). On the other hand, AGC1-KD cells showed significantly poorer ability to survive compared to control cells in Hanks' Buffered Salt Solution (HBSS) that contains 5.5mM glucose but lacks amino acids (Figure 17B). Supplementing HBSS with essential amino acids did not rescue this phenotype, but the addition of essential amino acids together with glutamine improved the survival and proliferation of AGC1-KD cells to the same degree as control cells (Figure 17B). To further test whether the loss of AGC1 impacts the cellular dependence on glutamine, we left cells to proliferate in DMEM-based low-glutamine media (0.1mM instead of 4mM). Low glutamine levels impair cell proliferation in control cells as previously reported (reviewed in Wise and Thompson, 2010). However, the impact of glutamine-depletion on cell proliferation was significantly stronger in AGC1-KD cells (Figure 17C), so much so that final cell numbers after low-glutamine treatment were lower than initial cell numbers, suggesting that cell survival was also compromised in low glutamine conditions. Annexin V/propidium iodide (PI) staining demonstrated that dead and apoptotic cell ratio is increased upon glutamine depletion (0.1mM) in both control and AGC1-KD cells (Figure 17E). Remarkably, AGC1-KD also caused some level of cell death in 4mM glutamine conditions and glutamine starvation (0.1mM) further exacerbated this phenotype (Figure 17E). Moreover, cleaved caspase 3 levels, a marker of apoptotic cells, was increased in low glutamine conditions, suggesting that glutamine starvation promotes cell death in AGC1-KD cells (Figure 17F).

Glutamine has various roles in cells based on different paths it can take. Some of the major fates of glutamine include being exchanged by plasma membrane transporters for importing other amino acids (Pochini et al., 2014), donating its amide nitrogen for nucleotide biosynthesis (Cory and Cory, 2006), or replenishing TCA cycle carbons (anaplerosis) by being converted to α -ketoglutarate (α -KG, also known as 2-oxoglutarate) (Wise and Thompson, 2010) (Figure 17D). In order to narrow down which particular function of glutamine is explicitly important for the proliferation and survival of AGC1-KD cells, we limited glutamine anaplerosis using glutaminase inhibitor CB-839 that blocks glutamine to glutamate conversion. Remarkably, CB-839 treatment phenocopies the effects of low-glutamine on AGC1-KD cells (Figure

RESULTS

17C). These data collectively suggest that AGC1-KD cells need glutamine anaplerosis for survival, rather than for other downstream reactions that do not require glutaminase activity.

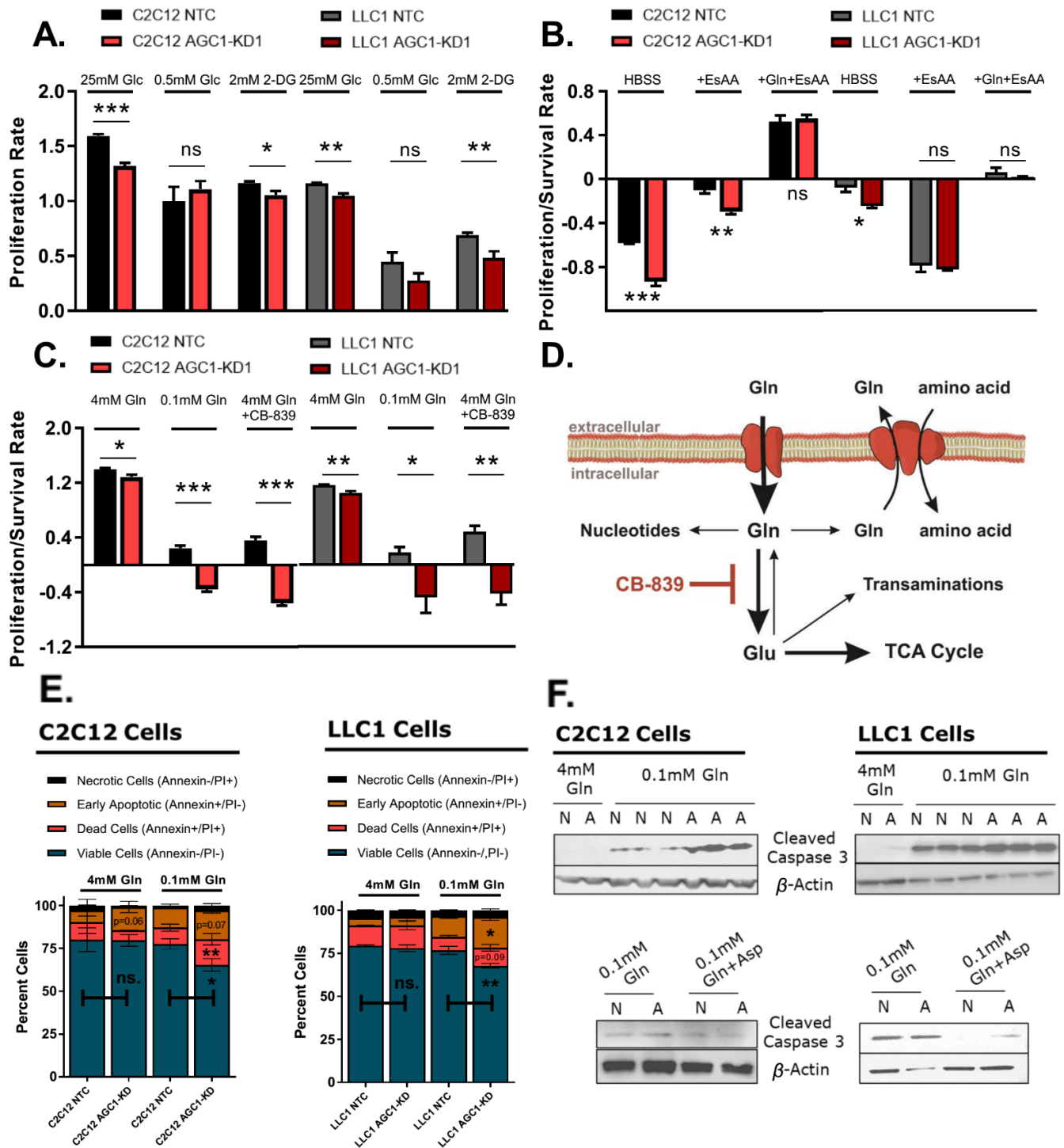


Figure 17: AGC1-knockdown cells depend on glutamine for survival. (A) The proliferation rate of C2C12 and LLC1 cells with or without AGC1-knockdown in pyruvate-free DMEM with either 25mM glucose, 0.5mM glucose (Glc), or 25mM glucose with 2mM 2-deoxyglucose (2-DG), as indicated (n=5). (B)

RESULTS

Proliferation/survival rate of C2C12 and LLC1 cells in pyruvate-free 5mM glucose HBSS (with 10% FBS and vitamins) containing either essential amino acids (EsAA) and or glutamine (Gln) as indicated (n=3). (C) Proliferation/survival rate of C2C12 and LLC1 cells in pyruvate-free DMEM containing either 4mM glutamine, 0.1mM glutamine (Gln), or 4mM glutamine with 1 μ M CB-839 (glutaminase inhibitor) as indicated (n=5). (D) Schematic demonstration of some potential fates of glutamine in a cell. (E) The percent annexin V and/or propidium iodide (PI) positive control (NTC) and AGC1-KD C2C12 and LLC1 cells cultured for 24h in 4mM glutamine or 0.1mM glutamine as indicated was determined by flow cytometry as shown (n=3) SDs are shown. (F) Cleaved caspase 3 protein expression as determined by Western Blot in control (N) or AGC1-knockdown (A) C2C12 and LLC1 cells cultured for 24h in the presence of 4mM glutamine or 0.1mM glutamine without or with 10mM aspartate as indicated is shown. the β -actin expression is also shown as a loading control. Data are representative of n=3 experiments. SEMs are shown unless indicated otherwise.

3.5 Glutamine dependence in AGC1-KD cells is not due to change in anaplerosis source

Because malate-aspartate shuttle can indirectly support redirecting glycolysis-derived pyruvate from lactate production to TCA cycle anaplerosis, we hypothesized that increased vulnerability of AGC1-knockdown cells to glutaminase inhibition might be due to a reduction of utilizing glucose for oxidative phosphorylation. In order to investigate this hypothesis, we measured the oxygen consumption of C2C12 cells after 6 hours of CB-839 treatment. Remarkably, CB-839 treatment reduced the mitochondrial oxygen consumption to 50% of untreated levels of corresponding AGC1-KD and control cells, suggesting that mitochondrial respiration requires proportionally comparable levels of glutamine in both cells (Figure 18A). Glucose uptake and consumption rates were also unchanged in AGC1-KD cells, compared to controls (Figure 18B). Interestingly, glutamate release was slightly elevated in AGC1-KD C2C12 cells, compared to controls (Figure 18C). However, only a small fraction of the consumed glutamine could be responsible for the excreted glutamate. This suggests that increased glutamate excretion is not the sole cause of glutamine dependency of AGC1-KD cells, but could rather be a side-effect of increased cytosolic glutamate levels upon loss of AGC1. In order to test this hypothesis, we inhibited plasma membrane glutamate exporter xCT (Slc7a11) (Dixon et al., 2014) using Erastin and demonstrated that Erastin inhibition has no specific impact on glutaminase-inhibited AGC1-KD cells (Figure 18D, E).

RESULTS

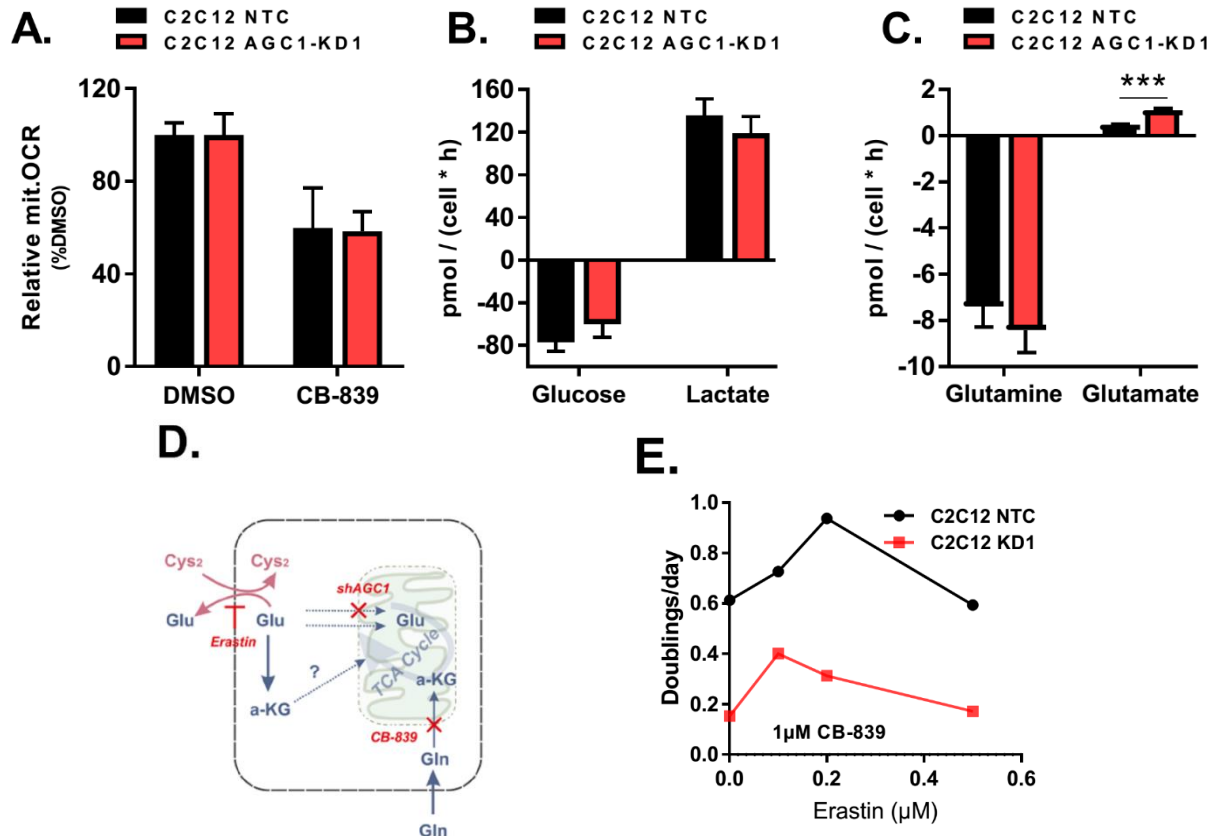
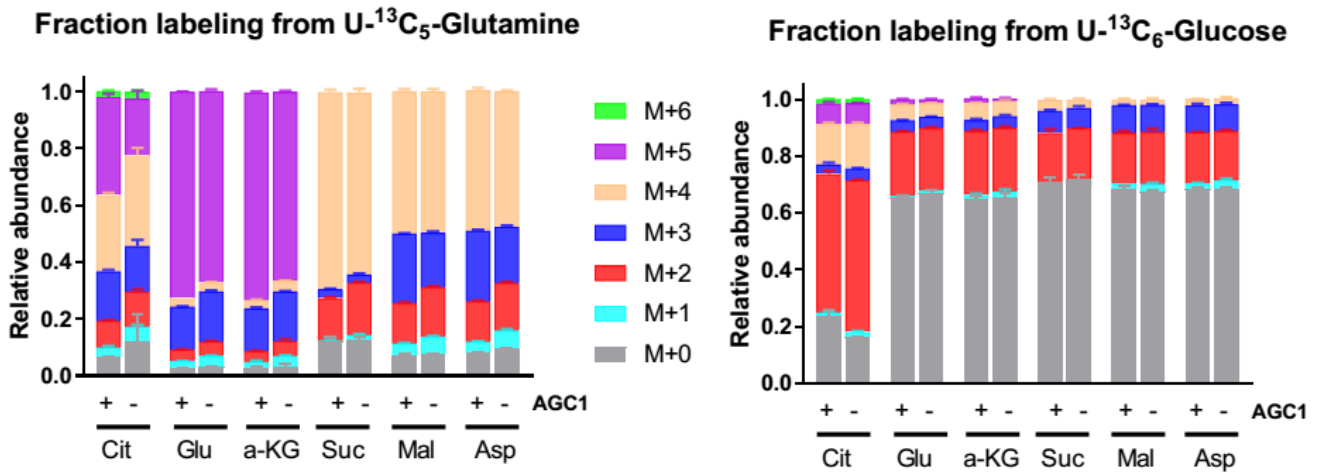


Figure 18: AGC1-knockdown cells do not consume more glucose or glutamine. (A) Relative mitochondrial oxygen consumption rate (mit.OCR) of control (NTC) and AGC1-KD1 C2C12 cells cultured for 6 hours in pyruvate-free DMEM containing 4mM glutamine with or without CB-839 (n=5), data normalized to percent change compared to DMSO treatments of each group, mean \pm SEMs are shown. (B-C) Glucose, lactate, glutamine, and glutamate uptake/consumption rate of control (NTC) and AGC1KD C2C12 cells cultured in pyruvate-free DMEM for 48h (n=3); mean \pm SDs are shown. (D) Schematic showing how Erastin inhibits glutamate export. (E) The proliferation rate of control (NTC) or AGC1-knockdown (KD1) C2C12 cells cultured in 1µM CB-839 and with varying concentrations of Erastin (n=1).

The changes in the cellular NAD⁺/NADH ratio upon hypoxia or mitochondrial dysfunction promote reductive glutamine metabolism (Metallo et al., 2011; Mullen et al., 2014; Mullen et al., 2011; Sullivan et al., 2015). To investigate whether AGC1-KD cells choose the metabolize glucose or glutamine differently, we traced [U¹³C]glucose or [U¹³C]glutamine into TCA cycle metabolites and amino acids using GC-MS. At the steady-state, there were no major changes in labeling from either carbon source. More specifically, glutamine is the major source of aspartate and other TCA intermediates in both AGC1-KD and control cells and the relative contributions of glucose and glutamine to the TCA cycle are not remarkably altered in AGC1-KD cells (Figure 19).

C2C12



LLC1

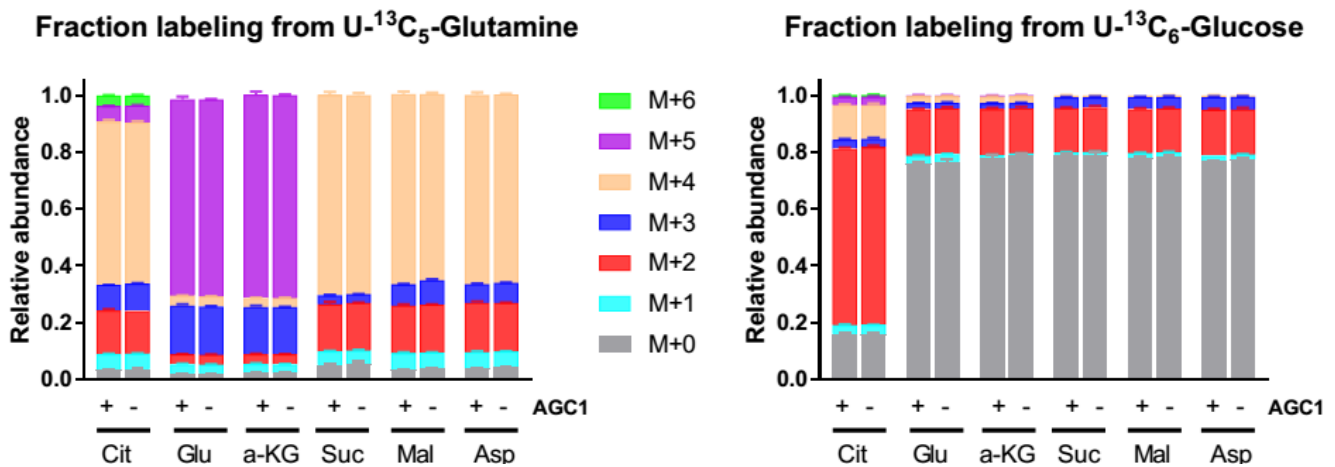


Figure 19: Glutamine is the predominant source of the TCA cycle in both AGC1-knockdown and control cells. Steady-state labeling of the glucose and glutamine when C2C12 or LLC1 cells without (+) or with (-) AGC1 knockdown are cultured for 24 hours in the presence of [¹³C]glutamine or [¹³C]glucose as noted (aspartate (Asp), citrate (Cit), glutamate (Glu), alpha-ketoglutarate (a-KG), malate (Mal), and succinate (Suc)) (n=3). The fraction of each metabolite with varying isotopomers is shown. Error bars represent standard deviations.

RESULTS

Interestingly, M+3 aspartate and M+5 citrate fractions from labeled glutamine were lower in AGC1-KD C2C12 cells (Figure 20A, 20B), suggesting a more oxidative TCA cycle path. Consistently, M+3 species of glutamate and α -KG are increased while M+5 species are decreased in AGC1-KD C2C12 cells without any significant changes in unlabeled (M+0) species (Figure 20C, 20D). These labeling patterns are in alignment with increased mitochondrial NAD⁺/NADH ratio promoting oxidative TCA cycling in AGC1-KD C2C12 cells (Figure 20E). Further supporting this interpretation, ¹⁴C-CO₂ release from [U¹⁴C]glutamine was significantly higher in AGC1-KD C2C12 cells, compared to controls (Figure 20E, 2F). However, unlike C2C12 cells, this decreased reductive carboxylation phenomenon was not present in LLC1 cells with AGC1 knockdown (Figure 19), arguing that changes in reductive carboxylation cannot be the universal cause of why AGC1-KD cells are sensitive to glutamine deprivation. Taken together, these findings suggest that, even though slight changes are observed in oxidative and reductive TCA pathways, overall glutamine utilization is not immensely altered in AGC1-KD cells, and glutamine remains the predominant source for aspartate independent of AGC1 expression.

It is also worth noting that, despite sources of those metabolites are unchanged, intracellular levels of several key metabolites, including non-essential amino acids and TCA cycle intermediates, were reduced in AGC1-KD cells (Figure 21). This indicates that AGC1-KD cells are still suffering from a metabolic deficiency, however that is not due to a change of the anaplerosis source they prefer.

RESULTS

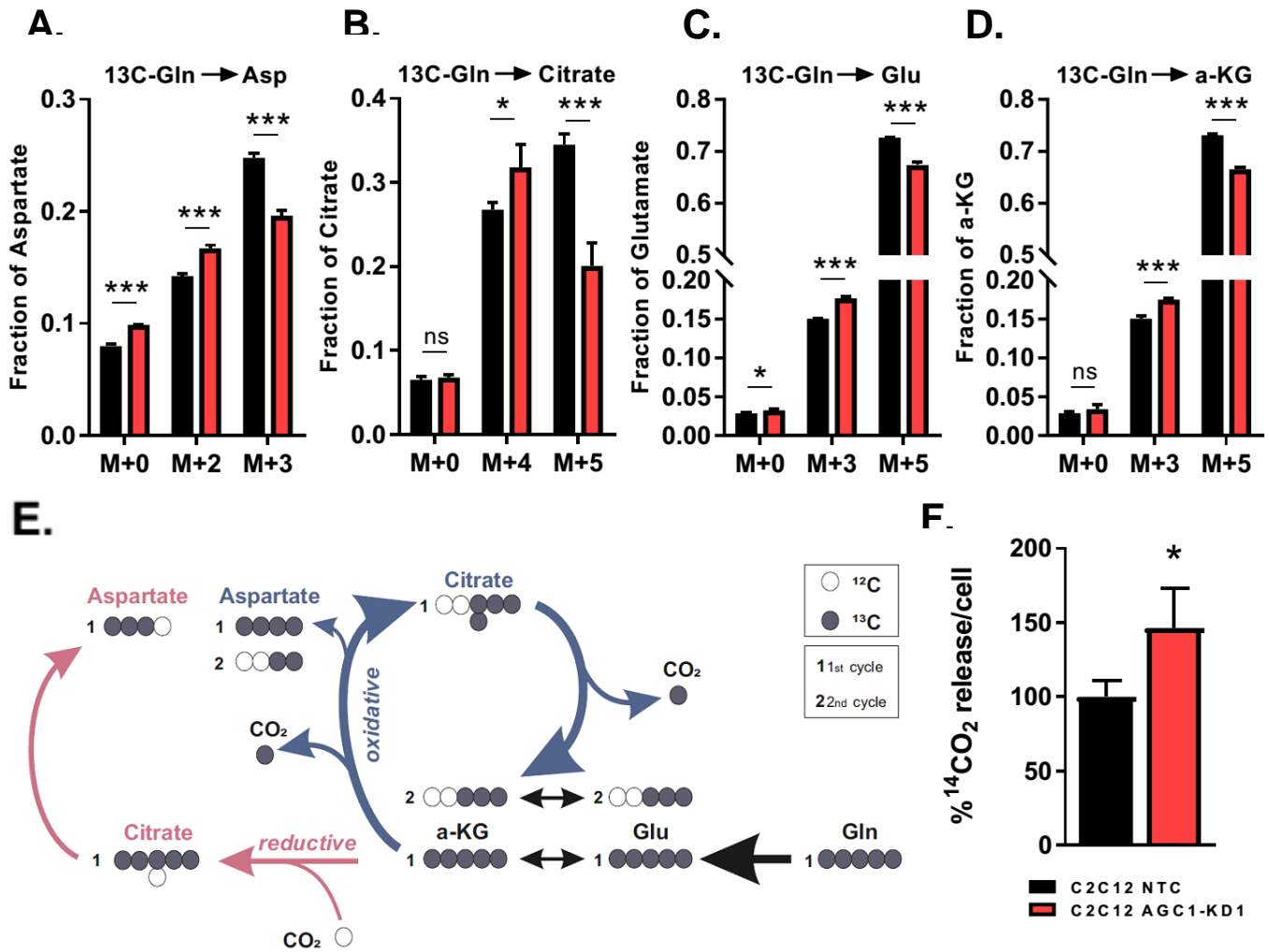


Figure 20: AGC1-knockdown C2C12 cells have increased oxidative TCA cycling. (A-D) Fractional labeling of aspartate (Asp), citrate, glutamate (Glu) and alpha-ketoglutarate (α -KG) after culturing of C2C12 control (black) or C2C12 AGC1-KD1 (red) cells in media containing [^{13}C]glutamine (Gln) for 24hours (n=3). This panel is a close-up to Figure 19 to highlight important changes of certain isotopomers relevant to the hypothesis. (E) Schematic overview of oxidative and reductive glutamine catabolism demonstrating how carbons from glutamine (Gln) label glutamate (Glu), α -ketoglutarate (a-KG) and the other indicated metabolites. (F) Relative $^{14}\text{CO}_2$ release from control (NTC) and AGC1-KD C2C12 cells cultured in media containing [^{14}C]-Glutamine for 1 hour (n=3). All figures show the mean \pm SD. * $p \leq 0.05$, ** $p \leq 0.01$, *** $p \leq 0.001$.

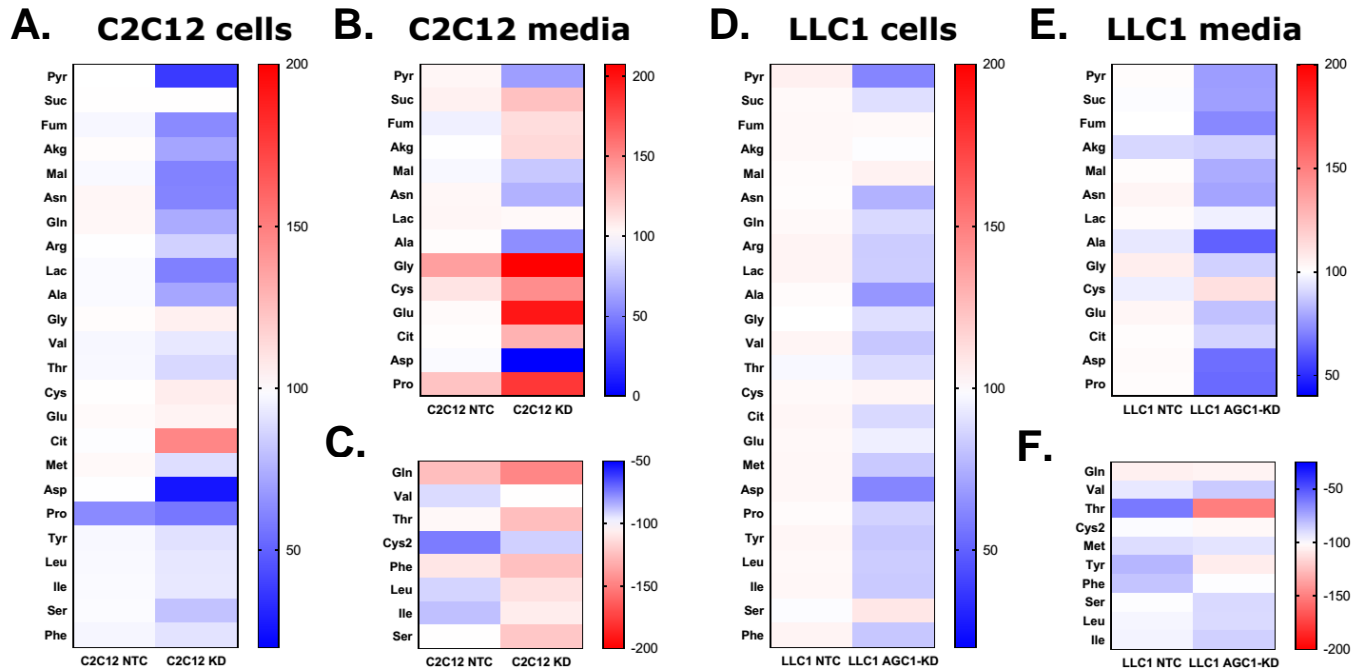


Figure 21: Changes of intracellular and media levels of several metabolites in AGC1-knockdown cells. (A, D) Heatmap showing relative total pool sizes of the indicated metabolites when control (NTC) or AGC1-knockdown (KD) (A) C2C12 and (D) LLC1 cells are cultured in full DMEM-Pyr media for 24h. Data were normalized to cell number and the median relative change compared to NTC are shown (n=3). (B, E) Heatmap showing relative levels of the indicated metabolite that increase in media after control (NTC) or AGC1-knockdown (B) C2C12 and (E) LLC1 cells are cultured in full DMEM-Pyr for 24 hours. Data normalized to cell number; median relative changes compared to NTC are shown (n=3). (C, F) Heatmap showing relative levels of the indicated metabolites that decreased in media when control (NTC) or AGC1-knockdown (J) C2C12 and (M) LLC1 cells are cultured in full DMEM-Pyr for 24 hours. Data normalized to cell number; median relative changes compared to NTC are shown (n=3).

3.6 AGC1-KD cells are unable to preserve cytosolic aspartate levels, causing cell death upon glutamine-deprivation

Maintaining cytosolic aspartate levels with aspartate production by the reverse function of cytosolic glutamate-oxaloacetate transaminase 1 (GOT1) is shown to be essential for cell survival when mitochondrial respiration is impaired (Birsoy et al., 2015). Therefore, we hypothesized that mitochondrial export of aspartate into the cytosol by AGC1 might be explicitly important to survive glutamine deprivation. Confirming this hypothesis, AGC1 protein expression is increased following glutamine limitation, implying a higher need for funneling mitochondrial aspartate into cytosol when anaplerosis source is missing (Figure 22A). Because glutamine withdrawal might plummet mitochondrial aspartate levels, we hypothesized that such low levels of aspartate may not be sufficient to activate other mitochondrial

RESULTS

transporters and cells upregulate AGC1 expression as a coping mechanism (Figure 22B). To investigate this, we supplemented cells with exogenous aspartate in low glutamine conditions. Remarkably, 5mM aspartate treatment rescues viability and proliferation of AGC1-KD cells during glutamine limitations (Figure 23A). Because aspartate is poorly permeable, non-physiological aspartate concentrations (5-20mM) are needed to deliver aspartate into the cells (Garcia-Bermudez et al, 2018; Sullivan et. al., 2018). However, expressing the plasma membrane aspartate transporter (SLC1A3) allowed 150 μ M aspartate (RPMI levels) to sufficiently rescue proliferation/survival in glutamine limitation (Figure 23B), suggesting that cytosolic aspartate delivery can be limiting for AGC1-KD cells.

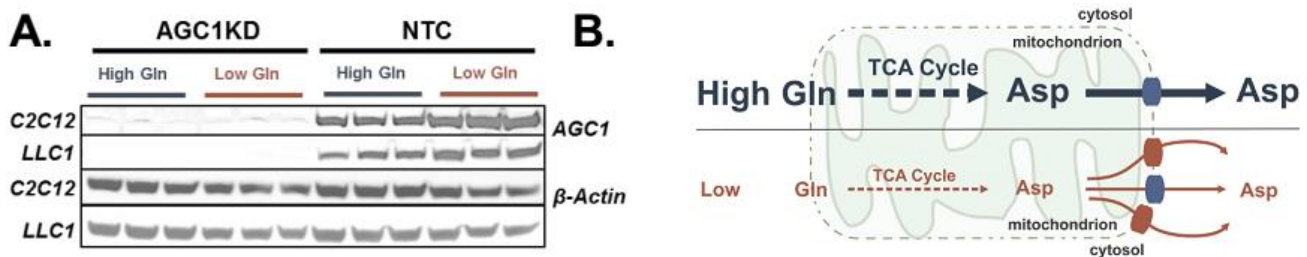


Figure 22: AGC1 protein expression is increased in low glutamine conditions. (A) Western blot analysis of AGC1 protein expression in whole-cell lysates (40 μ g/lane) from AGC1-knockdown (AGC1KD) or control (NTC) C2C12 or LLC1 cultured in DMEM with 10% FBS and 4mM glutamine (High Gln) or 0.1mM glutamine (Low Gln) for 24h as indicated. (B) Schematic depicting how low glutamine might lead to reduced cytosolic aspartate delivery and increased aspartate transporter expression.

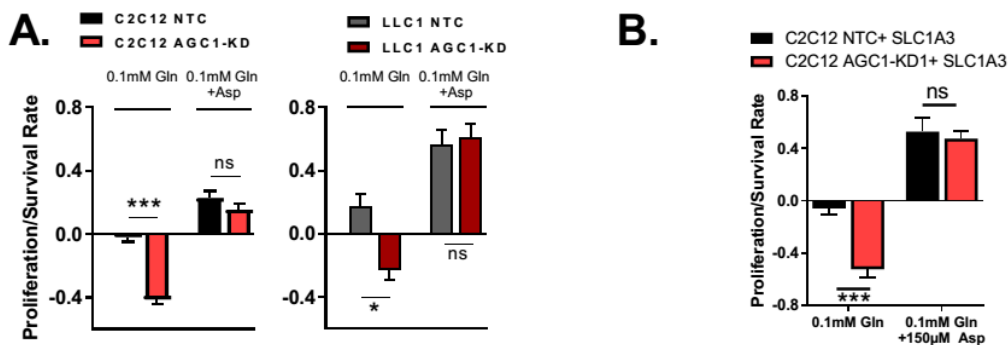


Figure 23: Aspartate supplementation recovers the viability and proliferation of AGC1-knockdown cells in glutamine limitations. (A) Survival/proliferation rate of control (NTC) and AGC1-knockdown (AGC1-KD) C2C12 cells cultured in pyruvate-free DMEM containing 0.1mM glutamine in the presence and absence of 5mM aspartate as indicated (n=3), mean \pm SEM. (B) Survival/proliferation rate of control (NTC) and ACG1-KD C2C12 cells expressing the plasma membrane aspartate transporter SLC1A3 cultured in pyruvate-free DMEM containing 0.1mM glutamine in the presence and absence of 0.15mM aspartate as indicated (n=3), mean \pm SD.

RESULTS

Afterward, we wanted to test whether the glutamine dependence of cells with AGC1 loss and the ability of aspartate to rescue this phenomenon is universal. Therefore, we knocked-down AGC1 in one other mouse cell line (AL1376 mouse pancreas adenocarcinoma cell line, see methods) and five human cell lines, including two lung adenocarcinoma (A549, H1299) and two pancreas adenocarcinoma (PANC1, CAPAN2) cell lines. Although each cell line showed varying sensitivities to glutamine deprivation and glutaminase inhibition, AGC1 loss exacerbated this sensitivity while aspartate supplementation consistently improved proliferation and/or survival (Figure 24).

In addition, we knocked-out AGC1 using the CRISPR/Cas9 system to investigate the effects of the total loss of AGC1. Knock-out of AGC1 (AGC1-KO) leads to comparable sensitivity to glutamine starvation or glutaminase inhibition in C2C12 cells (Figure 25). Similar to shRNA knockdowns, AGC1-KO cells exhibited reduced levels of aspartate and pyruvate/lactate ratio (Figure 26). Even though we failed to achieve total knockout, CRISPR/Cas9 blocking of AGC1 in LLC1 cells showed almost identical effects to those observed in C2C12 cells and with shRNA experiments (Figure 25). Interestingly, the total ablation of AGC1 also did not completely block proliferation in glutamine-replete media, suggesting that some cytosolic aspartate delivery is sustained by AGC2 or other mitochondrial transporters when glutamine is present.

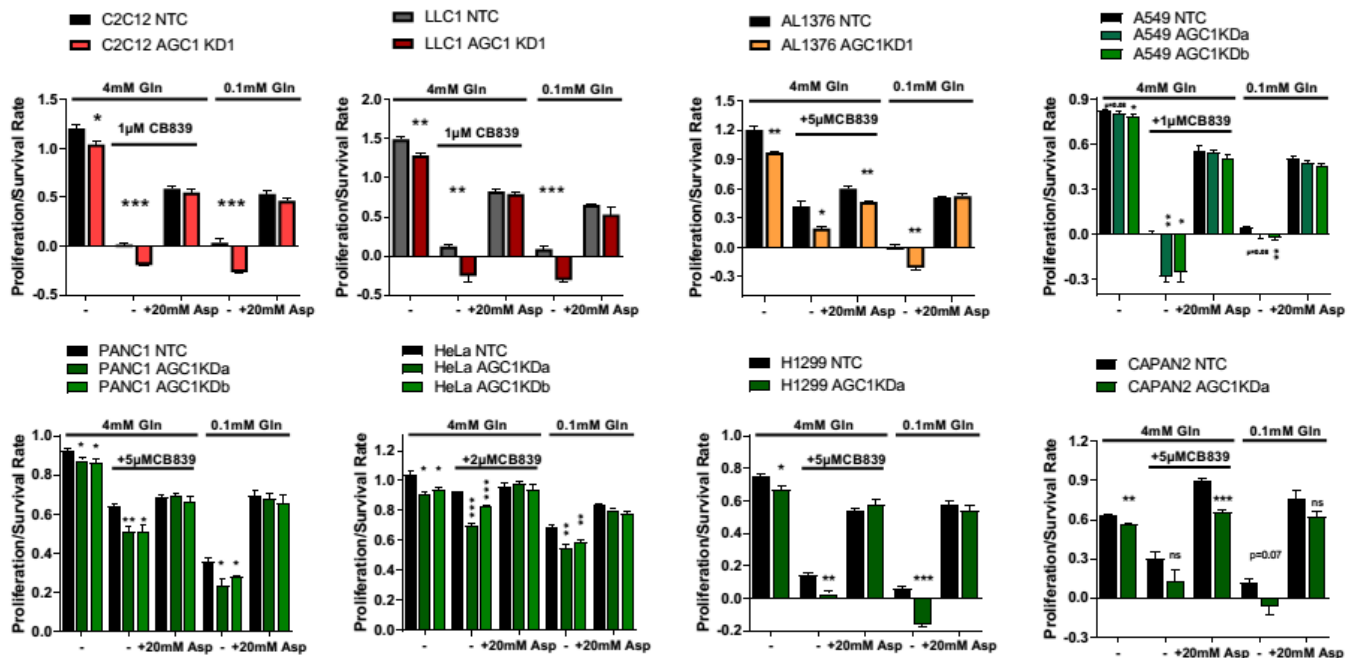


Figure 24: Proliferation/survival rate of eight different cell lines with AGC1-knockdown in glutamine limiting conditions. Proliferation/survival rate of control (NTC) and AGC1KD C2C12, LLC1, AL1376, A549, PANC1, HeLa, H1299 and CAPAN2 cells cultured in pyruvate-free DMEM containing 4mM or 0.1mM glutamine (Gln), or 4mM glutamine with CB839 at the specified concentrations in the presence or absence of 20mM aspartate (Asp) as indicated (n=3), mean \pm SEM. * $p \leq 0.05$, ** $p \leq 0.01$, *** $p \leq 0.001$.

RESULTS

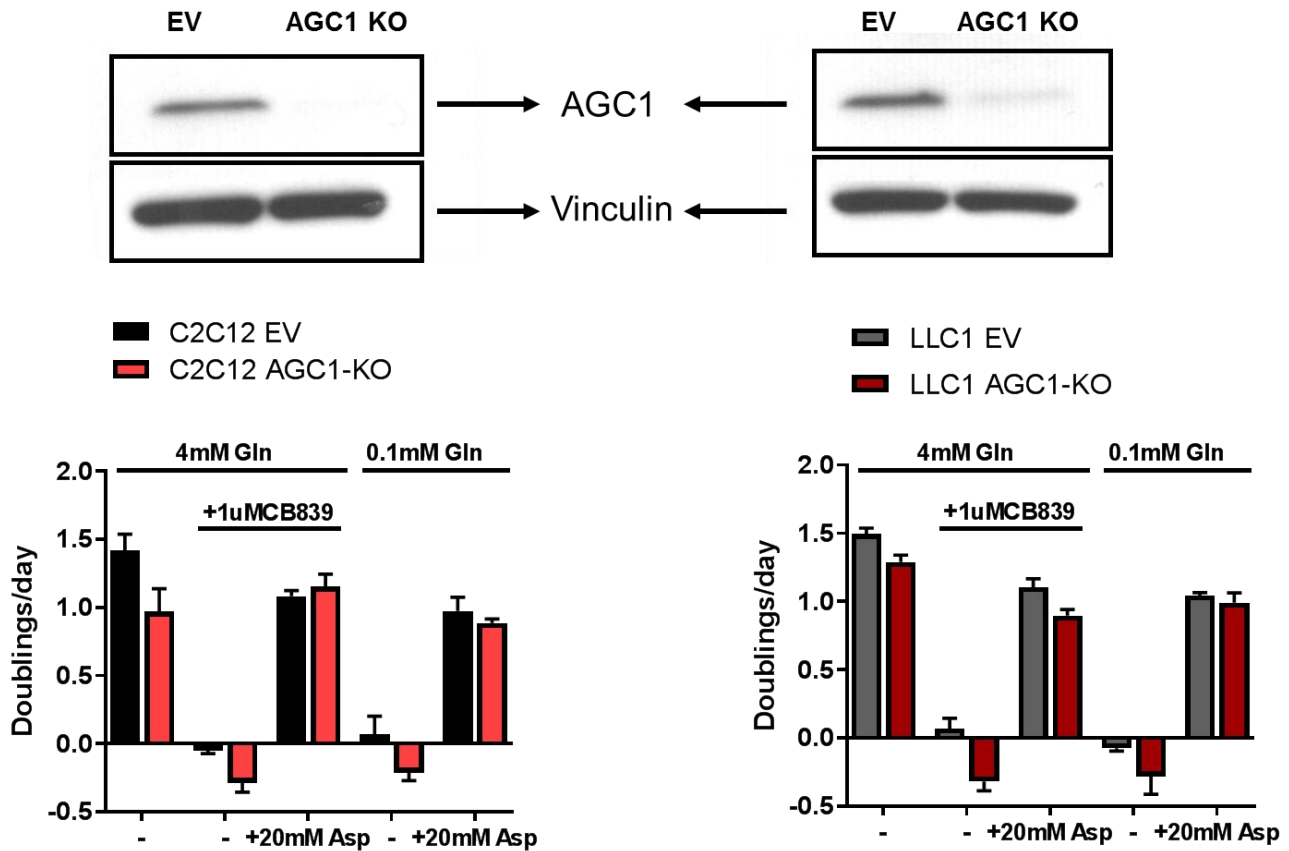


Figure 25: Proliferation/survival rate of AGC1-KO C2C12 and LLC1 cells. (Top) AGC1 protein expression as determined by Western blot (with Vinculin expression as a loading control). Survival/proliferation rate of control (EV) and CRISPR/Cas9-mediated AGC1 deleted (AGC1 KO) (Right) C2C12 and (Left) LLC1 cells cultured in indicated levels of glutamine (Gln), CB-839, and/or aspartate (Asp). All panels show mean \pm SDs.

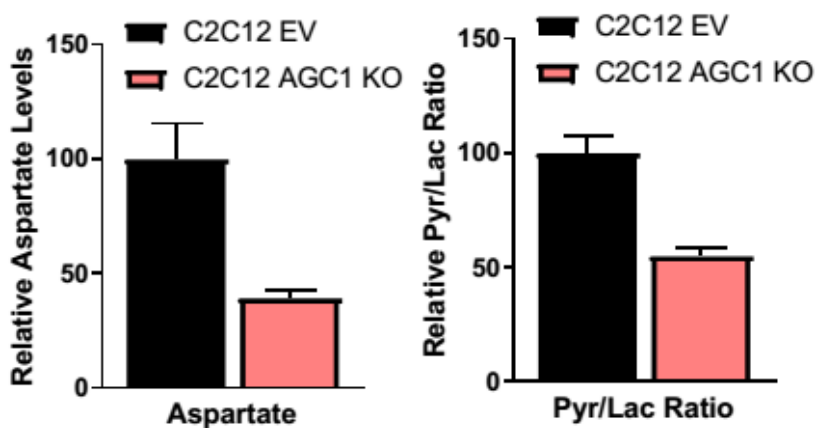


Figure 26: Aspartate levels and pyruvate/lactate ratio in AGC1-KO C2C12 cells. GCMS-measured (Right) aspartate levels and (Left) pyruvate/lactate (Pyr/Lac) ratio of control (EV) and CRISPR/Cas9-mediated AGC1 deleted C2C12 cells as indicated (n=3). All panels show mean \pm SDs.

3.7 High mitochondrial aspartate levels are required for AGC1-KD cells to activate aspartate export and maintain cytosolic aspartate levels

We next speculated that AGC1-KD cells need higher mitochondrial aspartate levels to sustain adequate amounts of aspartate delivery to the cytosol. Thus, we tested whether AGC1-deficient cells are also sensitive to other manipulations that plummet mitochondrial aspartate levels. For instance, metformin inhibits mitochondrial aspartate synthesis by blocking mitochondrial complex I and consequently reducing the NAD⁺/NADH ratio (Sullivan et al., 2015) (Figure 27A), and AGC1-KD cells are more vulnerable to metformin treatment than control cells (Figure 27B). Moreover, other anaplerotic carbon sources might maintain mitochondrial aspartate synthesis (Figure 27A), and both supplementation of dimethylalpha-ketoglutarate (daKG) and pyruvate recover proliferation/survival of AGC1-KD cells in low-glutamine and glutaminase-inhibited conditions (Figure 27C) and also boost aspartate levels (Figure 27D). These results imply that, in control cells, blocking glutamine anaplerosis for aspartate synthesis diminishes mitochondrial and cytosolic aspartate levels and restrict cell proliferation. On the other hand, in AGC1-deficient cells, the failure to export residual aspartate from mitochondria further decreases cytosolic aspartate and this compromises cell proliferation and cell survival (Figure 27E).

RESULTS

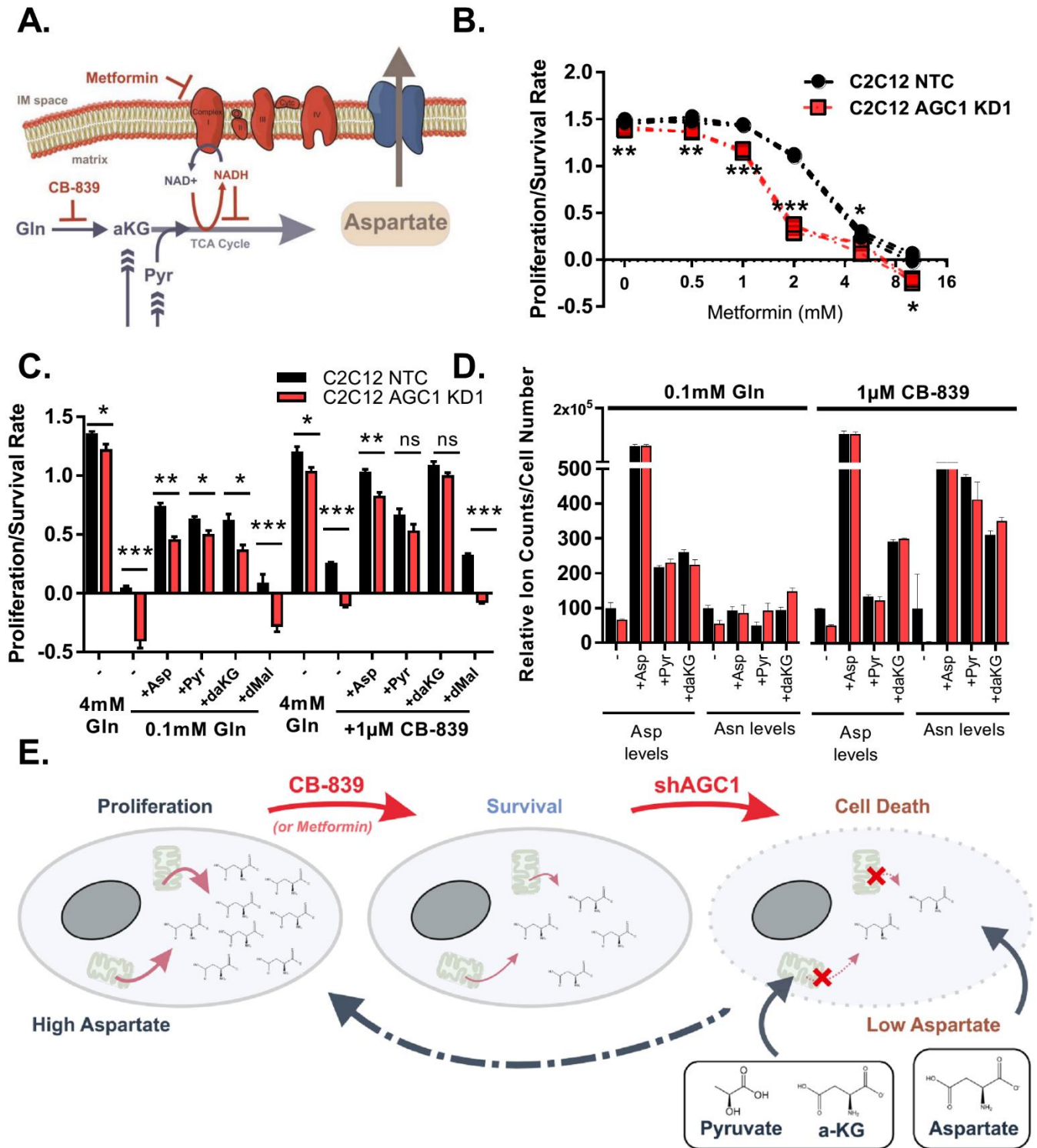


Figure 27: Sustaining cytosolic aspartate levels prevents cell death in glutamine limiting conditions. (A) Schematic demonstration of how glutamine and alternative anaplerotic substrates can feed the TCA cycle and sustain mitochondrial aspartate production. How CB-839-mediated blockage of glutaminase, and metformin inhibition of NAD⁺ regeneration, affect TCA cycling is also shown. (B) Proliferation/survival rate of control (NTC) and AGC1-KD C2C12 cells treated with varying concentrations of

RESULTS

metformin in pyruvate-free DMEM (n=3). (C) Proliferation/survival rate of control (NTC) and AGC1-KD C2C12 cells cultured in 4mM or 0.1 mM glutamine, or 4mM glutamine with 1 μ M CB-839, in the presence or absence of 20mM aspartate (Asp), 2mM sodium pyruvate (Pyr), 2mM dimethyl- α -ketoglutarate (daKG) or 2mM dimethylmalate (dMal) as indicated (n=3). (D) Relative cellular aspartate and asparagine levels in control (NTC) and AGC1-KD C2C12 cells were cultured in 0.1mM glutamine or 4mM glutamine with 1 μ M CB-839 in the presence or absence of 20mM aspartate (Asp), 2mM sodium pyruvate (Pyr) or 2mM dimethyl- α -ketoglutarate (daKG) as indicated (n=3). (E) Schematic depicting a model for how changes in cytosolic aspartate levels might correlate with cell survival. All figures denote mean \pm SEMs unless indicated otherwise. * $p \leq 0.05$, ** $p \leq 0.01$, *** $p \leq 0.001$.

3.8 Cytosolic aspartate is not crucial for non-essential amino acids in low-glutamine

After verifying the recovering effects of aspartate, we aimed to understand which downstream pathways of aspartate are most crucial when glutamine is limiting. Aspartate is a proteinogenic amino acid and is involved in various metabolic processes beyond its use for protein synthesis. Some of those processes have already been declared to be associated with cell proliferation (Birsoy et al., 2015; Krall et al., 2016; Sullivan et al., 2015; Zand et al., 2016)(Figure 28A). For instance, cytosolic aspartate could be transaminated to donate nitrogen for non-essential amino acid (NEAA) synthesis while remaining four-carbon units could either enter back to mitochondria to feed the TCA cycle or regenerate NAD⁺ through the cytosolic part of the MAS. Apart from the fates involving transamination, aspartate is essential for asparagine production by accepting an amide nitrogen from glutamine, it is necessary for de novo synthesis of both purine and pyrimidine nucleotides, and it can be acetylated via Nat8l enzyme to produce N-acetylaspartate (NAA), a metabolite usually found in brain that is speculated to have roles beyond central nervous system (Bogner-Strauss, 2017) (Figure 28A). Even though recent studies suggest an upregulation of Nat8l enzyme and its beneficial impacts on survival in some lung cancer cells (Lou et al., 2016; Zand et al., 2016), we failed to detect either endogenous NAA or mRNA expression of Nat8l in either C2C12 or LLC1 cells. Therefore, we assumed that potential disruption of NAA synthesis following AGC1-depletion cannot explain why cytosolic aspartate is a limitation for the cells we used in this study (Figure 28B) and decided to investigate other roles of aspartate.

First, we wanted to explore the transamination-related roles of cytosolic aspartate. First, we looked at the fluctuations of the mRNA levels of the enzymes relevant to amino acid metabolism under glutamine limitations. As expected, mRNA expression of many transaminases regulated by Activating transcription factor 4 (Atf4), a component of the amino acid starvation response (Chen et al., 2014), was upregulated following glutamine withdrawal in both C2C12 and LLC1 cells (Figure 28C). Because glutamine is a major carbon and nitrogen source for the cells, this is a response mechanism to endure with such stress. In line with that, levels of NEAAs (except for serine and glycine that are present in DMEM) are depleted upon

RESULTS

CB-839 treatment or in low glutamine (Figure 21A) and are further reduced in AGC1-KD cells compared to control cells, which is partially rescued by aspartate supplementation (Figure 28D). However, this does not distinguish between whether aspartate levels are limiting for production of NEAAs or NEAAs are spent to make aspartate when aspartate levels drop upon glutamine withdrawal because transaminases are highly reversible and the transfer of nitrogen between amino acids is not uni-directional (Berg et al., 2002; Wiechert, 2007).

To determine the directionality of whether aspartate or the other NEAAs are the limiting end product that rescue cell survival and proliferation during glutamine limitation, we supplemented cells with either a mixture of NEAAs or aspartate and stressed them further with the transaminase inhibitor aminooxyacetate (AOA) (Figure 29A). Because aspartate or NEAAs cannot be used for the synthesis of one another when the transaminases are inhibited, the metabolite that cannot rescue cells in glutamine limitation only in the presence of AOA is not the limiting end product needed for cell survival in these conditions. First, we observed that high levels of NEAAs, indeed, improve the proliferation of AGC1-KD cells following glutaminase inhibition and low-glutamine treatment, similar to observed with aspartate supplementation (Figure 29B-C). However, the rescuing effects of NEAAs supplementation are completely abolished by AOA treatment, suggesting that NEAA rescue of glutamine limitation requires transamination therefore NEAAs are likely to be not the limiting end product for these conditions (Figure 29B-C). Of note, we included a 0.1mM mixture of NEAAs when cells were treated with AOA because transaminase activity is required to make other NEAAs, and complete loss of NEAAs might impact proliferation/survival even when glutamine is not limiting. (Figure 29B-C). Markedly, none of the amino acids, including asparagine, can rescue glutaminase inhibition individually, except for a partial rescue by glutamate, which is itself the product of glutaminase (Figure 29D). Strikingly, AOA treatment reduces the proliferation/survival rate of control cells to the level of AGC1-KD cells upon CB-839 treatment (Figure 29B-C), implying that without the ability to produce aspartate, control cells do not have a survival advantage over AGC1-KD in glutamine limitations. Most importantly, the rescuing capacity of aspartate is unaffected by transaminase inhibition, implying that a transaminase-unrelated path of aspartate is necessary for recovering cell proliferation and survival under glutamine limitations (Figure 29B-C). These data suggest that aspartate is an essential end product of transamination reactions and is not particularly limiting for NEAA synthesis when glutamine anaplerosis is inhibited.

RESULTS

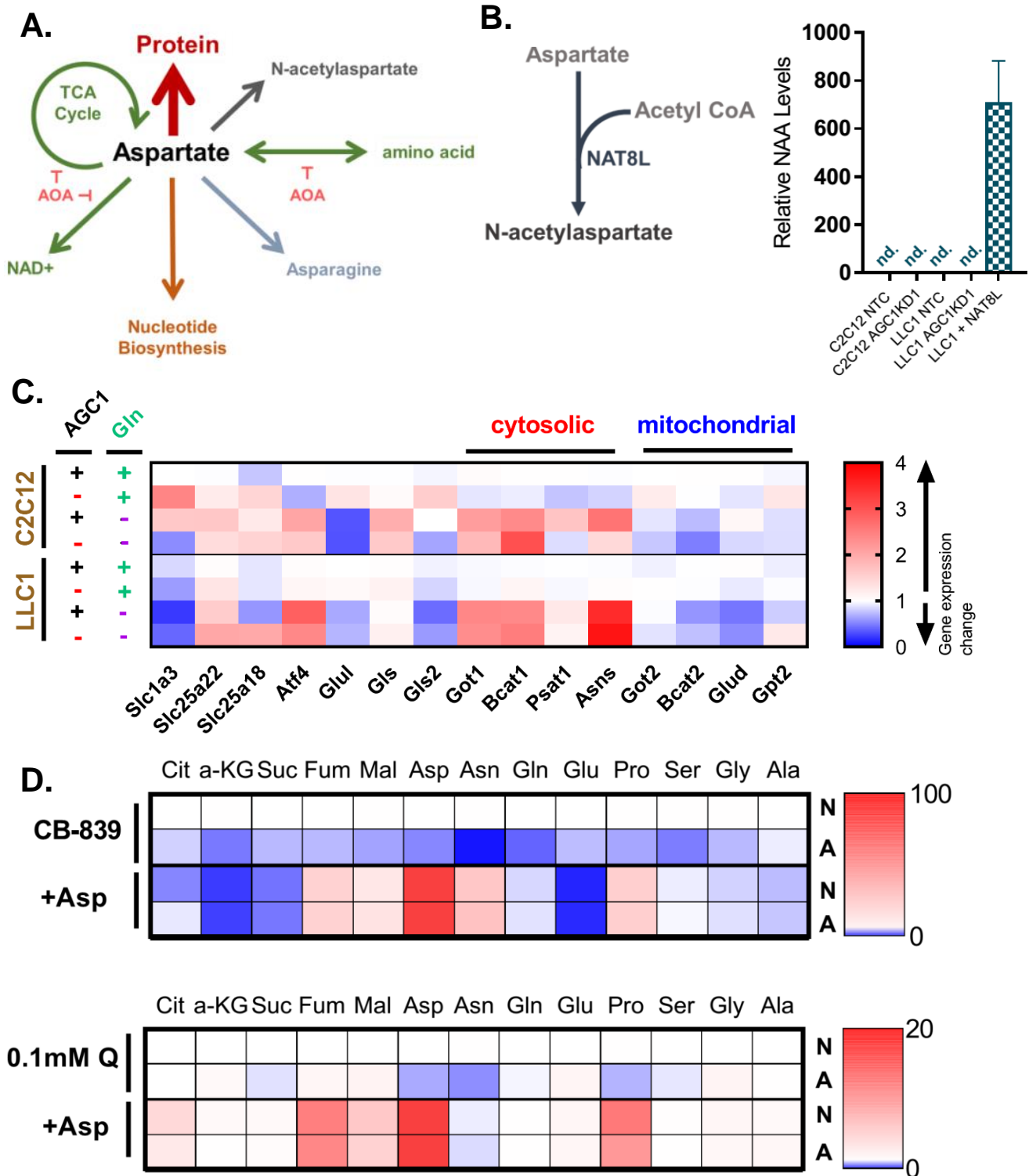


Figure 28: Changes in non-essential amino acid metabolism under glutamine limitation. (A) Drawing of the potential roles of cytosolic aspartate. Aspartate is a proteinogenic amino acid (red) that could be a substrate for transaminations (green) to donate nitrogen for non-essential amino acid synthesis, regenerate cytosolic NAD⁺ through the malate-aspartate shuttle, and supply carbon for fueling the

RESULTS

mitochondrial TCA cycle. Aspartate can also be a precursor to produce asparagine (blue), be acetylated to produce N-acetylaspartate (gray), or support purine and pyrimidine biosynthesis (orange). Aspartate fates that are affected by transaminase inhibition by AOA are indicated. (B) (Left) Schematic showing of N-acetylaspartate synthesis via the enzyme NAT8L. (Right) GCMS analysis of endogenous intracellular N-acetylaspartate (NAA) in control (NTC) and AGC1-knockdown (AGC1KD1) C2C12 and LLC1 cells as indicated. NAA levels in LLC1 cells engineered to express NAT8L to produce NAA is shown as a control. (nd. = not detected) (n=3) (C) mRNA expressions of genes involved in amino acid metabolism from control (+AGC1) or AGC1-KD (-AGC1) C2C12 or LLC1 cells cultured for 24h in 4mM glutamine (+Gln) or 0.1mM Gln (-Gln) as indicated. Shown is the median fold change in expression of the indicated gene compared to expression in control (NTC) cells cultured in 4mM glutamine (n=3). (D) Relative intracellular levels of non-essential amino acids and TCA cycle intermediates in control (N) and AGC1-KD (A) C2C12 cells cultured in 0.1mM glutamine (0.1mM Q) or 4mM glutamine with CB-839 for 24h in the presence and absence of 20mM aspartate, relative change compared to control with CB-839 or NTC with 0.1mM Q is shown (n=3) Cit, citrate; a-KG, alpha-ketoglutarate; Suc, succinate; Fum, fumarate; Mal, malate; Asp, aspartate; Asn, asparagine; Gln, glutamine; Glu, glutamate; Pro, proline; Ser, serine; Gly, glycine; Ala, alanine. mean ± SDs are shown

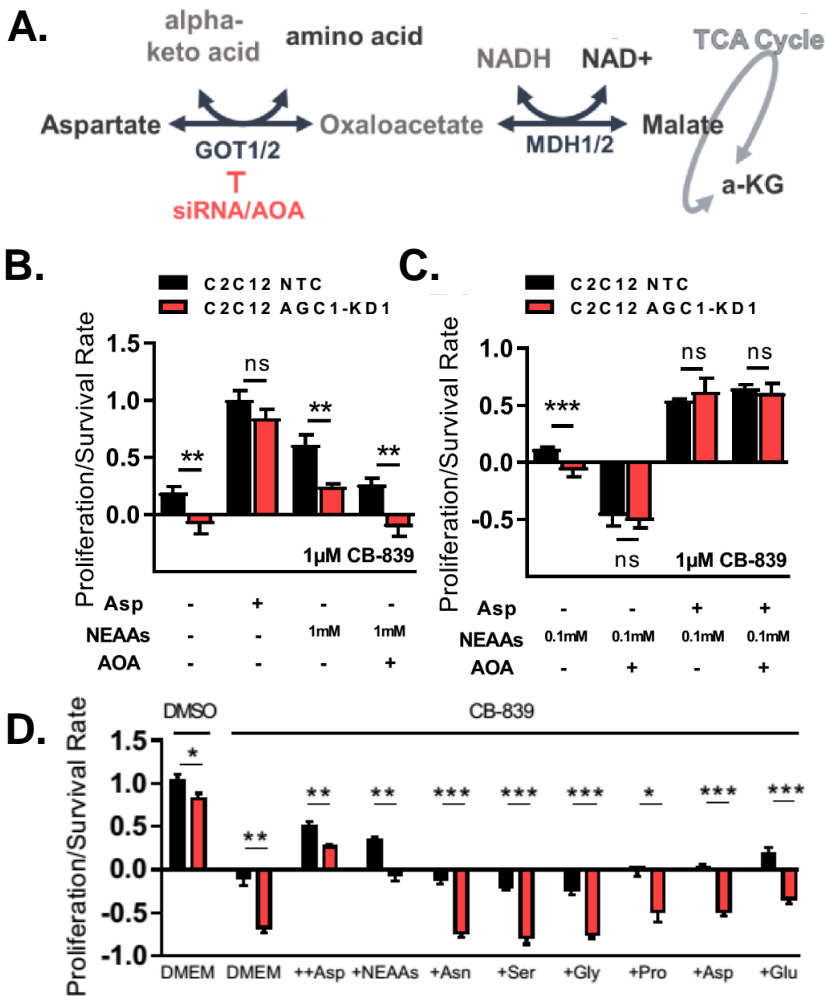


Figure 29: Cytosolic aspartate is not crucial for non-essential amino acids in low-glutamine. (A) Schematic showing how aspartate undergoes transaminations (Got1/2) to support amino acid biosynthesis, provide carbon to the TCA cycle, or oxidize NADH. To produce aspartate, TCA substrates or amino acids also require transamination.

Transamination to produce or consume aspartate is inhibited by AOA or by knockdown of aspartate transaminases (siGot1/2). (B-C) Proliferation/survival rates of control (NTC) and AGC1-KD C2C12 cells cultured in pyruvate-free DMEM and treated with 1µM CB-839 in the presence or absence of 20mM aspartate (Asp), 1mM or 0.1mM of a mixture of non-essential amino acids containing serine, glycine, alanine, aspartate, asparagine, proline, and glutamate (NEAAs), and/or 0.3mM AOA as indicated (n=3). (D) Proliferation/survival rates of control (NTC) and AGC1-KD C2C12 cells cultured in 4mM glutamine and treated with DMSO or with 1µM CB-839 in the presence of 10mM aspartate (Asp), 1mM of a mixture of non-essential amino acids containing asparagine (Asn), serine (Ser), glycine (Gly), proline (Pro), alanine, aspartate (Asp), and glutamate (Glu) (NEAAs) or 1mM of the individual specified free amino acid as indicated (n=3).

3.9 Cytosolic aspartate is not crucial for feeding the TCA cycle in low-glutamine

Because the ability of aspartate to rescue proliferation/survival in the presence of AOA is unaffected and the fates of aspartate to either feed the TCA cycle or be used for cytosolic NAD⁺ regeneration through malate-aspartate shuttle involve transamination reactions, we predicted that these functions of aspartate are not essential to recover cell proliferation/survival when glutamine is limiting (Figure 28A). As expected, supplementing cells with either a cell-permeable form of alpha-ketoglutarate (dimethyl alpha-ketoglutarate; daKG) or pyruvate as alternative anaplerosis sources fail to rescue glutamine limitation when aspartate production is inhibited via AOA or siRNA (Figure 30). This finding confirms that conversion of aspartate to oxaloacetate by Gots -either to regenerate cytosolic NAD⁺, to fuel the TCA cycle, or to donate nitrogen for amino acid synthesis- is not limiting in AGC1-KD cells upon glutamine-deprivation.

Strikingly, these data also speculate that a primary role of the TCA cycle anaplerosis in proliferation cells is to produce aspartate and the TCA cycle is not required for proliferation when aspartate is abundant. Nevertheless, it is paramount to state that these findings do not advocate that aspartate does not undergo transamination and/or fuel the TCA cycle and only suggests that those pathways are not limiting for survival in glutamine-limiting conditions. Consistently, we detected that labels from [U¹³C]aspartate is incorporated into the TCA cycle metabolites in low glutamine conditions (Figure 31A). Similarly, aspartate supplementation mildly increases the intracellular levels of some TCA cycle intermediates (Figure 28D), although these differences vary across different cell lines (Figure 21). Of note, [U¹³C]glutamate labels TCA cycle intermediates more strongly than [U¹³C]aspartate (Figure 31B), suggesting that even when transaminases are active, glutamate is a more prominent TCA cycle fuel than aspartate.

Asparagine synthesis is another downstream fate of cytosolic aspartate that does not require transamination, therefore it is not inhibited by AOA. Recent reports show that asparagine availability can regulate cell survival when glutamine is limiting (Ratnikov et al., 2015; Zhang et al., 2014), and plasma membrane transporters might be using intracellular asparagine as an exchange factor to import other extracellular amino acids when glutamine metabolism is blocked (Krall et al., 2016). Asparagine levels are also lower in AGC1-KD cells after glutamine-withdrawal and these levels are moderately improved by aspartate supplementation (Figure 28D). Nevertheless, asparagine supplementation alone failed to

RESULTS

rescue CB-839 treated AGC1-KD cells (Figure 29D), suggesting that asparagine production by itself is not a limiting role of aspartate to maintain AGC1-KD cell survival following CB-839 treatment.

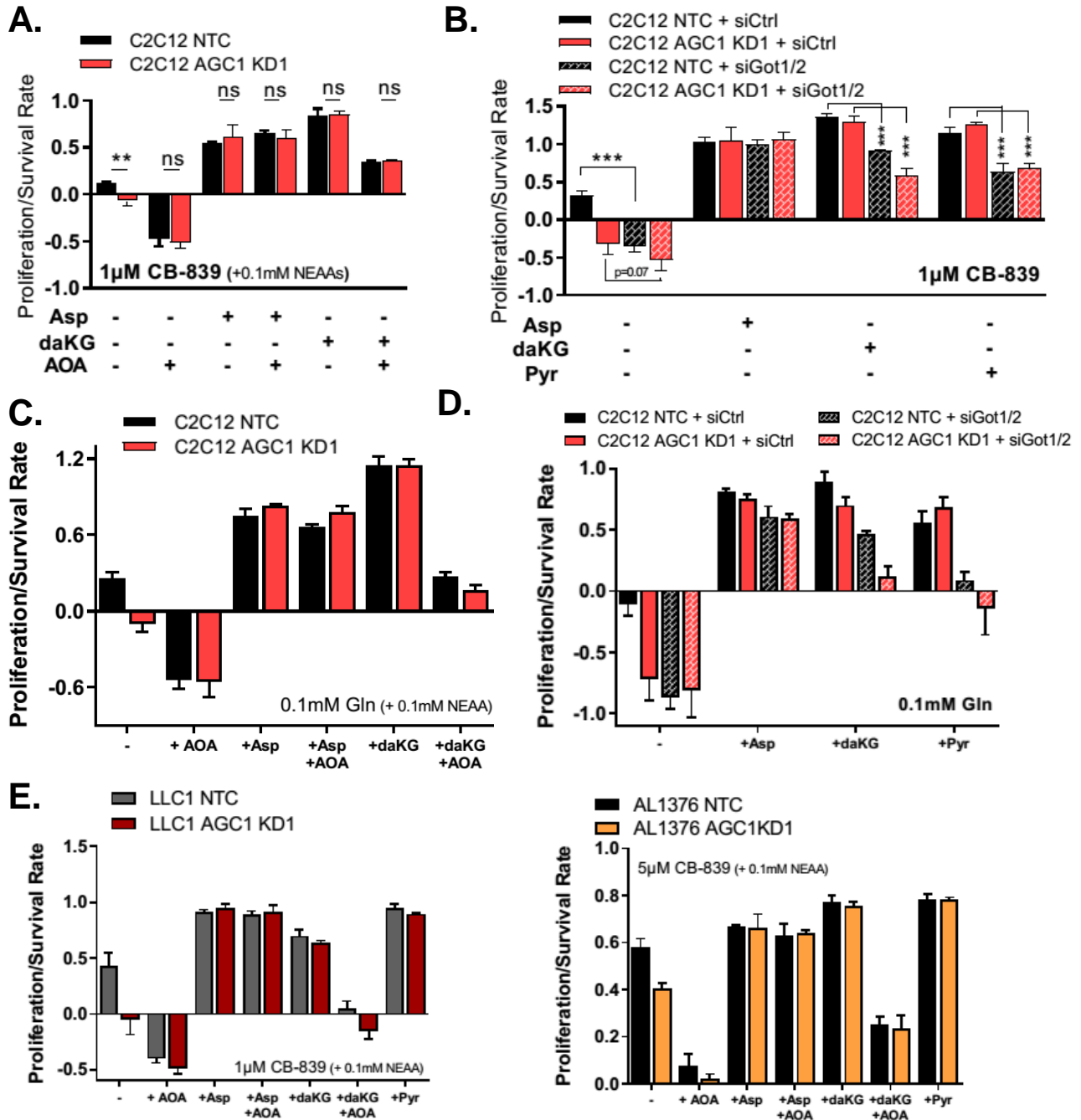


Figure 30: Cytosolic aspartate is not a crucial feeding TCA cycle or cytosolic NAD⁺ regeneration in low-glutamine. (A, C) Proliferation/survival rates of control (NTC) and AGC1-KD C2C12 cells cultured in (A) 4mM glutamine with 1µM CB-839 or (C) 0.1mM glutamine and 0.1mM mixture of non-essential amino acids (NEAAs) in the presence or absence of 20mM aspartate (Asp), 2mM dimethylalpha-ketoglutarate (daKG), and/or 0.3mM AOA as indicated (n=3). (B, D) Proliferation/survival rates of control (NTC) and AGC1-

RESULTS

KD C2C12 cells treated with either (B) 1 μ M CB-839 or (D) 0.1mM glutamine in the presence or absence of 20mM aspartate (Asp), 2mM dimethylalpha-ketoglutarate (daKG), and/or 2mM sodium pyruvate (Pyr), without (siCtrl) or with (siGot1/2) siRNA knockdown of Got1 and Got2 as indicated (n=3). (E) Proliferation/survival rates of control (NTC) and AGC1-KD LLC1 and AL1376 cells as described in (A). mean \pm SDs are shown.

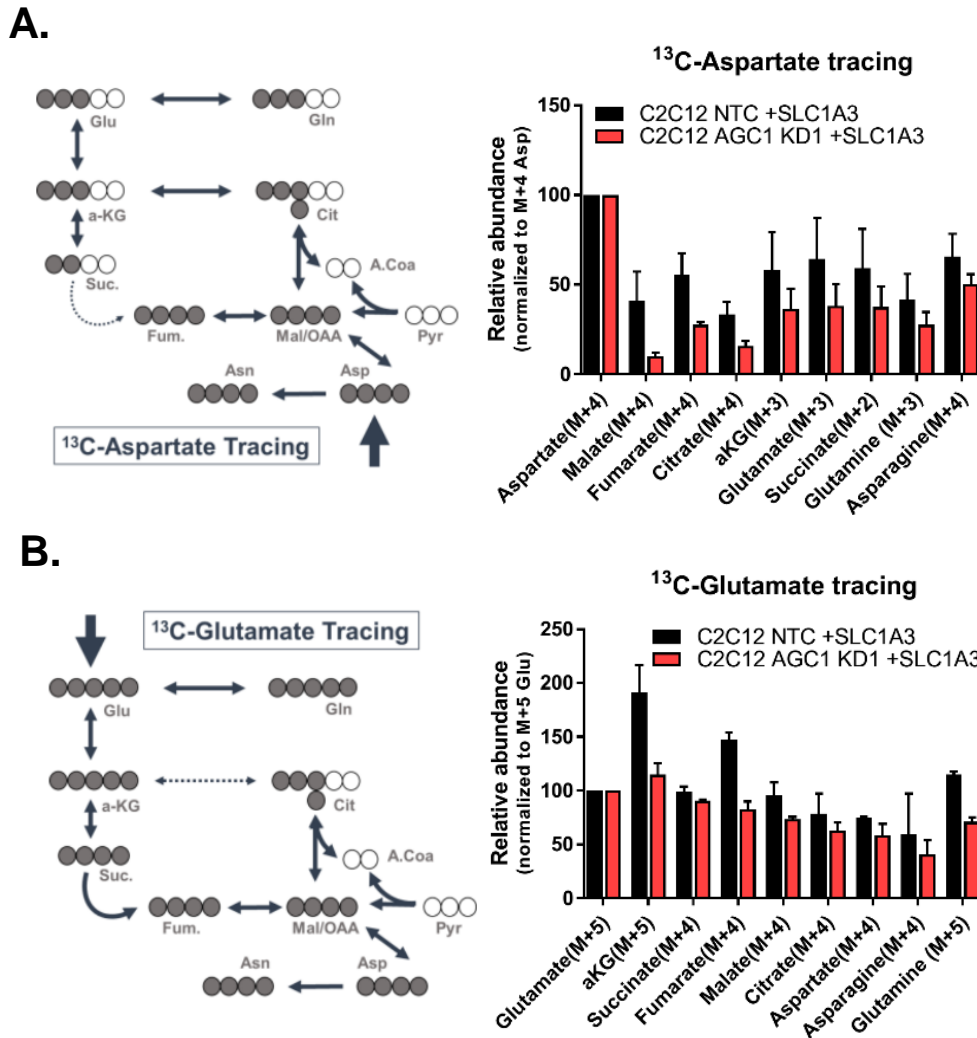


Figure 31: ¹³C-Aspartate and ¹³C-Glutamate tracing in C2C12 cells. (A) (Left) Tracing map showing the relationship between labeled aspartate carbon and the labeling of TCA cycle intermediates. (Right) Relative enrichment of the most abundant TCA intermediate isotopomers that were found to be labeled from [U-13C]aspartate when control (NTC) or AGC1-knockdown (AGC1-KD1) C2C12 cells expressing the aspartate/glutamate transporter SLC1A3 were cultured in media containing [U-13C]aspartate and 0.1mM glutamine. Data shown for each species were normalized to the enrichment of M+4 aspartate (n=3) (B) (Left) Tracing map showing the relationship between labeled glutamate carbon and the labeling of TCA cycle intermediates. (Right) Relative enrichment of the

most abundant TCA intermediate isotopomers that were found to be labeled from [U-13C]glutamate when control (NTC) or AGC1-knockdown (AGC1KD1) C2C12 cells expressing the aspartate/glutamate transporter SLC1A3 were cultured in media containing [U-13C]glutamate and 0.1mM glutamine. Data shown for each species were normalized to the enrichment of M+5 glutamate (n=3)

3.10 Cytosolic aspartate is required for nucleotide biosynthesis

Aspartate is a precursor for nucleotide biosynthesis that is required for cell proliferation (Sullivan et al., 2015). Inhibiting glutaminase in Von Hippel-Lindau (VHL)-deficient renal tumors reduces pyrimidine biosynthesis (Okazaki et al., 2017). Furthermore, when aspartate is used for purine production, fumarate is released as a byproduct (Lane and Fan, 2015). We speculated that this may explain the greater increase in fumarate levels compared to other TCA cycle metabolites after aspartate supplementation (Figure 29B). Together, these implied that the role of cytosolic aspartate to sustain cell survival in glutamine limitation might converge on nucleotide metabolism.

In order to investigate whether glutaminase inhibition influence nucleotide biosynthesis, we traced [¹⁵N-(amide)]glutamine into nucleotides during CB-839 treatment. Since nitrogen from aspartate is transferred to IMP for AMP synthesis, AMP production from IMP could be defective when cytosolic aspartate is sparse (Figure 32A). In line with this, the relative AMP/IMP ratio is reduced upon CB-839 treatment and is recovered by aspartate supplementation (Figure 32A), suggesting that a reduction in cytosolic aspartate levels impairs nucleotide biosynthesis. Likewise, intracellular UMP levels are also reduced in AGC1-KD cells upon CB-839 treatment compared to controls, implying that pyrimidine synthesis is also affected by decreased cytosolic aspartate delivery (Figure 32B). In order to examine whether nucleotides were indeed limiting end-product for AGC1-KD cells, we provided AGC1-KD and control cells with exogenous thymine, uridine, hypoxanthine, adenine, and guanine (Figure 32D). Strikingly, these nucleotide bases improved AGC1-KD cell proliferation/survival in low glutamine conditions or during glutaminase inhibition (Figure 32C, E), although this rescue was less prominent than that observed with aspartate. These data suggest that nucleotide biosynthesis is one limitation caused by decreased cytosolic aspartate delivery.

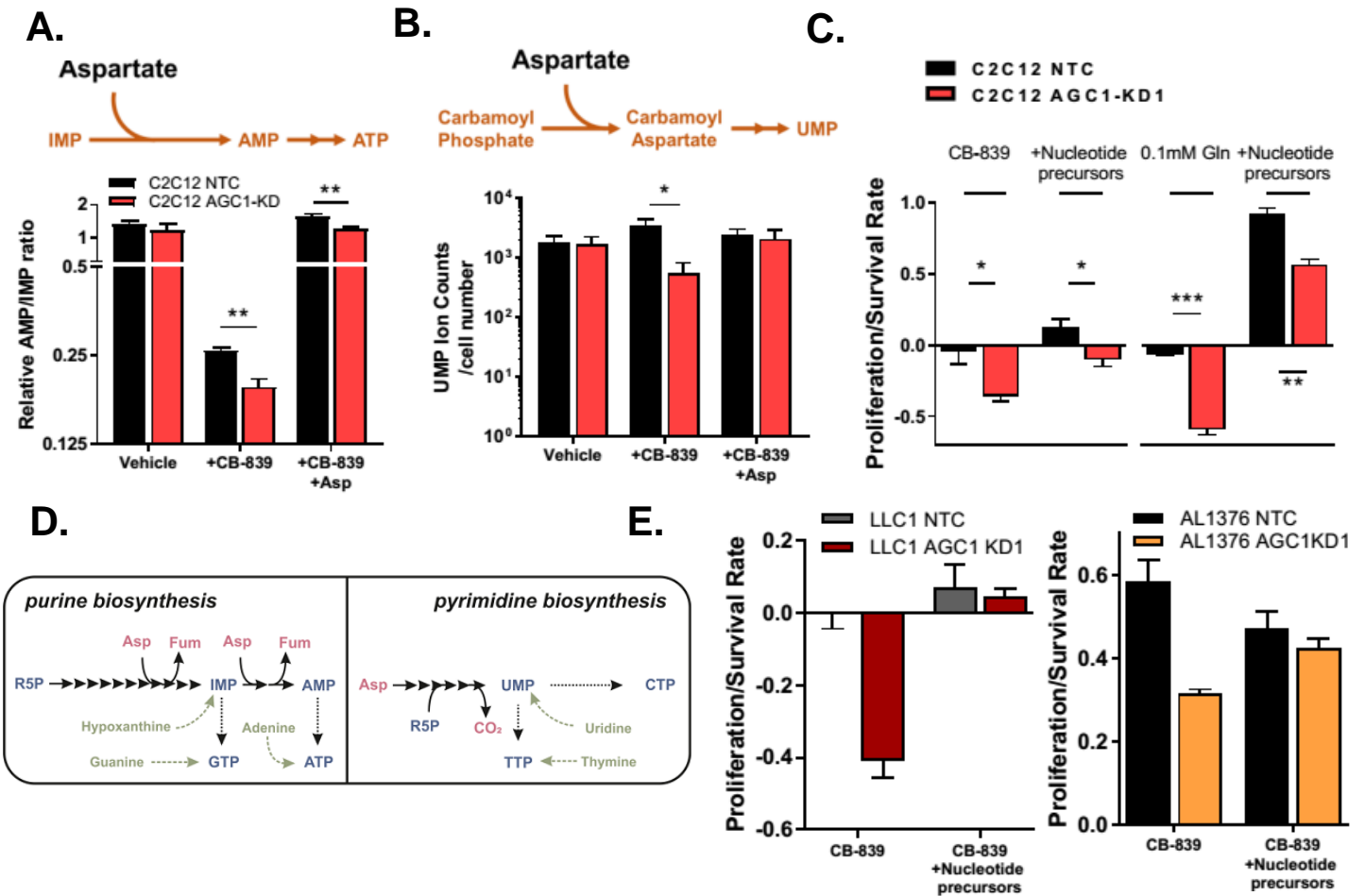


Figure 32: Cytosolic aspartate is required to produce nucleotides for maintaining cell survival in glutamine limitations. (A) (Top) Schematic showing the need for aspartate to make AMP from IMP. (Bottom) Relative AMP to IMP ratio in control (NTC) and AGC1-KD C2C12 cells cultured with 4mM glutamine for 24h in the absence (Vehicle) or presence of 1μM CB-839, without or with 20mM aspartate (Asp), as indicated (n=3). (B) (Top) Schematic showing the role of aspartate in UMP synthesis. (Bottom) Relative intracellular UMP levels in control (NTC) and AGC1-KD C2C12 cells cultured in 4mM glutamine for 24h in the absence (Vehicle) or presence of 1μM CB-839, without or with 20mM aspartate (Asp), as indicated (n=3). (C) Proliferation/survival rates of control (NTC) and AGC1-KD C2C12 cells cultured in 0.1mM Glutamine or 4mM glutamine with 1μM CB-839 in the presence or absence of a mix of nucleotide precursors containing 200μM hypoxanthine, 200μM adenine, 200μM guanine, 100μM thymine and 400μM uridine as indicated (n=3). (D) Schematic showing how Aspartate contributes to both purine and pyrimidine biosynthesis. R5P, ribose-5-phosphate; Asp, aspartate; Fum, fumarate; IMP, inosine monophosphate. (E) Proliferation/survival rates of control (NTC) and AGC1-KD LLC1 and AL1376 cells cultured in 4mM glutamine with 1μM (LLC1) or 5μM (AL1376) CB-839 in the presence and absence of a mixture of nucleotide precursors (200μM hypoxanthine, 200μM adenine, 200μM guanine, 100μM thymine and 400μM uridine) as indicated. (n=3). All figures denote mean ± SD unless indicated otherwise. * p ≤ 0.05, ** p ≤ 0.01, *** p ≤ 0.001.

3.11 AGC1 knockdown limits tumor growth

We next investigated whether knockdown of AGC1 would affect tumor growth *in vivo* as observed in cell culture. We injected two independent AGC1-knockdown (sh911 as KD1 and sh908 as KD2; as described above) and control (NTC) LLC1 cells subcutaneously, over the flanks of 8week-old, female wild-type syngeneic C57Bl/6J mice. We measured the tumor size using calipers 11 and 16 days after the injections. Strikingly, we observed significantly smaller tumors in mice injected with knocked-down cells at day 11 and this difference was even larger at day16 (Figure 33); demonstrating that AGC1-depletion inhibits tumor growth consistent with findings from cell culture experiments.

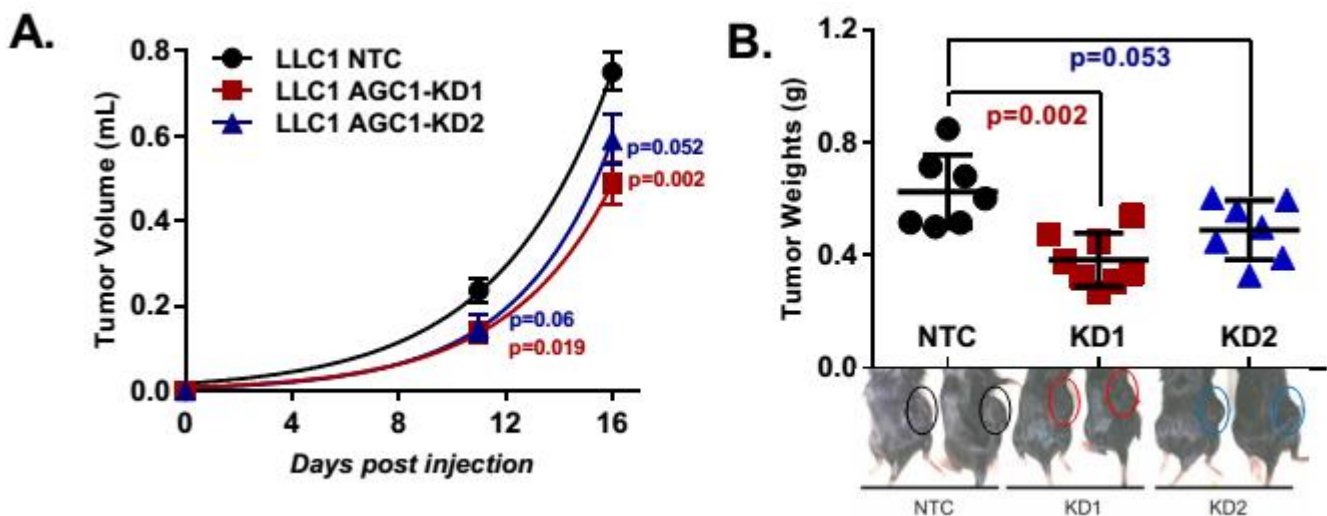


Figure 33: AGC1-knockdown reduces LLC1 tumor growth. (A) Tumor volume over time of allografts generated from control (NTC) and two independent AGC1-knockdown (AGC1-KD1 and AGC1-KD2) LLC1 cell lines implanted into the flanks of C57BL/6 mice ($n \geq 7$). (B) Tumor weights of the LLC1 allografts described in A at the experiment endpoint (day17). All figures denote mean \pm SEMs

3.12 AGC1 knockdown sensitizes tumors to CB-839 treatment

Despite prominent effects on cell proliferation and survival *in vitro*, glutaminase inhibitors such as CB-839 is unpredictably inefficient in blocking tumor growth in some cancer model *in vivo* (Biancur et al., 2017; Davidson et al., 2016). To investigate whether loss of AGC1 sensitizes tumors to CB-839 treatment *in vivo*, we gavaged mice tumor-bearing mice to CB-839 and monitor tumor growth over time. In line with previous studies, CB-839 treatment had modest effects on the growth of control LLC1 tumors (Figure 34). Remarkably, the growth of AGC1-KD LLC1 cells was further impaired by CB-839 (Figure 34), suggesting that loss of AGC1 synergizes with glutaminase inhibition to block tumor progression.

RESULTS

Because we observed little to no effect of CB-839 treatment on control tumors, we wanted to rule out the possibility that control tumors that being larger than AGC1-KD tumors at the starting point of the CB-839 gavage affected the efficiency of the applied dose of the drug. Therefore, we measured glutamate/glutamine ratio in these tumors and observed that control and AGC1-KD tumors responded in a comparable manner to CB-839 exposure, confirming that the treatment was equally effective to inhibit glutaminase activity (Figure 35A). In addition, we verified that the pyruvate/lactate ratio (as a proxy for NAD⁺/NADH ratio, as described previously) was lower in AGC1-KD tumors, as observed in cell culture experiments, highlighting that AGC1 depletion also alters the redox state of cells *in vivo* (Figure 35B). On the other hand, asparagine levels were strongly elevated in CB-839 treated tumors, unlike what we observed in the cell culture environment (Figure 35C). Nevertheless, these levels were still lower in AGC-KD tumors, compared to controls, suggesting lower levels of cytosolic aspartate (Figure 35C). These findings are in coherence with cytosolic aspartate delivery being crucial in tumors when glutaminase is blocked and is consistent with a failure to sustain cytosolic aspartate levels via mitochondrial aspartate export hindering the growth of AGC1-KD tumors upon CB-839 treatment. Furthermore, these findings also speculate that AGC1-KD increases tumor vulnerability to glutaminase inhibition.

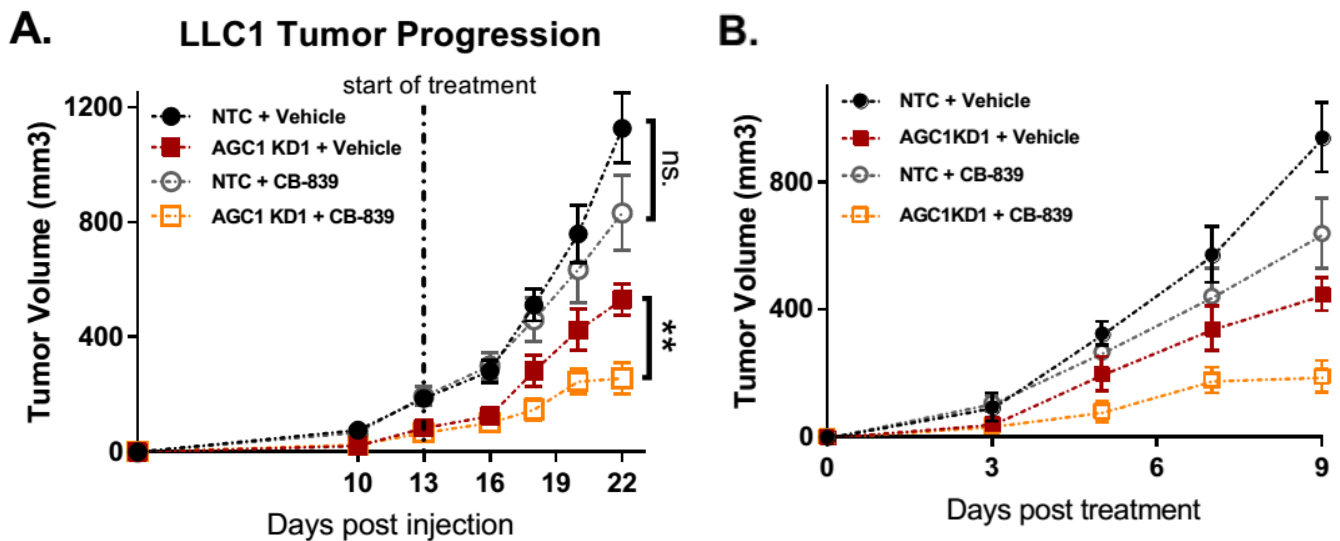


Figure 34: AGC1-deficiency sensitizes tumors to CB-839 treatment. (A) Growth of tumors generated from control (NTC) or AGC1-KD LLC1 in C56BL/6 mice flanks that were treated without (Vehicle) or with CB-839 dosed at 200mg/kg/twice daily starting on day 13 as indicated (n≥6). (B) Tumor volume over time of allografts generated from control (NTC) and AGC1-knockdown (AGC1KD1) LLC1 cells implanted into the flanks of C56BL/6 mice that are dosed with vehicle or 200mg/kg/twice daily of CB-839 starting on day 0 as indicated (n≥6). All figures denote mean ± SEMs

RESULTS

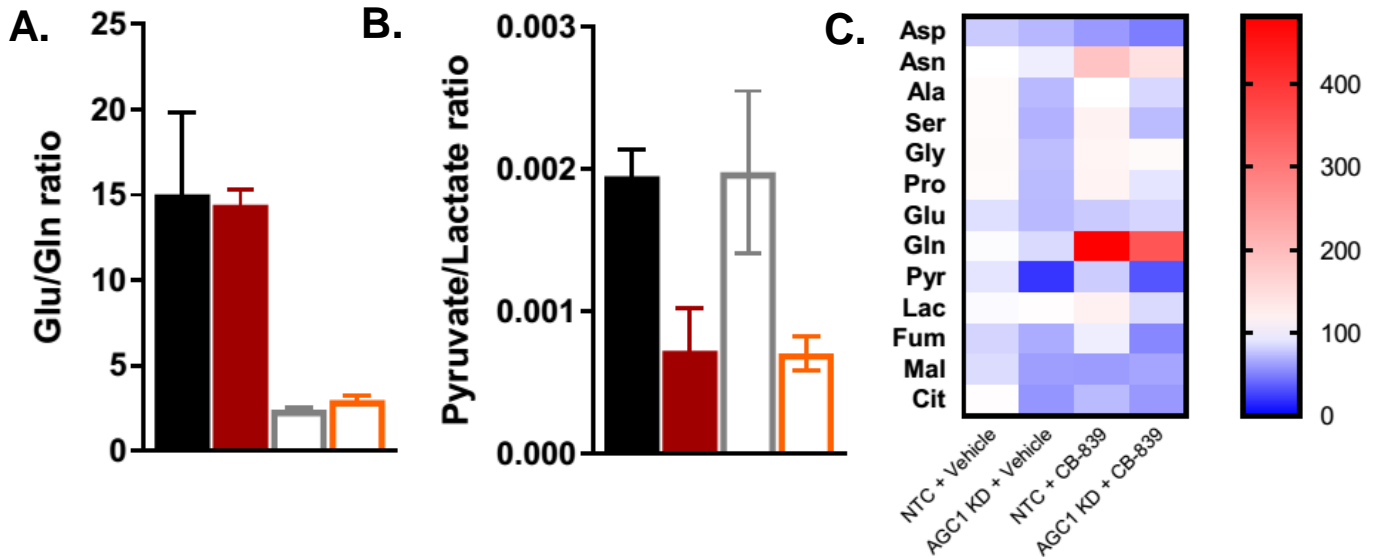


Figure 35: Metabolic profiling of LLC1 tumors. (A) Relative glutamate (Glu) to glutamine (Gln) ratio measured in metabolite extracts from the tumors shown in panel A at the experimental endpoint (day 22) ($n \geq 5$). (B) Relative pyruvate to lactate ratio measured in metabolite extracts from the tumors shown in panel A at the experimental endpoint (day 22) ($n \geq 5$). All figures denote mean \pm SEMs (C) Relative levels of the indicated non-essential amino acids and TCA intermediates (normalized to valine) from the tumors described in C. Data are presented as a relative change compared to vehicle-treated NTC control ($n \geq 5$), medians are shown.

Next, we decided to investigate whether the loss of AGC1 would have comparable effects on another cancer type. Thus, we allografted AL1376 pancreatic ductal adenocarcinoma cells that were derived from the LSL-KrasG12D, p53flox/flox, Pdx1-Cre mouse model (Bardeesy et al., 2006). Consistently, AGC1-depletion robustly slowed down AL1376 tumor growth (Figure 36). Of note, unlike LLC1, AL1376 tumors were completely resistant to CB-839 treatment, yet AGC1-KD introduced CB-839 vulnerability (Figure 36). These findings confirm that targeting AGC1 may synergize with the glutaminase inhibitors to limit the growth of some tumors.

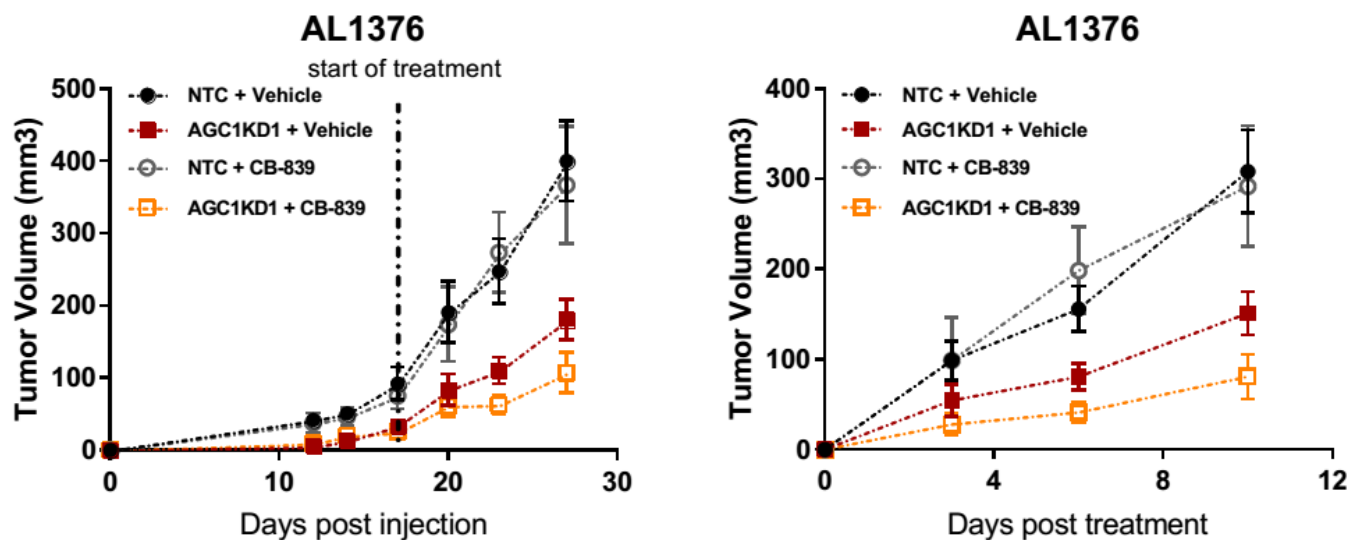


Figure 36: AGC1-knockdown sensitizes AL1376 pancreas allograft tumors to CB-839 treatment. (Left) Tumor volume over time of allografts generated from control (NTC) and AGC1-knockdown (AGC1KD1) AL1376 cells implanted into the flanks of C56BL/6 mice that are dosed with vehicle or 200mg/kg/twice daily of CB-839 as indicated ($n \geq 6$). Dosing of vehicle or CB-839 was started on day 16 as indicated. (Right) Growth of tumors derived from the AL1376 cells described in the left graph in C56BL/6 mice flanks that are dosed with vehicle or 200mg/kg/twice daily CB-839 as indicated starting on day 0 ($n \geq 6$). All figures denote mean \pm SEMs unless indicated otherwise.

3.13 AGC1 expression is upregulated in Pancreatic Ductal Adenocarcinomas

Next, we asked whether AGC1 is endogenously expressed in tumors. Using immunohistochemistry human cancer tissue-arrays, we identified that AGC1 is present in various cancer cells including glioblastoma, ovarian cancer, breast cancer, pheochromocytoma, leiomyosarcoma, and seminoma (Figure 37A).

We also investigated whether AGC1 is upregulated in cancers. From the non-cancerous pancreas histology samples, we first established that pancreatic islet cells have the strongest AGC1-positive signals (Figure 37B, top-left) and some, not all, exocrine glandular cells modestly express AGC1. On the other hand, all non-cancerous ductal cells seemed to be negative for AGC1 protein (Figure 37B, bottom-left). Strikingly, a number of ductal tumors, estimated to be 30-50% of all tumor cells, had positive AGC1 signals in a patient independent manner, suggesting that AGC1 might be upregulated in pancreatic ductal carcinomas (Figure 37B, right). It is important to note that AGC1 showed a heterogeneous expression in ductal tumors even within the same tissue slide, suggesting that tumor microenvironment or other factors might be involved in regulating AGC1 expression in tumors. These findings suggest that AGC1 could be a target to treat human cancers.

RESULTS

Because we performed *in vivo* tumor growth experiments using mouse lung and pancreas tumors, we wanted to verify that autochthonous mouse lung and pancreas tumors also express AGC1 protein. Even though AGC1 protein levels appeared to be only slightly upregulated in either KrasG12D, p53^{-/-} mouse lung (Davidson et al., 2016) or pancreatic (Mayers et al., 2014), we confirmed that both tumor types had abundant AGC1 expression (Figure 37C).

RESULTS

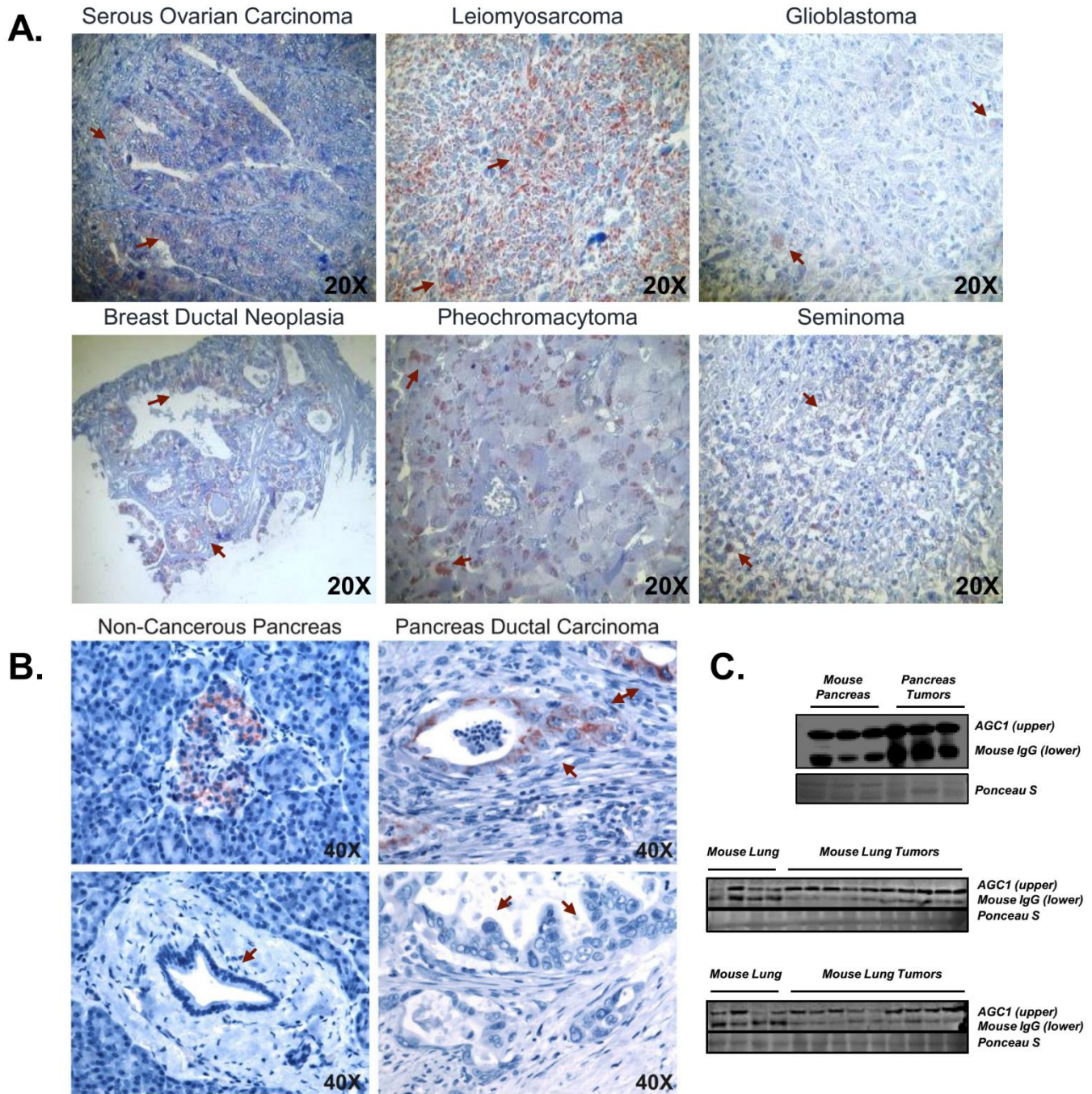


Figure 37: AGC1 is expressed in mouse and human tumors. (A) Representative immunohistochemistry staining for AGC1 in the indicated human cancer tissues. (B) Representative immunohistochemistry staining for AGC1 expression in normal and cancerous human pancreas tissue sections (n=5). AGC1 expression is observed in pancreatic islets [above left], and ductal carcinoma [right; above and below] but not in normal duct [below left]. (C) AGC1 expression assessed by Western blot in normal mouse pancreas and lung tissue as well as in KrasG12D, p53^{-/-} lung and pancreatic tumors arising in genetically engineered mouse models involving these organs as indicated.

3.14 High AGC1 expression may correlate with better prognosis in some cancers (Supplementary Finding)

During our first *in vivo* tumor growth experiment, after gathering preliminary data on tumor progression, we decided to leave the mice for additional time with unlimited water and food supply to gather information about their survival rate. We monitored the health status of the mice daily and euthanized when they reach critical levels of stress. Unexpectedly, we observed that mice bearing AGC1-KD tumors tended to die faster than the control group even though they showed slower tumor growth (Figure 38). Furthermore, our analysis of the mRNA-seq database of The Cancer Genome Atlas (TCGA) also showed that patients with high AGC1-expressing tumors were more inclined to survive longer (Figure 39) in most cancers, speculating that AGC1 might have a more diverse impact on cancers beyond its role in proliferation.

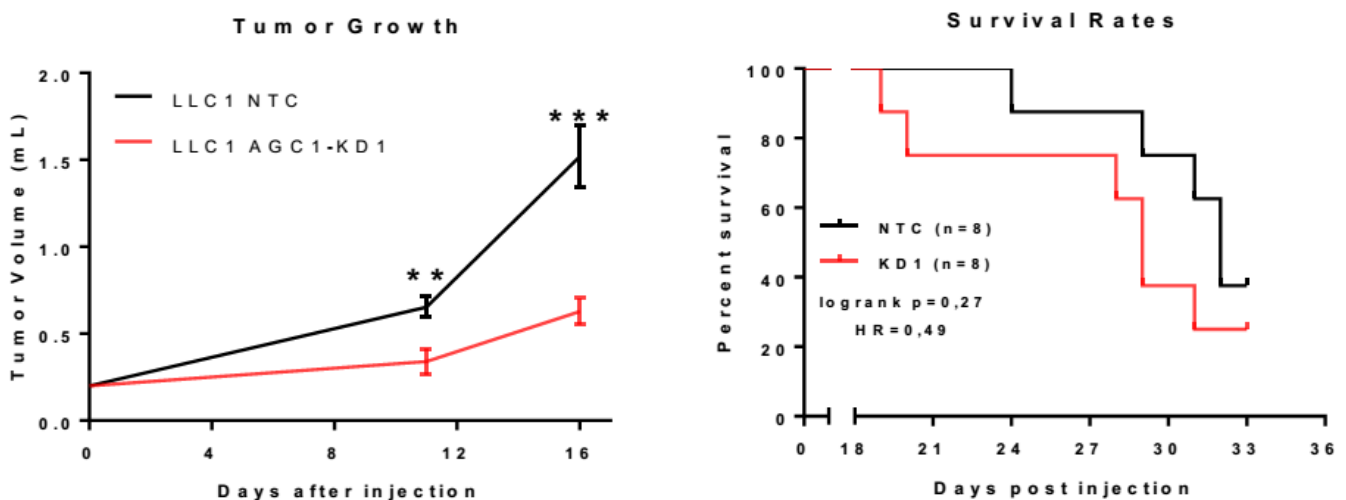


Figure 38: AGC1-deficient tumors tended to be more lethal for mice. (Left) Tumor progression of control (NTC) and AGC1-KD LLC1 tumors measured as described above. (Right) Survival rates of the mice bearing control (NTC) and AGC1-KD LLC1 tumors monitored over the course of 33 days.

3.15 AGC1-KD increased the pulmonary metastatic capacity of LLC1 and B16F10 cells (Supplementary Finding)

Because of the peculiar survival phenotype, we observed in our preliminary tumor growth experiment, one hypothesis we had was that AGC1-deficient cells might have a superior metastatic capacity compared to control cells. Thus, in our next LLC1 tumor growth experiment, we collected the lungs of the mice at the end of the experiment, embedded in paraffin, and screened for metastasis using a qualitative approach. Strikingly, none of the mice from the control group had pulmonary metastasis while approximately half of the mice bearing AGC1-KD tumors were metastasis positive (Figure 40A).

RESULTS

We next injected tumors behind the neck of the mice, instead of the flanks, because this approach allows us to inject a higher number of cells and inoculate the mice longer as we wanted to be able to quantify metastasis in each mice. We harvested the lungs 21 days after tumor injection and measured the percentage of tumor area within the whole lung. Consistently, the metastatic regions of the lungs from the mice with AGC1-KD LLC1 tumors were significantly larger than those from mice with control tumors (Figure 40B, C).

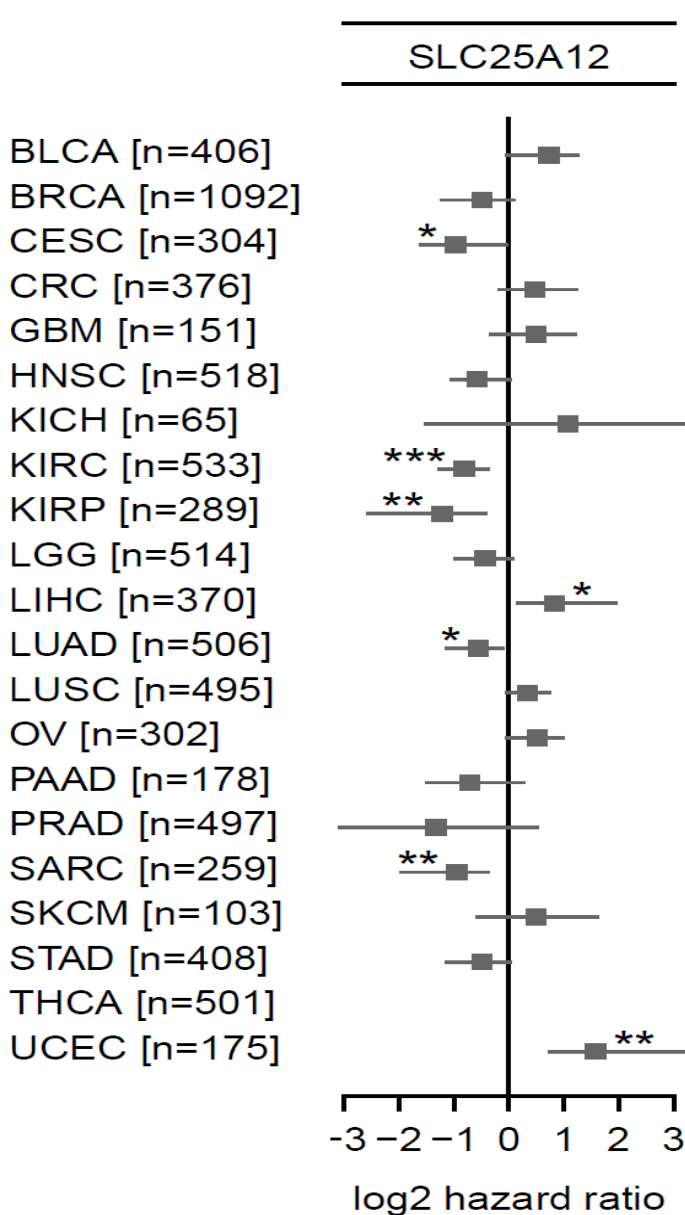


Figure 39: SLC25A12 expression often negatively correlates with cancer prognosis. Correlation of AGC1 (SLC25A12) expression with better (negative log₂hazard ratio) or worse (positive log₂hazard ratio) survival of patients from various cancers. Patients with higher or lower SLC25A12 expression was divided into two groups with a cut-off line where the separation of these groups was significantly most meaningful. Lower log₂hazard ratio for SLC25A12 means the group of the patients with tumors with lower SLC25A12 mRNA expression has worse overall survival than the higher expressing group. Cancers where high SLC25A12 expression is significantly correlated with worse for overall patient survival: LIHC (liver hepatocarcinoma) and UCEC (Uterine Corpus Endometrial Carcinoma). Cancer where low SLC25A12 expression is significantly correlated with worse for overall patient survival: CESC (Cervical Squamous Cell Carcinoma), KIRC (Kidney Renal Clear Cell Carcinoma), KIRP (Kidney Renal Papillary Cell Carcinoma), LUAD (Lung Adenocarcinoma), and SARC (Sarcoma). Cancers that are relevant to our study but did not show significant correlation: GBM (Glioblastoma), LGG (Lower-grade glioma), LUSC (Lung Squamous Cell Carcinoma), PAAAD (Pancreas Adenocarcinoma).

RESULTS

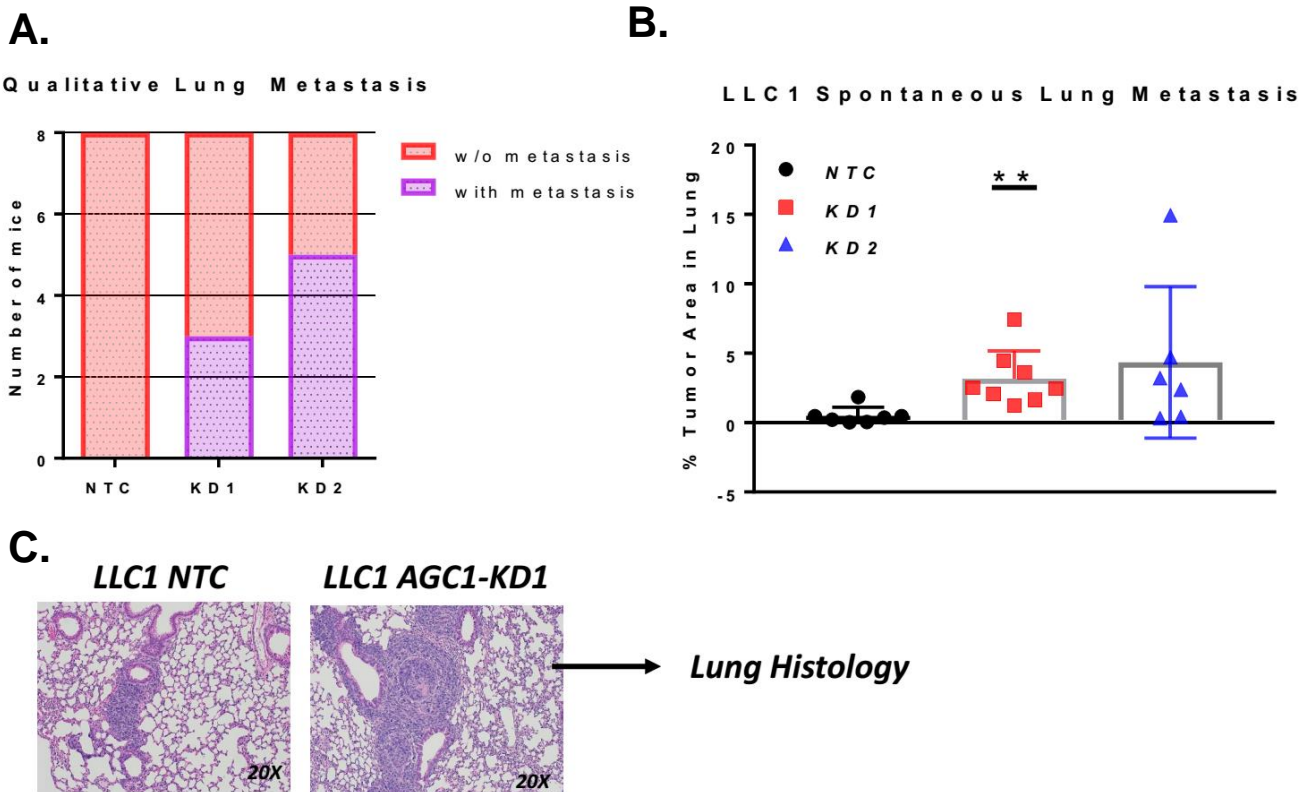


Figure 40: LLC1 tumors with AGC1-knockdown have higher chance to metastasize. (A) The number of mice with (purple) or without (pink) lung metastasis 16days after control (NTC), or AGC1-KD (KD1, sh911 or KD2, sh908) LLC1 cells were injected on the flanks. (B) Percent of the metastatic area in the lungs of mice bearing control (NTC), or AGC1-KD (KD1, sh911 or KD2, sh908) LLC1 tumors, measured 21days after cells being injected behind the necks of mice. (C) Representative histology pictures of the metastatic areas of mice injected with control (NTC) or AGC1-KD LLC1 tumors.

Next, we wanted to verify these findings in the B16F10 cell line that is specifically generated for their metastatic potential and a proper model for metastasis studies (Hart et al., 1979). AGC1 is abundantly expressed in B16F10 cells and depletion of AGC1 reduced cell proliferation as observed in LLC1 cells (Figure 10). To test the impact of AGC1-knockdown on the metastatic capacity of B16F10 cells *in vivo*, we injected them intravenously into 8-9 week-old, female wild-type C57Bl/6J mice. We harvested the lungs 16 days after and measured the percentage of tumor area within the whole lung. Strikingly, AGC1-KD cells yielded more metastasis in the lung in three independent experiments (Figure 41). These findings suggest that AGC1-loss is correlated with increased metastatic capacity. Whether this is a direct cause-effect relationship or the reason why cells with low AGC1 expression have higher metastatic potential remains to be further investigated. Because suppressing oxidative stress can assist the survival of circulating cells (Piskounova, et al., 2015), lower baseline levels of reactive oxygen species (ROS)

RESULTS

observed in AGC1-KD cells (Figure 42) might be one explanation why AGC1-depletion has a peculiar impact on metastatic capacity. These findings could lead to a follow-up project, aiming to understand the metabolic requirements of metastasis.

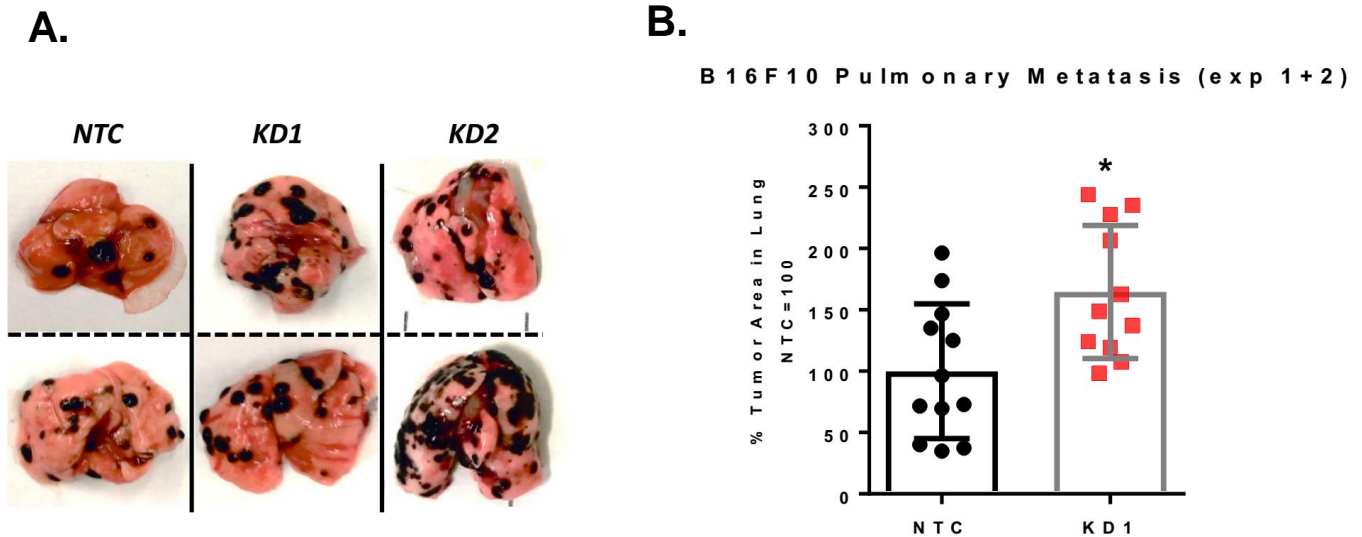


Figure 41: B16F10 cells with AGC1-knockdown have higher pulmonary metastasis capacity. (A) Representative pictures from the lungs with metastasis harvested 16 days after control (NTC), and AGC1-KD (KD1, sh911; KD2, sh908) B16F10 cells intravenously injected. (B) Percent of the metastatic area in the lungs of mice with control (NTC), or AGC1-KD LLC1 cells, measured 16 days after cells intravenously injected.

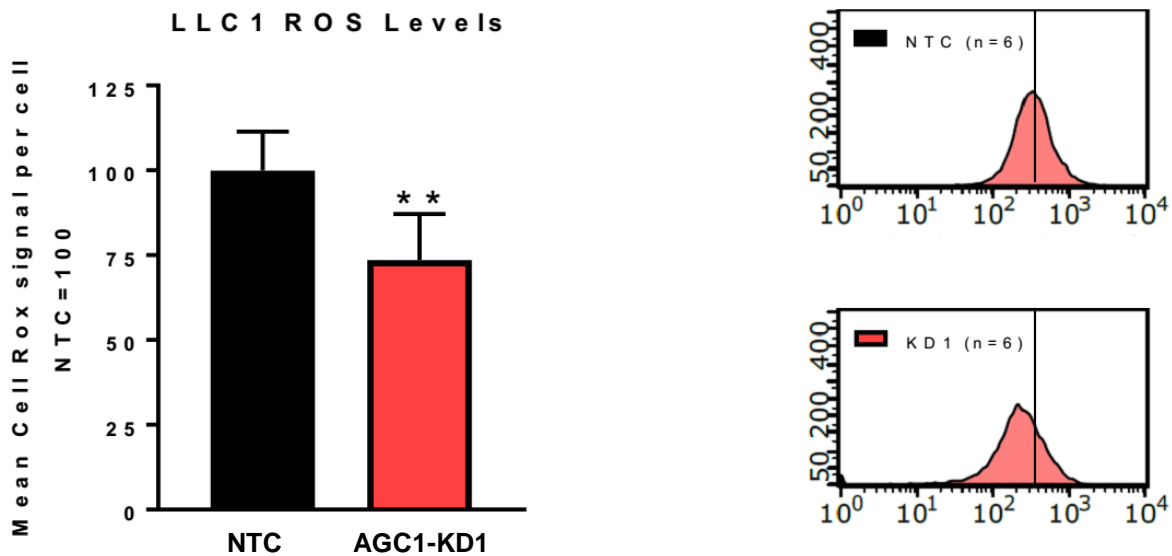


Figure 42: AGC1-knockdown cells have lower baseline levels of ROS. Relative levels of reactive oxygen species in control (NTC) and AGC1-KD LLC1 cells cultured in full DMEM.

3.15 AGC1-KD impaired myogenic differentiation of C2C12 (Supplementary Finding)

Because AGC1 expression is very high in skeletal muscle (Begum et al., 2002), we wanted to test whether its expression would affect myogenic differentiation. During the differentiation of C2C12 cells, both mRNA and protein levels of AGC1 are strongly upregulated during myogenesis in C2C12 cells (Figure 43A). Morphologically, AGC1-KD cells appeared unhealthy after 6 days of differentiation and could not form myotubes (Figure 43B). Confirming defective myogenesis, protein levels of myosin heavy chain II (MHCII), a differentiation marker (Kim et al., 2015), were significantly reduced in differentiated AGC1-KD C2C12 cells, compared to controls (Figure 43C). Interestingly, the mRNA levels of the transcription factors involved in myogenesis (Myf5, MyoD, MyoG) and satellites marker (Pax7) were not changed in AGC-KD cells (data not shown), suggesting that impaired differentiation is not due a genetic regulation. We suspect that the metabolic dysregulation that impairs cell survival and proliferation in AGC1-KD cells also affect myogenesis. We determined that the levels of aspartate and several other amino acids were significantly lower in our stable-knockdown model (data not are shown) unlike recent reports on transient AGC1 silencing after myogenic differentiation (Agudelo et al., 2019). However, supplementing cells aspartate failed to rescue the differentiation of AGC1-KD cells, contrary to the proliferation of phenotype. Likewise, increasing levels of non-essential or essential amino acids in differentiation media also could not improve the differentiation of AGC1-KD cells, suggesting a more complicated mechanism is at work. Therefore, which branches of metabolism cause this deficiency remain to be investigated, and these findings could lead to follow-up projects, targeting to identify metabolic requirements of muscle differentiation.

RESULTS

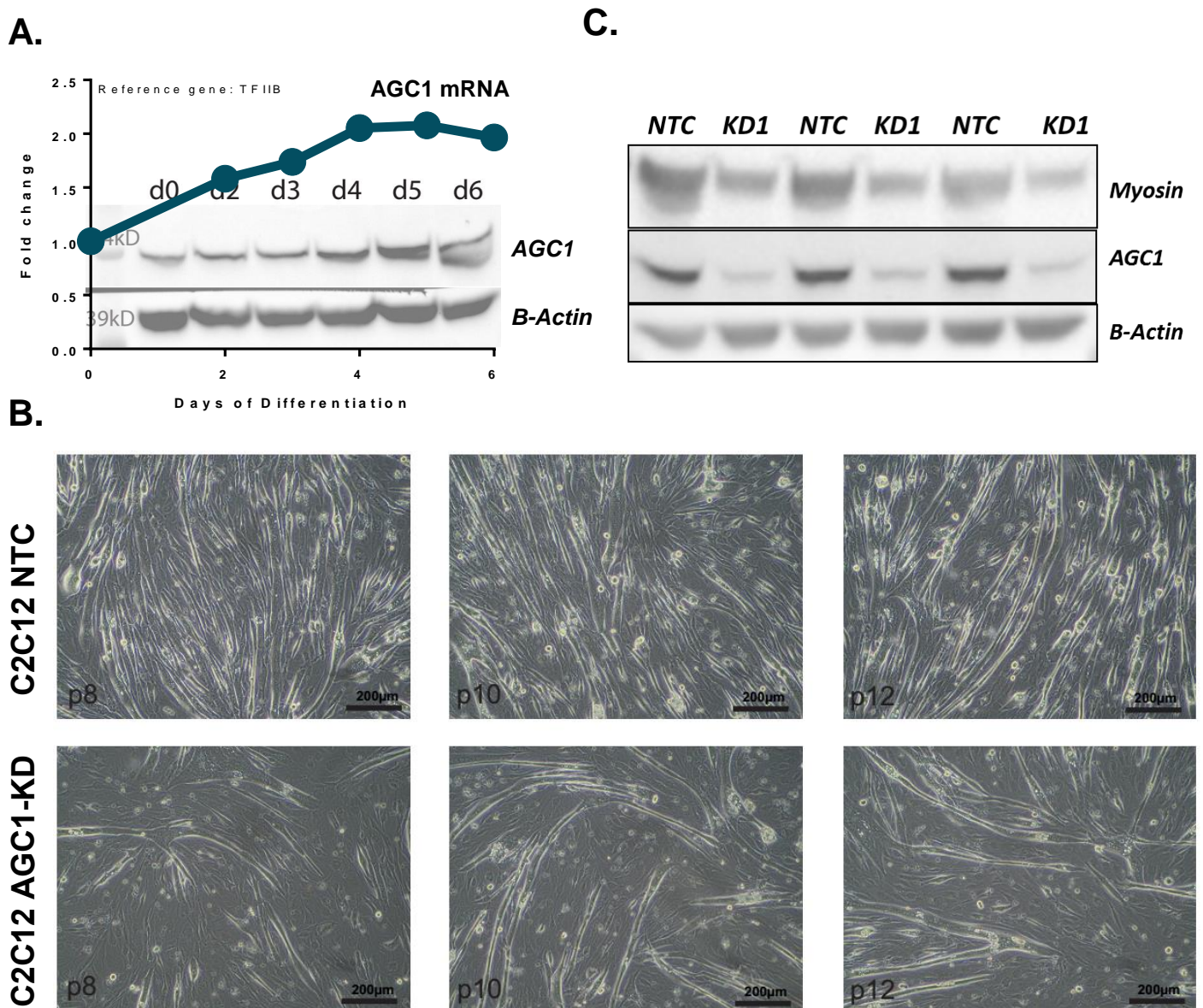


Figure 43: AGC1-KD impaired myogenic differentiation of C2C12. (A) mRNA and protein levels of AGC1 throughout the myogenic differentiation of C2C12 cells. (B) Representative pictures of myotube formation in control (NTC) and AGC1-KD C2C12 cells six days after myogenic induction. (C) Western blot analysis of Myosin Heavy Chain, AGC1 and B-Actin protein in control (NTC) and AGC1-KD C2C12 cells six days after myogenic induction.

DISCUSSION

4. Discussion

4.1 High mitochondrial export or exogenous aspartate supply maintain cell proliferation and survival when glutamine is limiting

As detailed in our published manuscript (Alkan et al., 2018; Alkan and Bogner-Strauss, 2019), this thesis presents three main conclusions that could be important for understanding metabolism of cell proliferation and inventing new ways to target cancers: 1) the primary function of glutamine anaplerosis is to produce aspartate, 2) the decline in cytosolic aspartate levels can induce cell death, and 3) blocking cytosolic aspartate levels sensitizes resistant tumors to glutaminase inhibition.

Our discovery that AGC1-depleted cells are vulnerable to glutaminase inhibition is in line with a recent report pointing out that AGC1-deficient neuroblastoma cells grow slower in low-glutamine media (Profilo et al., 2017) and provides a more mechanistic understanding as to why AGC1 function is required. Based on our results, one crucial function of AGC1 appears to maintain the proliferation/survival of glutamine-deprived cells by supplying aspartate to the cytosol. Although we concluded that cytosolic aspartate becomes limiting for de novo nucleotide biosynthesis when glutamine metabolism is compromised, other paths of aspartate could be more important for other conditions. It is also very important to state that, when we rescue one fate of aspartate by exogenous supplementations, more aspartate will be accessible for the other pathways, making it challenging to reach to a definitive conclusion that nucleotide synthesis is the only crucial fate of aspartate, especially when we observe clear correlations among non-essential amino acids, TCA cycle intermediates, and cytosolic aspartate levels in glutamine distress. Another important fate of aspartate we failed to address in this study was the use of aspartate for protein synthesis because it is almost impossible to specifically rescue the proteinogenic function of aspartate in the same way that aspartate use for de novo nucleotide biosynthesis is rescued by supplementation of exogenous bases. We presume that the role of aspartate in protein synthesis may be equally or more important in the cell lines we studied.

Moreover, because AGC1 and AGC2, structurally and functionally, are very much alike (Thangaratnarajah et al., 2014) and found at varying levels in different cell types (Begum et al., 2002) AGC2 loss could be more fatal for some cell types than AGC1 loss. More importantly, the total ablation of both isoforms simultaneously could lead to a more drastic metabolic limitation to hinder cell survival, even when glutamine and/or pyruvate present.

DISCUSSION

Central carbon metabolism and glutamine dependence in cancer can be manipulated by the environment (Davidson et al., 2016). For instance, Muir et al. discovered that high cystine concentration in conventional cell culture media stimulate glutaminase activity and lead to an artificial dependency on glutamine (Muir et al., 2017). In accordance with these observations, glutamine anaplerosis is remarkably lower in some cancers *in vivo* where glucose and lactate become the predominant contributors feeding the TCA cycle. (Davidson et al., 2016; Hensley et al., 2016; Faubert et al, 2017). Similar to the effects of supra-physiological cystine levels, we speculate that higher ratios of mitochondrial NAD⁺/NADH could also boost oxidative mitochondrial pathways and push glutamine flux into aspartate production. We detected that AGC1-KD suppressed reductive glutamine metabolism in C2C12 cells while the baseline levels of reductive carboxylation in LLC1 cells were too low to be inhibited via AGC1-KD (Figure 19). However, in a hypoxic tumor microenvironment where reductive carboxylation is expected to be a more prominent AGC1-loss might have the same effect on LLC1 that could be another explanation why AGC1-KD tumors are sensitive to glutaminase inhibition *in vivo*.

In mammalian cells, the mitochondrial isoform of glutaminase KGA (GAC, also known as glutaminase C) is the enzymatically most effective glutaminase isoform and is often associated with cancer and glutamine anaplerosis (Cassago et al., 2012). When GAC is inhibited by CB-839 treatment, cells may try to compensate for the lack of mitochondrial glutaminolysis via utilizing cytosolic glutamate as an alternative. Since AGC1 is an anti-porter that exports aspartate from mitochondria in exchange of cytosolic glutamate, a drop in mitochondrial glutamate levels are also expected, which can be partly responsible for the glutamine dependency and the CB-839 toxicity in AGC1-KD cells. Consistently, the TCA cycle contribution of [U¹³C]glutamate was lower in AGC1-KD cells compared to controls (Figure 31). This suggests that glutamate entry to mitochondria might be damaged, however, it does not inherently prove that reduced mitochondrial glutamate uptake is the primary cause of glutamine dependency in AGC1-KD cells. First, in addition to AGC2 (Slc25a13) that is functionally identical to AGC1 (Slc25a12), there are two other mitochondrial transporters (Slc25a22 and Slc25a18) that import glutamate (Palmieri, 2013), and these transporters may sustain some mitochondrial glutamate delivery in AGC1-KD cells. Nevertheless, glutamate is still required to be deaminated and converted to alpha-ketoglutarate (either via transaminases or glutamate dehydrogenase) to feed the TCA cycle, and we have no indication to speculate that mitochondrial alpha-ketoglutarate was affected. Supporting this, alpha-ketoglutarate supplementation failed to completely recover glutamine limitation when aspartate production is inhibited via AOA or siRNA. These findings are more in line with cytosolic aspartate delivery function of AGC1 being more crucial to endure glutamine limitations than its role to uptake glutamate into mitochondria.

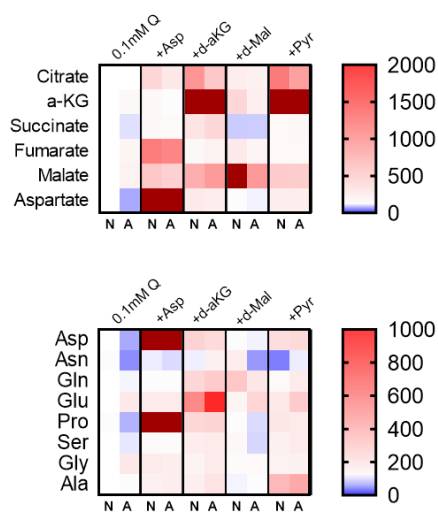
DISCUSSION

Upon glutamine starvation, we observed that the enzymes using aspartate in the cytosol (Got1 and Asns) are upregulated but the mitochondrial isoform (Got2) is downregulated (Figure 28C). Likewise, other cytosolic transaminases are also upregulated, while the mitochondrial isoforms of the same transaminases remain either unchanged or are down-regulated (Figure 28C). Even though we are hesitant to make major conclusions based solely on mRNA data, we believe these findings can hint that regulating cytosolic amino acid metabolism could be more important than regulating mitochondrial amino acid metabolism to cope with glutamine starvation. This might be due to cells needing to rewire their nitrogen metabolism as the major nitrogen donor is missing (Walker and Van der Donk, 2016).

It is important to note that despite having comparable effects on certain conditions, glutamine starvation and CB-839 treatment are not exactly identical. Low levels or depletion of glutamine undermines more pathways than CB-839 treatment which only blocks the consumption of glutamine by the glutaminase enzyme predominantly located in the mitochondria and therefore is selectively more important for TCA cycle metabolism. This is why reduction of cell proliferation/survival and the levels of certain non-essential amino acids and TCA metabolites were more noticeable in low-glutamine treatment than CB-839. However, because AGC1-loss synergizes with both glutaminase inhibition and glutamine starvation in a comparable manner, impaired TCA cycle anaplerosis is likely to be the reason why AGC1-KD cells are more sensitive to glutamine withdrawal than control cells.

Mitochondrial transporters can be notoriously unspecific and carry several different metabolites across membranes with varying binding efficiencies (Fiermonte et al., 2009; Gutierrez-Aguilar and Baines, 2013). For example, uncoupling protein 2 (UCP2) can export aspartate and other four-carbon intermediates across the mitochondrial membrane (Vozza et al., 2014). Based on this knowledge, we hypothesized that various mitochondrial transporters, including AGC2, sustain some degree of cytosolic aspartate delivery in AGC1-KD cells when anaplerotic substrates (such as pyruvate and alpha-ketoglutarate) are present and therefore mitochondrial aspartate levels are sufficiently high. Unexpectedly, another anaplerotic substrate Dimethylmalate (dMal, a cell-permeable form of malate) (Heart et al., 2009) failed to improve cell proliferation or survival following low glutamine or CB-839 treatment (Figure 27C), was unable to recover intracellular aspartate levels (Figure 44) or other TCA intermediates. Relative levels of some TCA cycle intermediates were even decreased upon dMal supplementation, implying that dMal is likely to have toxic effects on cells other than solely supplying four carbon units to the TCA cycle.

C2C12 Cells



LLC1 Cells

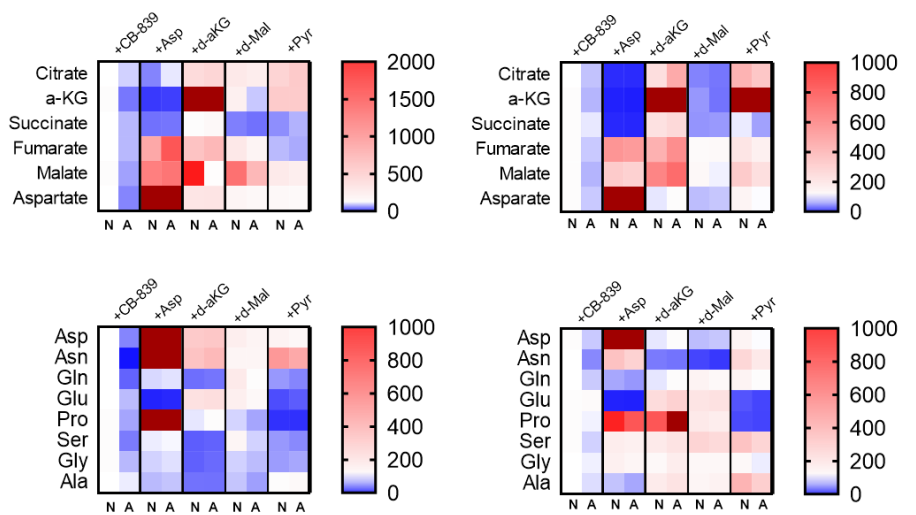


Figure 44: Relative changes in levels of intracellular TCA cycle intermediates and non-essential amino acids in low glutamine and glutaminase inhibition. Relative intracellular levels of TCA cycle intermediates and non-essential amino acids in C2C12 or LLC1 cells cultured in low glutamine or with CB-839, normalized to levels of individual metabolites in control cells under low glutamine or CB-839 treated conditions. (Mean of n=3 are shown)

We included pyruvate in our experiments because similar to aspartate, it can both feed the TCA cycle and improve the NAD⁺/NADH ratio. We hypothesized that if recovering NAD⁺/NADH ratio was limiting for AGC1-KD cells in glutamine starvation, pyruvate cannot rescue cell survival in the presence of transaminase inhibitor AOA. Despite all the evidence to the contrary, pyruvate rescue was not affected by AOA treatment, similar to aspartate rescue which requires transamination to improve the NAD⁺/NADH ratio. We were perplexed by this inconsistency, and in trying to sort out why, we realized that a non-enzymatic condensation of pyruvate and aminooxyacetate (AOA) has been reported in the literature (Zhang et al., 2011) and that this could explain our inconsistent results. Given this complication, we excluded pyruvate from AOA-related mechanistic experiments and used Got1/2 siRNA as a more direct way to explore whether pyruvate can rescue loss of aspartate transamination, and found that knockdown of Got1 and Got2 diminishes the ability of pyruvate to rescue cells in low glutamine (Figure 30), suggesting that the need of cytosolic aspartate to recover cell survival under glutamine limitation is independent of its potential impact on NAD⁺/NADH ratio. Consistently, we found that low glutamine inherently does not cause a significant drop in this ratio, nor was this ratio affected by aspartate supplementation (Figure 45A). Furthermore, duroquinone treatment (which can independently

DISCUSSION

regenerate NAD⁺ (Merker et al., 2006; Gui et al., 2016)) was unable to rescue proliferation in low glutamine (Figure 45B), further confirming that regenerating NAD⁺ is not most limiting in these conditions.

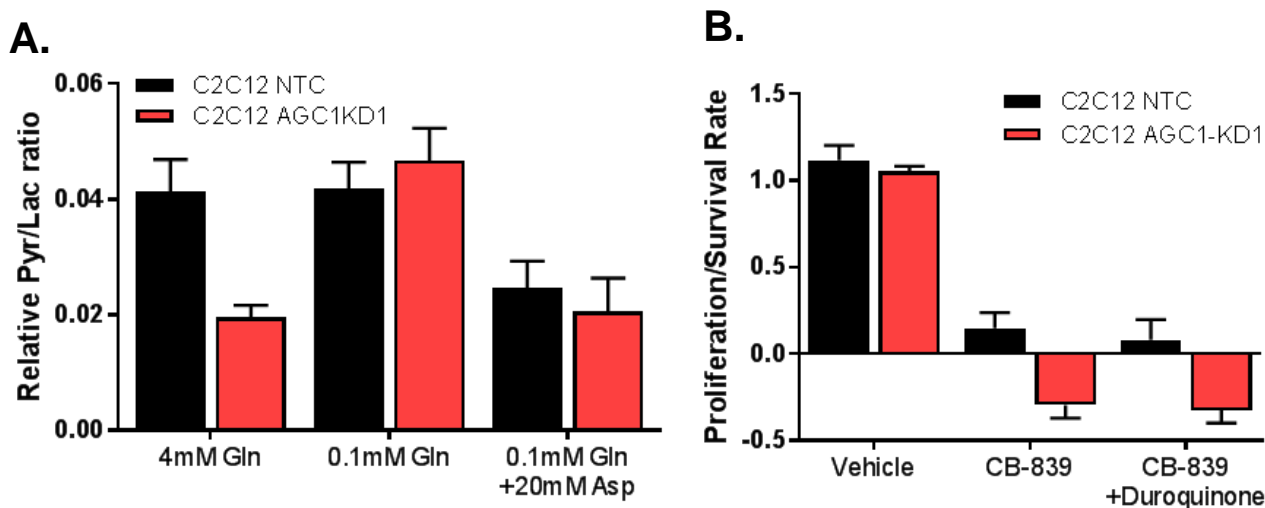


Figure 45: Aspartate is not required to regenerate NAD⁺ in order to rescue glutamine limitations. (A) Pyruvate/lactate ratio and (B) duroquinone treatment of cells cultured in low glutamine or following CB-839 treatment, for cells cultured with or without aspartate (Asp, 20mM), (n=3, SD are shown).

Throughout the study, we considered asparagine levels as a proxy for cytosolic aspartate for cell culture experiments because asparagine is produced from aspartate in the cytosol and is not found in our culture conditions. On the other hand, there is a circulating asparagine in mouse plasma (Rivera et al., 1987). This may illustrate why asparagine levels of AGC1-KD tumors are comparable to controls *in vivo*. Strikingly, intra-tumor asparagine levels were strongly increased following CB-839 treatment consistently in both control and AGC1-KD tumors, unlike any other measured metabolite except glutamine of which consumption is directly blocked by CB-839. This finding is consistent with reports suggesting that the expression of asparagine synthase (ASNS) is upregulated when cells develop resistance to CB-839 (Biancur et al., 2017). This may be explained by a recently proposed anti-apoptotic role for asparagine (Zhang et al., 2014). Notably, exogenous asparagine had no impact on CB-839 treated cell *in vitro* in our experimental models, this might be different if cells were adapted to grow in the presence of glutaminase inhibitors (Krall et al., 2016). According to our understanding, an increase in asparagine levels and ASNS may solely be a side-effect of glutamine accumulation. In addition, aspartate is also not a proper proxy for cytosolic aspartate levels in low-glutamine experiments, because another substrate required for asparagine production is cytosolic glutamine, in which case there is no way distinguishing between whether cytosolic aspartate or cytosolic glutamine levels were dictating asparagine concentration.

DISCUSSION

Aspartate levels can be a sole limitation for tumor growth *in vivo* (Sullivan et al., 2018, Birsoy 2018) and we observed that AGC1-loss plummets cytosolic aspartate levels and increases dependence on glutaminase activity. Similarly, cellular starvation response mechanisms following glutamine withdrawal can also stimulate aspartate uptake (Tajan et al., 2018). Our observations propose that combination therapy with low-toxicity drugs targeting aspartate production -such as Metformin- (Gui et al., 2016) and glutaminolysis (such as CB-839) could be synergistic. Because our study highlights that mitochondrial aspartate export plays a crucial role in maintaining cytosolic aspartate levels, especially in conditions where the main source of the TCA cycle is depleted, a potential small-molecule inhibitor targeting AGCs could sensitize resistant tumors to glutaminase treatment.

Despite aiming to be mechanistically detailed, our study has limitations on including the number of cancer models with various genetic backgrounds and different tissues of origin and these are critical elements to consider before targeting metabolism (Mayers et al., 2016; Yuneva et al., 2012). Therefore, future work is essential to determine the subset of cancers that more likely to respond to our proposed combination therapy alternatives. Because total loss or loss-of-function mutations of AGC1 in mice or in humans, respectively, instigate epilepsy-like seizures, impaired motor coordination, and neuronal degeneration (Falk et al., 2014; Jalil et al., 2005; Sakurai et al., 2010; Wibom et al., 2009), while the loss of AGC2 cause urea cycle-associated disorder type II-citrullinemia (Saheki et al., 2002; Yasuda et al., 2000); it is also paramount to study potential toxicities of AGC1 inhibition in non-cancerous tissues. For instance, we also observed that AGC1-KD strongly inhibited the differentiation of C2C12 cells into muscles, and this phenotype should be further examined *in vivo*. Similarly, AGC1-KD impairs pancreatic beta-cell function *in vitro* (Rubi et al., 2008), Furthermore, considering the TCGA data on the poor prognosis of the cancer patient with lower AGC1 expression and our observation that the loss of AGC1 promotes metastatic phenotype in B16F10 and LLC1 cells, a potential cancer therapy involving AGCs might be a long way ahead. Nevertheless, my thesis work provides solid evidence that tumor-specific deletion of AGC1 impairs tumor growth and this effect can be exacerbated by glutaminase inhibition via CB-839.

In conclusion, this thesis presents proof that one primary role of the TCA cycle in proliferating cells is to produce aspartate which is used for further biosynthetic pathways in the cytosol. Because providing exogenous aspartate is sufficient to sustain cell proliferation and survival when the TCA cycle is shut-down, we speculate that mitochondrial energy production is not crucial for cell proliferation, suggesting that glycolysis-derived ATP can fulfill energy needs of a proliferating cell. Moreover, this thesis also emphasizes that local concentrations (i.e. mitochondria) of a metabolite (i.e. aspartate) or the amount of

its transporter (i.e. AGC1) could be the decisive component regulating cell proliferation or survival in certain nutrient starvation (glutamine).

4.2 Knockdown of AGC1 increased the pulmonary metastatic capacity of LLC1 and B16F10 cells

One of the most unexpected findings throughout my thesis work was that mice bearing AGC1-deficient tumors did not exhibit any improved survival despite smaller tumors and if anything, they showed tendencies to die earlier. Because we were more concerned about the metabolic roles of AGC1 and its impact on tumor growth at the time, we first did not design the mouse experiments specifically to investigate this phenomenon. In one of the first preliminary experiments, we noticed that mice with AGC1-KD tumors gained less weight compared to control cells after tumor weights were subtracted (data not shown). Within the same experiment, mice with AGC1-KD tumors also had smaller skeletal muscles. We did not follow-up because of this observation because the results were inconsistent among different experiments. However, these experiments were designed to monitor tumor growth and drug-responsivity, and therefore a fewer number of cells were injected subcutaneously to the mice. Injecting a higher number of cells intramuscularly as in cachexia studies might provide more consistent results.

Because increased lung metastasis capacity of AGC1-KD tumors was more consistent than cachexia, we decided to give our priority to investigate as to why AGC1-KD has this unexpected advantage. First, we tried to explore this phenotype *in vitro* where we can manipulate the environment more easily. However, despite several trials of migration, invasion or sphere formation assays, we failed to find a condition where AGC1-KD cells performed better than controls (data not shown). The only difference between control and AGC1-KD cells was that it can potentially explain the peculiar metastatic phenotype was that AGC1-KD cells have lower levels of ROS in full media conditions. Maintaining oxidative stress is a crucial challenge for cells to survive in circulation (Fendt, 2017). It is reported that metastasizing cells deregulate cellular pathways to either prevent the production of reactive oxygen species (ROS) or to better detoxify existing ROS (Peiris-Pagès et al., 2015; Piskounova, et al., 2015). Because AGC1-KD cells have lower levels of intracellular ROS levels, this mechanism might explain their metastatic phenotype. To investigate whether superior metastatic capacity of AGC1-KD cells are due to higher chance of survival in circulation and having lower ROS levels, future experiments including a measure of cell survival under oxidative stress and a metastasis assay where tumors were treated with agent either increasing (BSO treatment) or diminishing (NAC treatment) are required.

REFERENCES

5. References

Agudelo, L. Z., Ferreira, D. M. S., Dadvar, S., Cervenka, I., Ketscher, L., Izadi, M., Zhengye, L., Furrer, R., Handschin, C., Venckunas, T., Brazaitis, M., Kamandulis, S., Lanner, J. T. & Ruas, J. L. (2019). Skeletal muscle PGC-1alpha1 reroutes kynurenine metabolism to increase energy efficiency and fatigue-resistance. *Nat Commun*, 10, 2767.

Ahn, C.S., and Metallo, C.M. (2015). Mitochondria as biosynthetic factories for cancer proliferation. *Cancer & metabolism* 3, 1.

Alberts, B., Johnson, A., Lewis, J., Raff, M., Robests, K., Walter, P. *The Molecular Biology of The Cell*. 5th Edition. New York: Garland Science; (2008). Section 20, Cancer.

Alkan, H. F., Walter, K. E., Luengo, A., Madreiter-Sokolowski, C. T., Stryeck, S., Lau, A. N., ... Bogner-Strauss, J. G. (2018). Cytosolic Aspartate Availability Determines Cell Survival When Glutamine Is Limiting. *Cell Metabolism*, 28(5). doi: 10.1016/j.cmet.2018.07.021

Alkan, H. F., & Bogner-Strauss, J. G. (2019). Maintaining cytosolic aspartate levels is a major function of the TCA cycle in proliferating cells. *Molecular & Cellular Oncology*, 6(5). doi: 10.1080/23723556.2018.1536843

Amoedo, N.D., Punzi, G., Obre, E., Lacombe, D., De Grassi, A., Pierri, C.L., and Rossignol, R. (2016). AGC1/2, the mitochondrial aspartate-glutamate carriers. *Biochimica et biophysica acta* 1863, 2394-2412.

Bardeesy, N., Aguirre, A.J., Chu, G.C., Cheng, K.H., Lopez, L.V., Hezel, A.F., Feng, B., Brennan, C., Weissleder, R., Mahmood, U., et al. (2006). Both p16(Ink4a) and the p19(Arf)-p53 pathway constrain progression of pancreatic adenocarcinoma in the mouse. *Proceedings of the National Academy of Sciences of the United States of America* 103, 5947-5952.

Begum, L., Jalil, M.A., Kobayashi, K., Iijima, M., Li, M.X., Yasuda, T., Horiuchi, M., del Arco, A., Satrustegui, J., and Saheki, T. (2002). Expression of three mitochondrial solute carriers, citrin, aralar1 and ornithine transporter, in relation to urea cycle in mice. *Biochimica et biophysica acta* 1574, 283-292.

Berg, J. M., Tymoczko, J. L., Stryer, L. *Biochemistry*. 5th edition. New York: W H Freeman; (2002). Section 18.5, Many Shuttles Allow Movement Across the Mitochondrial Membranes.

Biancur, D.E., Paulo, J.A., Malachowska, B., Del Rey, M.Q., Sousa, C.M., Wang, X., Sohn, A.S.W., Chu, G.C., Gygi, S.P., Harper, J.W., et al. (2017). Compensatory metabolic networks in pancreatic cancers upon perturbation of glutamine metabolism. *Nature communications* 8, 15965.

Birsoy, K., Wang, T., Chen, W.W., Freinkman, E., Abu-Remaileh, M., and Sabatini, D.M. (2015). An Essential Role of the Mitochondrial Electron Transport Chain in Cell Proliferation Is to Enable Aspartate Synthesis. *Cell* 162, 540-551.

REFERENCES

Bogner-Strauss, J.G. (2017). N-Acetylaspartate Metabolism Outside the Brain: Lipogenesis, Histone Acetylation, and Cancer. *Frontiers in endocrinology* 8, 240.

Cancer Research UK, <https://www.cancerresearchuk.org/health-professional/cancer-statistics/worldwide-cancer/mortality#heading-Zero>, Accessed [10] [2018].

Cantor, J.R., and Sabatini, D.M. (2012). Cancer cell metabolism: one hallmark, many faces. *Cancer discovery* 2, 881-898.

Cassago, A., Ferreira, A.P., Ferreira, I.M., Fornezari, C., Gomes, E.R., Greene, K.S., Pereira, H.M., Garratt, R.C., Dias, S.M., and Ambrosio, A.L. (2012). Mitochondrial localization and structure-based phosphate activation mechanism of Glutaminase C with implications for cancer metabolism. *Proceedings of the National Academy of Sciences of the United States of America* 109, 1092-1097.

Catalina-Rodriguez, O., Kolukula, V.K., Tomita, Y., Preet, A., Palmieri, F., Wellstein, A., Byers, S., Giaccia, A.J., Glasgow, E., Albanese, C., et al. (2012). The mitochondrial citrate transporter, CIC, is essential for mitochondrial homeostasis. *Oncotarget* 3, 1220-1235.

Chen, R., Zou, Y., Mao, D., Sun, D., Gao, G., Shi, J., Liu, X., Zhu, C., Yang, M., Ye, W., et al. (2014). The general amino acid control pathway regulates mTOR and autophagy during serum/glutamine starvation. *The Journal of cell biology* 206, 173-182.

Christensen, C.E., Karlsson, M., Winther, J.R., Jensen, P.R., and Lerche, M.H. (2014). Non-invasive in-cell determination of free cytosolic [NAD⁺]/[NADH] ratios using hyperpolarized glucose show large variations in metabolic phenotypes. *The Journal of biological chemistry* 289, 2344-2352.

Contreras, L., Gomez-Puertas, P., Iijima, M., Kobayashi, K., Saheki, T. & Satrustegui, J. (2007). Ca²⁺ Activation kinetics of the two aspartate-glutamate mitochondrial carriers, aralar and citrin: role in the heart malate-aspartate NADH shuttle. *J Biol Chem*, 282, 7098-106.

Cory, J.G., and Cory, A.H. (2006). Critical roles of glutamine as nitrogen donors in purine and pyrimidine nucleotide synthesis: asparaginase treatment in childhood acute lymphoblastic leukemia. *In vivo* 20, 587-589.

Davidson, S.M., Papagiannakopoulos, T., Olenchock, B.A., Heyman, J.E., Keibler, M.A., Luengo, A., Bauer, M.R., Jha, A.K., O'Brien, J.P., Pierce, K.A., et al. (2016). Environment Impacts the Metabolic Dependencies of Ras-Driven Non-Small Cell Lung Cancer. *Cell metabolism* 23, 517-528.

DeBerardinis, R.J., and Chandel, N.S. (2016). Fundamentals of cancer metabolism. *Science advances* 2, e1600200.

del Arco, A., Morcillo, J., Martinez-Morales, J.R., Galian, C., Martos, V., Bovolenta, P., and Satrustegui, J. (2002). Expression of the aspartate/glutamate mitochondrial carriers aralar1 and citrin during development and in adult rat tissues. *European journal of biochemistry* 269, 3313-3320.

REFERENCES

del Arco, A., Satrustegui J. (1998). Molecular Cloning of Aralar, a New Member of the Mitochondrial Carrier Superfamily That Binds Calcium and Is Present in Human Muscle and Brain. *Journal of Biological Chemistry*. 273(36):23327-23334

Dixon, S.J., Patel, D.N., Welsch, M., Skouta, R., Lee, E.D., Hayano, M., Thomas, A.G., Gleason, C.E., Tatonetti, N.P., Slusher, B.S., et al. (2014). Pharmacological inhibition of cystine-glutamate exchange induces endoplasmic reticulum stress and ferroptosis. *eLife* 3, e02523.

Falk, M.J., Li, D., Gai, X., McCormick, E., Place, E., Lasorsa, F.M., Otieno, F.G., Hou, C., Kim, C.E., Abdel-Magid, N., et al. (2014). AGC1 Deficiency Causes Infantile Epilepsy, Abnormal Myelination, and Reduced N-Acetylaspartate. *JIMD reports* 14, 77-85.

Farber, S. & Diamond, L. K. (1948). Temporary remissions in acute leukemia in children produced by folic acid antagonist, 4-aminopteroyl-glutamic acid. *N Engl J Med*, 238, 787-93.

Faubert, B., Li, K.Y., Cai, L., Hensley, C.T., Kim, J., Zacharias, L.G., Yang, C., Do, Q.N., Doucette, S., Burguete, D., Li, H., Huet, G., Yuan, Q., Wigal, T., Butt, Y., Ni, M., Torrealba, J., Oliver, D., Lenkinski, R.E., Malloy, C.R., Wachsmann, J.W, Young, J.D., Kernstine, K., and DeBerardinis, R.J. (2017) Lactate Metabolism in Human Lung Tumors. *Cell* 171, 358-371.

Fendt, S. M. (2017). Is There a Therapeutic Window for Metabolism-Based Cancer Therapies? *Front Endocrinol (Lausanne)*, 8, 150.

Fernandez, C.A., Des Rosiers, C., Previs, S.F., David, F., and Brunengraber, H. (1996). Correction of ¹³C mass isotopomer distributions for natural stable isotope abundance. *Journal of mass spectrometry : JMS* 31, 255-262.

Fiermonte, G., Paradies, E., Todisco, S., Marobbio, C.M., and Palmieri, F. (2009). A novel member of solute carrier family 25 (SLC25A42) is a transporter of coenzyme A and adenosine 3',5'-diphosphate in human mitochondria. *The Journal of biological chemistry* 284, 18152-18159.

Finley, LWS, Zhang, J, Ye, J, Ward, PS & Thompson, CB (2013), 'SnapShot: Cancer metabolism pathways', *Cell Metabolism*, vol. 17, no. 3. <https://doi.org/10.1016/j.cmet.2013.02.016>

Garcia-Bermudez, J., Baudrier, L., La, K., Zhu, X. G., Fidelin, J., Sviderskiy, V. O., Papagiannakopoulos, T., Molina, H., Snuderl, M., Lewis, C. A., Possemato, R. L. & Birsoy, K. (2018). Publisher Correction: Aspartate is a limiting metabolite for cancer cell proliferation under hypoxia and in tumours. *Nat Cell Biol*, 20, 1228.

Gatenby, R. A. & Gillies, R. J. (2004). Why do cancers have high aerobic glycolysis? *Nat Rev Cancer*, 4, 891-9.

REFERENCES

Greenhouse, W.V., and Lehninger, A.L. (1976). Occurrence of the malate-aspartate shuttle in various tumor types. *Cancer research* 36, 1392-1396.

Gross, M.I., Demo, S.D., Dennison, J.B., Chen, L., Chernov-Rogan, T., Goyal, B., Janes, J.R., Laidig, G.J., Lewis, E.R., Li, J., et al. (2014). Antitumor activity of the glutaminase inhibitor CB-839 in triple-negative breast cancer. *Molecular cancer therapeutics* 13, 890-901.

Gui, D.Y., Sullivan, L.B., Luengo, A., Hosios, A.M., Bush, L.N., Gitego, N., Davidson, S.M., Freinkman, E., Thomas, C.J., and Vander Heiden, M.G. (2016). Environment Dictates Dependence on Mitochondrial Complex I for NAD⁺ and Aspartate Production and Determines Cancer Cell Sensitivity to Metformin. *Cell metabolism* 24, 716-727.

Gutierrez-Aguilar, M., and Baines, C.P. (2013). Physiological and pathological roles of mitochondrial SLC25 carriers. *The Biochemical journal* 454, 371-386.

Hart, I. R. (1979). The selection and characterization of an invasive variant of the B16 melanoma. *Am J Pathol*, 97, 587-600.

Hayasaka, K. & Numakura, C. (2018). Adult-onset type II citrullinemia: Current insights and therapy. *Appl Clin Genet*, 11, 163-170.

Heart, E., Cline, G. W., Collis, L. P., Pongratz, R. L., Gray, J. P. & Smith, P. J. (2009). Role for malic enzyme, pyruvate carboxylation, and mitochondrial malate import in glucose-stimulated insulin secretion. *Am J Physiol Endocrinol Metab*, 296, E1354-62.

Heidelberger, M. (1957). The Formation of Antibodies in Man after Injection of Pneumococcal Polysaccharides. *Proc Natl Acad Sci U S A*, 43, 883-7.

Hensley, C.T., Faubert, B., Yuan, Q., Lev-Cohain, N., Jin, E., Kim, J., Jiang, L., Ko, B., Skelton, R., Loudat, L., et al. (2016). Metabolic heterogeneity in human lung tumors. *Cell* 164, 681–694.

Hosios, A.M., Hecht, V.C., Danai, L.V., Johnson, M.O., Rathmell, J.C., Steinhauser, M.L., Manalis, S.R., and Vander Heiden, M.G. (2016). Amino Acids Rather than Glucose Account for the Majority of Cell Mass in Proliferating Mammalian Cells. *Developmental cell* 36, 540-549.

Jalil, M.A., Begum, L., Contreras, L., Pardo, B., Iijima, M., Li, M.X., Ramos, M., Marmol, P., Horiuchi, M., Shimotsu, K., et al. (2005). Reduced N-acetylaspartate levels in mice lacking aralar, a brain- and muscle-type mitochondrial aspartate-glutamate carrier. *The Journal of biological chemistry* 280, 31333-31339.

Jiang, L., Boufersaoui, A., Yang, C., Ko, B., Rakheja, D., Guevara, G., Hu, Z., and DeBerardinis, R.J. (2017). Quantitative metabolic flux analysis reveals an unconventional pathway of fatty acid synthesis in cancer cells deficient for the mitochondrial citrate transport protein. *Metabolic engineering* 43, 198-207.

REFERENCES

Katt, W. P., Lukey, M. J. & Cerione, R. A. (2017). A tale of two glutaminases: homologous enzymes with distinct roles in tumorigenesis. *Future Med Chem*, 9, 223-243.

Kim, M., Sung, B., Kang, Y. J., Kim, D. H., Lee, Y., Hwang, S. Y., Yoon, J. H., Yoo, M. A., Kim, C. M., Chung, H. Y. & Kim, N. D. (2015). The combination of ursolic acid and leucine potentiates the differentiation of C2C12 murine myoblasts through the mTOR signaling pathway. *Int J Mol Med*, 35, 755-62.

Krall, A.S., Xu, S., Graeber, T.G., Braas, D., and Christofk, H.R. (2016). Asparagine promotes cancer cell proliferation through use as an amino acid exchange factor. *Nature communications* 7, 11457.

Lane, A.N., and Fan, T.W. (2015). Regulation of mammalian nucleotide metabolism and biosynthesis. *Nucleic acids research* 43, 2466-2485.

Lewis, C.A., Parker, S.J., Fiske, B.P., McCloskey, D., Gui, D.Y., Green, C.R., Vokes, N.I., Feist, A.M., Vander Heiden, M.G., and Metallo, C.M. (2014). Tracing compartmentalized NADPH metabolism in the cytosol and mitochondria of mammalian cells. *Molecular cell* 55, 253-263.

Lou, T.F., Sethuraman, D., Dospoy, P., Srivastva, P., Kim, H.S., Kim, J., Ma, X., Chen, P.H., Huffman, K.E., Frink, R.E., et al. (2016). Cancer-Specific Production of N-Acetylaspartate via NAT8L Overexpression in Non-Small Cell Lung Cancer and Its Potential as a Circulating Biomarker. *Cancer prevention research* 9, 43-52.

Lunt, S.Y., and Vander Heiden, M.G. (2011). Aerobic glycolysis: meeting the metabolic requirements of cell proliferation. *Annual review of cell and developmental biology* 27, 441-464.

Mates, J. M., Campos-Sandoval, J. A. & Marquez, J. (2018). Glutaminase isoenzymes in the metabolic therapy of cancer. *Biochim Biophys Acta Rev Cancer*, 1870, 158-164.

Mayers, J.R., Torrence, M.E., Danai, L.V., Papagiannakopoulos, T., Davidson, S.M., Bauer, M.R., Lau, A.N., Ji, B.W., Dixit, P.D., Hosios, A.M., et al. (2016). Tissue of origin dictates branched-chain amino acid metabolism in mutant Kras-driven cancers. *Science* 353, 1161-1165.

Merker, M.P., Audi, S.H., Bongard, R.D., Lindemer, B.J., and Krenz, G.S. (2006). Influence of pulmonary arterial endothelial cells on quinone redox status: effect of hyperoxia-induced NAD(P)H:quinone oxidoreductase 1. *American journal of physiology. Lung cellular and molecular physiology* 290, L607-619.

Metallo, C.M., Gameiro, P.A., Bell, E.L., Mattaini, K.R., Yang, J., Hiller, K., Jewell, C.M., Johnson, Z.R., Irvine, D.J., Guarente, L., et al. (2011). Reductive glutamine metabolism by IDH1 mediates lipogenesis under hypoxia. *Nature* 481, 380-384.

REFERENCES

- Mráček T, Drahotka Z, Houštěk J. (2013). The function and the role of the mitochondrial glycerol-3-phosphate dehydrogenase in mammalian tissues. *Biochimica et Biophysica Acta (BBA) - Bioenergetics.* 1827(3):401-410.
- Muir, A., Danai, L.V., Gui, D.Y., Waingarten, C.Y., Lewis, C.A., and Vander Heiden, M.G. (2017). Environmental cystine drives glutamine anaplerosis and sensitizes cancer cells to glutaminase inhibition. *eLife* 6.
- Mullen, A.R., Hu, Z., Shi, X., Jiang, L., Boroughs, L.K., Kovacs, Z., Boriack, R., Rakheja, D., Sullivan, L.B., Linehan, W.M., et al. (2014). Oxidation of alpha-ketoglutarate is required for reductive carboxylation in cancer cells with mitochondrial defects. *Cell reports* 7, 1679-1690.
- Mullen, A.R., Wheaton, W.W., Jin, E.S., Chen, P.H., Sullivan, L.B., Cheng, T., Yang, Y., Linehan, W.M., Chandel, N.S., and DeBerardinis, R.J. (2011). Reductive carboxylation supports growth in tumour cells with defective mitochondria. *Nature* 481, 385-388.
- Okazaki, A., Gameiro, P.A., Christodoulou, D., Laviollette, L., Schneider, M., Chaves, F., Stemmer-Rachamimov, A., Yazinski, S.A., Lee, R., Stephanopoulos, G., et al. (2017). Glutaminase and poly(ADP-ribose) polymerase inhibitors suppress pyrimidine synthesis and VHL-deficient renal cancers. *The Journal of clinical investigation* 127, 1631-1645.
- Palmieri, F. (2013). The mitochondrial transporter family SLC25: identification, properties and physiopathology. *Molecular aspects of medicine* 34, 465-484.
- Palmieri, L., Pardo, B., Lasorsa, F.M., del Arco, A., Kobayashi, K., Iijima, M., Runswick, M.J., Walker, J.E., Saheki, T., Satrustegui, J., et al. (2001). Citrin and aralar1 are Ca(2+)-stimulated aspartate/glutamate transporters in mitochondria. *The EMBO journal* 20, 5060-5069.
- Peiris-Pagès M, Martinez-Outschoorn U, Sotgia F, Lisanti M. (2015). Metastasis and Oxidative Stress: Are Antioxidants a Metabolic Driver of Progression?. *Cell Metabolism.* 22(6):956-958.
- Piskounova E, Agathocleous M, Murphy M, Hu Z, Huddlestun S, Zhao Z et al. (2015). Oxidative stress inhibits distant metastasis by human melanoma cells. *Nature.* 527(7577):186-191.
- Pochini, L., Scalise, M., Galluccio, M., and Indiveri, C. (2014). Membrane transporters for the special amino acid glutamine: structure/function relationships and relevance to human health. *Frontiers in chemistry* 2, 61.
- Profilo, E., Pena-Altamira, L.E., Corricelli, M., Castegna, A., Danese, A., Agrimi, G., Petralla, S., Giannuzzi, G., Porcelli, V., Sbrana, L., et al. (2017). Down-regulation of the mitochondrial aspartate-glutamate carrier isoform 1 AGC1 inhibits proliferation and N-acetylaspartate synthesis in Neuro2A cells. *Biochimica et biophysica acta* 1863, 1422-1435.

REFERENCES

- Prokesch, A., Graef, F.A., Madl, T., Kahlhofer, J., Heidenreich, S., Schumann, A., Moyschewitz, E., Pristoynik, P., Blaschitz, A., Knauer, M., et al. (2017). Liver p53 is stabilized upon starvation and required for amino acid catabolism and gluconeogenesis. *FASEB journal : official publication of the Federation of American Societies for Experimental Biology* 31, 732-742.
- Radovic, B., Vujic, N., Leopold, C., Schlager, S., Goeritzer, M., Patankar, J.V., Korbelius, M., Kolb, D., Reindl, J., Wegscheider, M., et al. (2016). Lysosomal acid lipase regulates VLDL synthesis and insulin sensitivity in mice. *Diabetologia* 59, 1743-1752.
- Rivera, S., Lopez-Soriano, F.J., Azcon-Bieto, J., and Argiles, J.M. (1987). Blood amino acid compartmentation in mice bearing Lewis lung carcinoma. *Cancer research* 47, 5644-5646.
- Robinson, M. M., Mcbryant, S. J., Tsukamoto, T., Rojas, C., Ferraris, D. V., Hamilton, S. K., Hansen, J. C. & Curthoys, N. P. (2007). Novel mechanism of inhibition of rat kidney-type glutaminase by bis-2-(5-phenylacetamido-1,2,4-thiadiazol-2-yl)ethyl sulfide (BPTES). *Biochem J*, 406, 407-14.
- Rubi, B., del Arco, A., Bartley, C., Satrustegui, J., and Maechler, P. (2004). The malate-aspartate NADH shuttle member Aralar1 determines glucose metabolic fate, mitochondrial activity, and insulin secretion in beta cells. *The Journal of biological chemistry* 279, 55659-55666.
- Saheki, T., Kobayashi, K., Iijima, M., Nishi, I., Yasuda, T., Yamaguchi, N., Gao, H.Z., Jalil, M.A., Begum, L., and Li, M.X. (2002). Pathogenesis and pathophysiology of citrin (a mitochondrial aspartate glutamate carrier) deficiency. *Metabolic brain disease* 17, 335-346.
- Sakurai, T., Ramoz, N., Barreto, M., Gazdoui, M., Takahashi, N., Gertner, M., Dorr, N., Gama Sosa, M.A., De Gasperi, R., Perez, G., et al. (2010). Slc25a12 disruption alters myelination and neurofilaments: a model for a hypomyelination syndrome and childhood neurodevelopmental disorders. *Biological psychiatry* 67, 887-894.
- Satrustegui, J., Contreras, L., Ramos, M., Marmol, P., Del Arco, A., Saheki, T. & Pardo, B. (2007). Role of aralar, the mitochondrial transporter of aspartate-glutamate, in brain N-acetylaspartate formation and Ca(2+) signaling in neuronal mitochondria. *J Neurosci Res*, 85, 3359-66. (a)
- Satrustegui, J., Pardo, B. & Del Arco, A. (2007). Mitochondrial transporters as novel targets for intracellular calcium signaling. *Physiol Rev*, 87, 29-67. (b)
- Sanjana, N.E., Shalem, O., Zhang, F. (2014) Improved lentiviral vectors and genome-wide libraries for CRISPR screening. *Nature Methods*, 11(8):783-784
- Shalem, O., Sanjana, N.E., Hartenian, E., Shi, X., Scott, D.A., Mikkelsen, T., Heckl, D., Ebert, B.L., Root, D.E., Doench, J.G., Zhang, F. (2014). Genome-scale CRISPR-Cas9 knockout screening in human cells. *Science*, 343, 83-7

REFERENCES

- Sullivan, L.B., Gui, D.Y., Hosios, A.M., Bush, L.N., Freinkman, E., and Vander Heiden, M.G. (2015). Supporting Aspartate Biosynthesis Is an Essential Function of Respiration in Proliferating Cells. *Cell* 162, 552-563.
- Sullivan, L.B., Luengo, A., Danai, L.V., Bush, L.N., Diehl, F.F., Hosios, A.M., Lau, A.N., Elmiligy, S., Malstrom, S., Lewis, C.A., et al. (2018). Aspartate is an endogenous metabolic limitation for tumour growth. *Nature cell biology* 20, 782-788.
- Thangaratnarajah, C., Ruprecht, J.J., and Kunji, E.R. (2014). Calcium-induced conformational changes of the regulatory domain of human mitochondrial aspartate/glutamate carriers. *Nature communications* 5, 5491.
- Tajan, M., Hock, A. K., Blagih, J., Robertson, N. A., Labuschagne, C. F., Kruiswijk, F., Humpton, T. J., Adams, P. D. & Vousden, K. H. 2018. A Role for p53 in the Adaptation to Glutamine Starvation through the Expression of SLC1A3. *Cell Metab*, 28, 721-736 e6.
- Vander Heiden, M.G., Cantley, L.C., and Thompson, C.B. (2009). Understanding the Warburg effect: the metabolic requirements of cell proliferation. *Science* 324, 1029-1033.
- Vander Heiden, M.G., and DeBerardinis, R.J. (2017). Understanding the Intersections between Metabolism and Cancer Biology. *Cell* 168, 657-669.
- Voza, A., Parisi, G., De Leonardis, F., Lasorsa, F.M., Castegna, A., Amorese, D., Marmo, R., Calcagnile, V.M., Palmieri, L., Ricquier, D., et al. (2014). UCP2 transports C4 metabolites out of mitochondria, regulating glucose and glutamine oxidation. *Proceedings of the National Academy of Sciences of the United States of America* 111, 960-965.
- Vyas, S., Zaganjor, E., and Haigis, M.C. (2016). Mitochondria and Cancer. *Cell* 166, 555-566.
- Walker, M. C. & Van Der Donk, W. A. (2016). The many roles of glutamate in metabolism. *J Ind Microbiol Biotechnol*, 43, 419-30.
- Warburg, O. (1956). On the origin of cancer cells. *Science* 123, 309-314.
- Weir HK, Anderson RN, Coleman King SM, Soman A, Thompson TD, Hong Y, et al. Heart Disease and Cancer Deaths — Trends and Projections in the United States, (1969–2020). *Prev Chronic Dis* 2016;13:160211. DOI: http://dx.doi.org/10.5888/pcd13.160211external_icon.
- Wibom, R., Lasorsa, F.M., Tohonen, V., Barbaro, M., Sterky, F.H., Kucinski, T., Naess, K., Jonsson, M., Pierri, C.L., Palmieri, F., et al. (2009). AGC1 deficiency associated with global cerebral hypomyelination. *The New England journal of medicine* 361, 489-495.
- Wiechert, W. (2007). The thermodynamic meaning of metabolic exchange fluxes. *Biophysical journal* 93, 2255-2264.

REFERENCES

Williamson, D.H., Lund, P., and Krebs, H.A. (1967). The redox state of free nicotinamide-adenine dinucleotide in the cytoplasm and mitochondria of rat liver. *The Biochemical journal* 103, 514-527.

Wise, D. R., Deberardinis, R. J., Mancuso, A., Sayed, N., Zhang, X. Y., Pfeiffer, H. K., Nissim, I., Daikhin, E., Yudkoff, M., McMahon, S. B. & Thompson, C. B. (2008). Myc regulates a transcriptional program that stimulates mitochondrial glutaminolysis and leads to glutamine addiction. *Proc Natl Acad Sci U S A*, 105, 18782-7.

Wise, D.R., and Thompson, C.B. (2010). Glutamine addiction: a new therapeutic target in cancer. *Trends in biochemical sciences* 35, 427-433.

Yasuda, T., Yamaguchi, N., Kobayashi, K., Nishi, I., Horinouchi, H., Jalil, M.A., Li, M.X., Ushikai, M., Iijima, M., Kondo, I., et al. (2000). Identification of two novel mutations in the SLC25A13 gene and detection of seven mutations in 102 patients with adult-onset type II citrullinemia. *Human genetics* 107, 537-545.

Yuneva, M., Zamboni, N., Oefner, P., Sachidanandam, R., and Lazebnik, Y. (2007). Deficiency in glutamine but not glucose induces MYC-dependent apoptosis in human cells. *The Journal of cell biology* 178, 93-105.

Yuneva, M.O., Fan, T.W., Allen, T.D., Higashi, R.M., Ferraris, D.V., Tsukamoto, T., Mates, J.M., Alonso, F.J., Wang, C., Seo, Y., et al. (2012). The metabolic profile of tumors depends on both the responsible genetic lesion and tissue type. *Cell metabolism* 15, 157-170.

Zand, B., Previs, R.A., Zacharias, N.M., Rupaimoole, R., Mitamura, T., Nagaraja, A.S., Guindani, M., Dalton, H.J., Yang, L., Baddour, J., et al. (2016). Role of Increased n-acetylaspartate Levels in Cancer. *Journal of the National Cancer Institute* 108, djv426.

Zhang, G.F., Sadhukhan, S., Tochtrop, G.P., and Brunengraber, H. (2011). Metabolomics, pathway regulation, and pathway discovery. *The Journal of biological chemistry* 286, 23631-23635.

Zhang, J., Fan, J., Venneti, S., Cross, J.R., Takagi, T., Bhinder, B., Djaballah, H., Kanai, M., Cheng, E.H., Judkins, A.R., et al. (2014). Asparagine plays a critical role in regulating cellular adaptation to glutamine depletion. *Molecular cell* 56, 205-218.

Zong, W.X., Rabinowitz, J.D., and White, E. (2016). Mitochondria and Cancer. *Molecular cell* 61, 667-676.

FIGURE & TABLE LEGENDS

6. Figure and Table Legends

6.1 Figure Legends

Figure 1: Aerobic and anaerobic glycolysis in proliferative and non-proliferative cells.	3
Figure 2: FDG-PET/CT imaging is used to monitor tumor regression.	4
Figure 3: Mitochondria and cancers.	6
Figure 4: Central carbon metabolism in proliferating cells.	8
Figure 5: Glycerol 3-phosphate shuttle	9
Figure 6: Malate-aspartate shuttle	10
Figure 7: Aspartate-glutamate carriers.	11
Figure 8: mRNA expression of MAS components.	31
Figure 9: AGC1 expression in tumor vs healthy tissues.	32
Figure 10: Knockdown of AGC1 decreases proliferation in C2C12, B16F10 and LLC1 cell lines.	33
Figure 11: AGC1 knockdown reduced the proliferation rate.	34
Figure 12: AGC1 knockdown decreases cellular and cytosolic NAD ⁺ /NADH ratio	35
Figure 13: AGC1 knockdown decreases basal mitochondrial oxygen consumption rate	36
Figure 14: AGC1-KD reduced aspartate and asparagine levels.	36
Figure 15: AGC1 overexpression increased proliferation rate, NAD ⁺ /NADH ratio and aspartate levels in C2C12 cells	37
Figure 16: AGC1-knockdown reduced cellular aspartate levels.	37
Figure 17: AGC1-knockdown cells depend on glutamine for survival.	39
Figure 18: AGC1-knockdown cells do not consume more glucose or glutamine.	41
Figure 19: Glutamine is the predominant source of the TCA cycle in both AGC1-knockdown and control cells.	42
Figure 20: AGC1-knockdown C2C12 cells have increased oxidative TCA cycling.	44
Figure 21: Changes of intracellular and media levels of several metabolites in AGC1-knockdown cells.	45
Figure 22: AGC1 protein expression is increased in low glutamine conditions.	46
Figure 23: Aspartate supplementation recovers the viability and proliferation of AGC1-knockdown cells in glutamine limitations.	46

FIGURE AND TABLE LEGENDS

Figure 24: Proliferation/survival rate of eight different cell lines with AGC1-knockdown in glutamine limiting conditions.	47
Figure 25: Proliferation/survival rate of AGC1-KO C2C12 and LLC1 cells.	48
Figure 26: Aspartate levels and pyruvate/lactate ratio in AGC1-KO C2C12 cells.	48
Figure 27: Sustaining cytosolic aspartate levels prevents cell death in glutamine limiting conditions.	50
Figure 28: Changes in non-essential amino acid metabolism under glutamine limitation.	53
Figure 29: Cytosolic aspartate is not crucial for non-essential amino acids in low-glutamine.	54
Figure 30: Cytosolic aspartate is not a crucial feeding TCA cycle or cytosolic NAD ⁺ regeneration in low-glutamine.	56
Figure 31: ¹³ C-Aspartate and ¹³ C-Glutamate tracing in C2C12 cells.	57
Figure 32: Cytosolic aspartate is required to produce nucleotides for maintaining cell survival in glutamine limitations.	59
Figure 33: AGC1-knockdown reduces LLC1 tumor growth.	60
Figure 34: AGC1-deficiency sensitizes tumors to CB-839 treatment.	61
Figure 35: Metabolic profiling of LLC1 tumors.	62
Figure 36: AGC1-knockdown sensitizes AL1376 pancreas allograft tumors to CB-839 treatment.	63
Figure 37: AGC1 is expressed in mouse and human tumors.	65
Figure 38: AGC1-deficient tumors tended to be more lethal for mice.	66
Figure 39: SLC25A12 expression often negatively correlates with cancer prognosis.	67
Figure 40: LLC1 tumors with AGC1-knockdown have higher chance to metastasize.	68
Figure 41: B16F10 cells with AGC1-knockdown have higher pulmonary metastasis capacity.	69
Figure 42: AGC1-knockdown cells have lower baseline levels of ROS.	69
Figure 43: AGC1-KD impaired myogenic differentiation of C2C12.	71
Figure 44: Relative changes in levels of intracellular TCA cycle intermediates and non-essential amino acids in low glutamine and glutaminase inhibition.	76
Figure 45: Aspartate is not required to regenerate NAD ⁺ in order to rescue glutamine limitations.	77

6.2 Table Legends

Table 1: Key resources table.	25
-------------------------------	----

ABBREVIATIONS

ABBREVIATIONS

7. Abbreviations

2-DG	2-deoxyglucose
5-FU	5-fluorouracil
AGC1/2	Mitochondrial aspartate-glutamate carrier 1/2
AMP	Adenosine monophosphate
AOA	aminoxyacetate
Asns	Asparagine synthetase
Atf4	Activating transcription factor 4
ATP	Adenosine triphosphate
BCA	Bicinchoninic acid
BPTES	(bis-2-(5-phenylacetamido-1,2,4-thiadiazol-2-yl)ethyl sulfide)
BSO	Buthionine sulfoximine
CB-839	Calithera Glutaminase Inhibitor Telaglenastat
CACLE	Cancer Cell Line Encyclopedia
daKG	dimethylalpha-ketoglutarate
dMal	dimethylalpha-malate
DMEM	Dulbecco's Modified Eagle Medium
DMSO	Dimethyl sulfoxide
DNA	Deoxyribonucleic Acid
EDTA	Ethylenediaminetetraacetic acid
EsAA	Essential aminoacid
FAD	flavin adenine dinucleotide (oxidized)
FADH ₂	flavin adenine dinucleotide (reduced)
FBS	Fetal Bovine Serum
FCCP	carbonyl cyanide p-trifluoromethoxyphenylhydrazone
FDG-PET	Fluro-deoxyglucose positron-emission-tomography
FITC	Fluorescein isothiocyanate
G3P	glycerol 3-phosphate
GAC	glutaminase kidney isoform, mitochondrial
GC-MS	Gas chromatography–mass spectrometry
GOT1/2	glutamate-oxaloacetate transaminase 1/2
HBSS	Hank's Balanced Salt Solution

ABBREVIATIONS

HS	Horse Serum
IMP	inosine monophosphate
KD	knockdown
KGA	glutaminase kidney isoform
KO	knockout
LC-MS	Liquid chromatography–mass spectrometry
LGA	glutaminase liver isoform
MAS	Malate-Aspartate Shuttle
MDH1/2	malate dehydrogenase
MHCII	myosin heavy chain II
mRNA	messenger Ribonucleic Acid
mRNA-seq	mRNA sequencing
Myf5	Myogenic Factor 5, gene name
MyoD	myoblast determination protein 1, gene name
MyoG	myogenin, gene name
NAA	N-acetyl aspartate
NAC	N-acetyl cystein
NAD+	nicotinamide adenine dinucleotide, oxidized
NADH	nicotinamide adenine dinucleotide, reduced
NEAA	Non-essential amino acid
NMR	Nuclear magnetic resonance spectroscopy
NTC	non-targetting control
OCR	Oxygen Consumption Rate
Pax7	Paired Box 7, gene name
PBS	Phosphate Buffered Saline
PCR	Polymerase Chain Reaction
PI	Propidium Iodide
ROS	Reactive Oxygen Species
RPMI	Roswell Park Memorial Institute Medium
SD	Standard Deviation
SDS	sodium dodecyl sulfate
SEM	Von Hippel-Lindau
shRNA	small-hairpin RNA

ABBREVIATIONS

siRNA	Small interfering RNA
SLC1A3	Excitatory amino acid transporter 1, gene name
SLC25A12	Solute Carrier Family 25 Member 12, gene name of AGC1
SLC25A13	Solute Carrier Family 25 Member 13, gene name of AGC2
Slc7a11	Solute Carrier Family 7 Member 11, gene name
TCA cycle	tricarboxylic acid cycle
TCGA	The Cancer Genome Atlas
VHL	Von Hippel-Lindau syndrome
α -KG	alpha-ketoglutarate
β -actin	beta-actin, protein name

8. Appendices

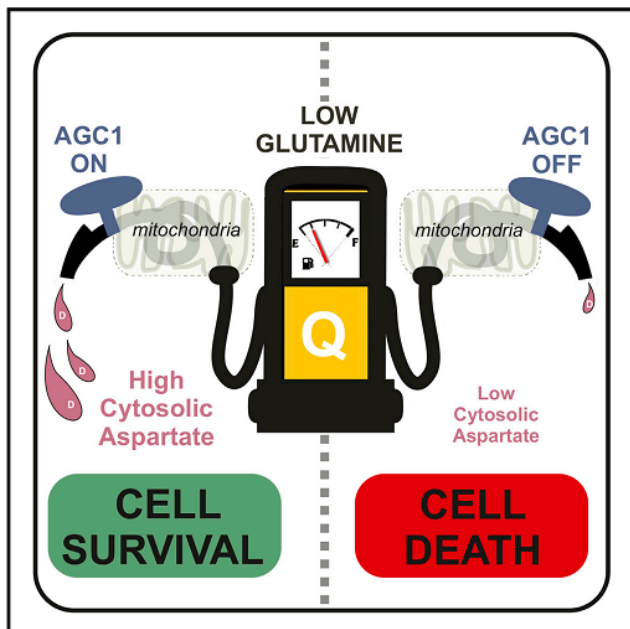
8.1 Published Original Article: Cytosolic Aspartate Availability Determines Cell Survival When Glutamine Is Limiting.

Alkan, H. F., Walter, K. E., Luengo, A., Madreiter-Sokolowski, C. T., Stryeck, S., Lau, A. N., ... **Bogner-Strauss, J. G.** (2018). Cytosolic Aspartate Availability Determines Cell Survival When Glutamine Is Limiting. *Cell Metabolism*, 28(5). doi: 10.1016/j.cmet.2018.07.021

Cell Metabolism

Cytosolic Aspartate Availability Determines Cell Survival When Glutamine Is Limiting

Graphical Abstract



Authors

H. Furkan Alkan, Katharina E. Walter, Alba Luengo, ..., Tobias Madl, Matthew G. Vander Heiden, Juliane G. Bogner-Strauss

Correspondence

mvh@mit.edu (M.G.V.H.),
juliane.bogner-strauss@tugraz.at (J.G.B.-S.)

In Brief

Alkan et al. show that, under conditions in which cytosolic glutamine is limiting, mitochondrial aspartate export, via the aspartate-glutamate carrier 1 (AGC1), supports cell proliferation and cellular redox homeostasis and that AGC1 inhibition can synergize with glutaminase inhibition to limit tumor growth.

Highlights

- Cells lacking the mitochondrial aspartate exporter (AGC1) require glutamine metabolism
- Cytosolic aspartate is required to sustain survival when glutamine is limiting
- Glutamine anaplerosis supports aspartate production
- AGC1 loss sensitizes tumors to glutaminase inhibition *in vivo*



Alkan et al., 2018, Cell Metabolism 28, 706–720
November 6, 2018 © 2018 Published by Elsevier Inc.
<https://doi.org/10.1016/j.cmet.2018.07.021>

CellPress

Cytosolic Aspartate Availability Determines Cell Survival When Glutamine Is Limiting

H. Furkan Alkan,^{1,2} Katharina E. Walter,¹ Alba Luengo,² Corina T. Madreiter-Sokolowski,³ Sarah Stryeck,³ Allison N. Lau,² Wael Al-Zoughbi,⁴ Caroline A. Lewis,⁵ Craig J. Thomas,^{6,7} Gerald Hoefler,^{4,8} Wolfgang F. Graier,^{3,8} Tobias Madl,^{3,8} Matthew G. Vander Heiden,^{2,9,*} and Juliane G. Bogner-Strauss^{1,8,10,*}

¹Institute of Biochemistry, Graz University of Technology, Humboldtstrasse 46/III, 8010 Graz, Austria

²The Koch Institute for Integrative Cancer Research and Department of Biology, Massachusetts Institute of Technology, Cambridge, MA 02139, USA

³Gottfried Schatz Research Center, Molecular Biology and Biochemistry, Medical University of Graz, Neue Stiftingtalstrasse 6/6, A-8010 Graz, Austria

⁴Diagnostic and Research Institute of Pathology, Medical University of Graz, Neue Stiftingtalstraße 6, A-8010 Graz, Austria

⁵Whitehead Institute for Biomedical Research, 455 Main Street, Cambridge, MA 02142, USA

⁶Division of Preclinical Innovation, National Center for Advancing Translational Sciences, National Institutes of Health, Bethesda, MD 20892, USA

⁷Lymphoid Malignancies Branch, National Cancer Institute, Bethesda, MD 20892, USA

⁸BioTechMed-Graz, Graz, Austria

⁹Dana-Farber Cancer Institute, Boston, MA 02115, USA

¹⁰Lead Contact

*Correspondence: mvh@mit.edu (M.G.V.H.), juliane.bogner-strauss@tugraz.at (J.G.B.-S.)

<https://doi.org/10.1016/j.cmet.2018.07.021>

SUMMARY

Mitochondrial function is important for aspartate biosynthesis in proliferating cells. Here, we show that mitochondrial aspartate export via the aspartate-glutamate carrier 1 (AGC1) supports cell proliferation and cellular redox homeostasis. Insufficient cytosolic aspartate delivery leads to cell death when TCA cycle carbon is reduced following glutamine withdrawal and/or glutaminase inhibition. Moreover, loss of AGC1 reduces allograft tumor growth that is further compromised by treatment with the glutaminase inhibitor CB-839. Together, these findings argue that mitochondrial aspartate export sustains cell survival in low-glutamine environments and AGC1 inhibition can synergize with glutaminase inhibition to limit tumor growth.

INTRODUCTION

Proliferation increases the energetic and biosynthetic needs of cells. To meet these demands, proliferating cells alter their metabolism and utilize nutrients differently than non-proliferating cells (Vander Heiden and DeBerardinis, 2017; Cantor and Sabatini, 2012; Warburg, 1956). In culture, most proliferating cells depend on two main carbon sources: glucose and glutamine (Hosios et al., 2016). Although oxidative glucose catabolism is energetically the most efficient means to produce ATP, proliferating cells often exhibit increased lactate production—also known as aerobic glycolysis (Cantor and Sabatini, 2012; Vander Heiden et al., 2009). In addition, glutamine is a primary anaplerotic tricarboxylic acid (TCA) cycle substrate for many cells, making those cells

vulnerable to glutamine withdrawal or glutaminase inhibition by drugs such as CB-839 (Gross et al., 2014; Yuneva et al., 2007).

Despite prominent lactate production, mitochondrial function remains important for proliferating cells (DeBerardinis and Chandel, 2016). Mitochondrial one-carbon metabolism is strongly up-regulated in many cancer types to maintain purine and thymidine biosynthesis (Vyas et al., 2016; Zong et al., 2016). Initiating *de novo* lipogenesis in mitochondria through citrate production is also vital for proliferation in some contexts (Catalina-Rodriguez et al., 2012; Jiang et al., 2017). Another important role for mitochondrial respiration in proliferating cells is to support aspartate production, as aspartate is essential to make protein as well as for purine and pyrimidine biosynthesis (Birsoy et al., 2015; Gui et al., 2016; Sullivan et al., 2015). Because of these biosynthetic roles of mitochondria, movement of macromolecule precursors across the mitochondrial membranes might also become a limitation for tumor growth. For instance, blocking the mitochondrial citrate transporter impairs *de novo* lipogenesis and inhibits cell proliferation in some contexts (Catalina-Rodriguez et al., 2012). In addition, transferring electrons between the cytosolic and mitochondrial compartments may also be important because accumulation of reducing equivalents in either compartment could cause proliferation defects. For instance, inhibiting mitochondrial electron transport leads to NADH accumulation in mitochondria, which hampers oxidation reactions, impairs aspartate synthesis, and slows proliferation (Sullivan et al., 2015). Regenerating cytosolic NAD⁺ is also vital for glycolysis and the biosynthesis of certain amino acids and nucleotides (Lunt and Vander Heiden, 2011). Therefore, understanding the role of mitochondrial transporters in proliferating cells could not only provide insight into cancer metabolism, but also suggest novel cancer drug targets.

The malate-aspartate shuttle (MAS) is important for transferring electrons from cytosolic NADH to the mitochondria, where they can be transferred to oxygen via the electron transport



chain (Greenhouse and Lehninger, 1976). Exchange of mitochondrial aspartate for cytosolic glutamate and a proton by the aspartate-glutamate carrier (AGC) is proposed to be the only irreversible step of the MAS (del Arco et al., 2002). Both AGC isoforms are predicted to be functionally identical (Thangaratnarajah et al., 2014), yet many tissues selectively express one isoform: AGC1 (*SLC25A12*, Aralar) is abundant in brain, skeletal muscle, and pancreatic beta cells, while AGC2 (*SLC25A13*, Citrin) is primarily found in liver and kidney (Begum et al., 2002; Palmieri et al., 2001). Previous studies have shown that AGC1 is involved in neuronal development, supports aspartate and N-acetylaspartate production, and reduces lactate secretion (Jalil et al., 2005; Rubi et al., 2004).

Although MAS activity in tumors has been reported (Greenhouse and Lehninger, 1976) and the expression of AGCs in cancer has been predicted (Amoedo et al., 2016), the functional importance of mitochondrial aspartate-glutamate transport in proliferating cells has not been extensively studied. Here, we show that AGC1 knockdown (KD) slows cell proliferation, reduces the cellular NAD⁺/NADH ratio, and impairs aspartate delivery to the cytosol. We also show that mitochondrial aspartate export is essential for cell survival in glutamine-limited conditions, and that loss of AGC1 can synergize with glutaminase inhibitors to suppress tumor growth. These findings argue that sustaining cytosolic aspartate levels is required for cell survival in low-glutamine environments and suggest that AGC1 might be a target to treat some cancers.

RESULTS

Knockdown of AGC1 Reduces Proliferation Due to Impaired Aspartate Synthesis

AGC1 exports aspartate produced in mitochondria to the cytosol, where it can be used for nucleotide, amino acid, and protein synthesis. In addition, mitochondrial aspartate export can contribute to cytosolic redox homeostasis by serving as a substrate for cytosolic glutamate-oxaloacetate transaminase (Got1, producing oxaloacetate from aspartate) and malate dehydrogenase (Mdh1, reducing oxaloacetate to malate while oxidizing NADH) as part of the MAS (Figures 1A and S1A). mRNA expression analysis suggests that proliferating cells in culture display robust expression of MAS components (Figure S1B).

To test whether AGC1 is important for cell proliferation, we used short hairpin RNA (shRNA) to knock down AGC1 in non-transformed mouse C2C12 myoblasts because AGC1 levels in these cells are about 8-fold higher than AGC2 levels (Figure S1B). We observed that AGC1-KD leads to a slight, yet significant, proliferation rate reduction when cells are cultured in standard DMEM containing 1 mM pyruvate (Figure 1B). Because extracellular pyruvate can act as an electron acceptor to provide oxidized NAD⁺ to cells (Figure 1A), we excluded pyruvate from the media for subsequent experiments unless otherwise indicated. The effect of AGC1-KD on cell proliferation becomes more apparent following pyruvate withdrawal, and this change is rescued by pyruvate or aspartate supplementation (Figure 1C), as reported previously for cells with mitochondrial dysfunction (Birsoy et al., 2015; Sullivan et al., 2015). Interestingly, however, AGC1-KD cells remain viable and retain the ability to proliferate slowly in pyruvate-free media (Figure 1C).

Disruption of the MAS is expected to decrease the NAD⁺/NADH ratio in the cytosol and increase the NAD⁺/NADH ratio in the mitochondria (del Arco et al., 2002). Indeed, the whole-cell NAD⁺/NADH ratio is lower in AGC1-KD cells compared to non-targeting control (NTC) cells, hereafter referred to as control cells (Figure 1D). In addition, because the lactate dehydrogenase reaction is coupled to cytosolic NAD⁺/NADH, the pyruvate/lactate ratio is sometimes used as a proxy for this ratio (Christensen et al., 2014; Williamson et al., 1967), and indeed AGC1-KD cells have a lower pyruvate/lactate ratio (Figure 1E). Basal oxygen consumption rate is also lower in AGC1-KD cells (Figure 1F), a finding that is consistent with the expected increase in mitochondrial NAD⁺/NADH ratio. To determine whether AGC1-KD leads to similar phenotypes in transformed cells, we examined mouse Lewis lung carcinoma (LLC1) cells. As observed in C2C12 cells, AGC1-KD LLC1 cells proliferate slower than control LLC1 cells and have reduced NAD⁺/NADH and pyruvate/lactate ratios (Figures S1C–S1E).

The low NAD⁺/NADH ratio of AGC1-KD cells is accompanied by reduced aspartate levels in both C2C12 and LLC1 cells (Figures 1G and S1F). To assess whether cytosolic aspartate is changed, we examined how AGC1-KD affects asparagine levels, an amino acid that is not present in the culture media, because the conversion of aspartate to asparagine is mediated by the cytosolic enzyme asparagine synthetase (Asns) (Ahn and Metallo, 2015). KD of AGC1 leads to reduced asparagine levels, indicative of lower cytosolic aspartate levels in these cells (Figures 1G and S1F).

We also tested the effects of increased AGC1 expression and found that overexpression of mouse AGC1 promotes C2C12 cell proliferation (Figure S1G). Increased expression of mouse AGC1 elevates whole-cell NAD⁺/NADH ratio and aspartate levels, the opposite of what was observed following AGC1 KD using three independent shRNAs (Figures S1H–S1J). Furthermore, expression of human AGC1 that is resistant to KD rescues the proliferation defect observed in AGC1-KD C2C12 cells (Figure S1K).

AGC1-KD Increases Cellular Dependence on Glutamine

We hypothesized that AGC1-deficient cells maintain proliferation by rewiring metabolism to obtain cytosolic aspartate from a different source. To test this hypothesis, we individually removed glucose or select amino acids from the media and assessed whether these interventions further affected cell proliferation upon AGC1 KD. We found that culturing cells in low glucose (0.5 mM, instead of 25 mM contained in regular DMEM) or with the glycolysis inhibitor 2-deoxyglucose (2-DG) does not affect proliferation or survival of AGC1-KD cells more than control cells (Figure 2A). However, survival of AGC1-KD cells was compromised more than control cells in Hank's Buffered Salt Solution (HBSS) that contains 5.5 mM glucose but lacks amino acids (Figure 2B). Addition of essential amino acids did not rescue this phenotype, but addition of essential amino acids and glutamine to HBSS was able to rescue AGC1-KD cell proliferation to the same degree as control cells (Figure 2B). To further explore whether AGC1-KD alters dependence on glutamine, we cultured cells in DMEM-based low-glutamine media (0.1 mM instead of 4 mM). In line with previous studies (Wise and Thompson, 2010), low glutamine impairs cell proliferation, but in contrast to control cells, AGC1-KD cell survival is compromised in

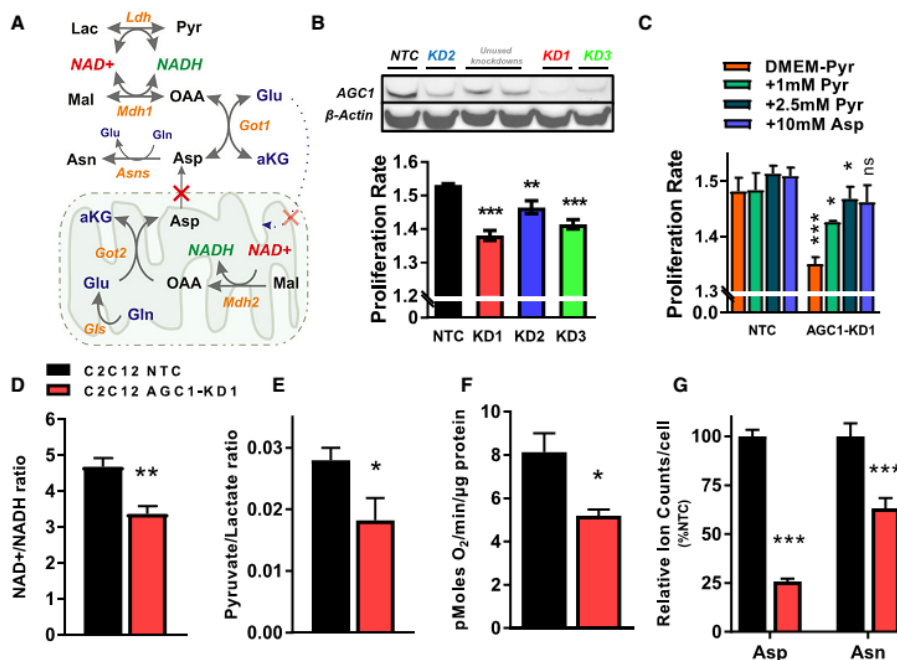


Figure 1. AGC1 Knockdown Decreases Cytosolic Aspartate Levels and Increases Dependence on Exogenous Electron Acceptors

(A) Schematic showing how aspartate can regenerate NAD⁺ in the cytosol through the MAS involving glutamate-oxaloacetate transaminase (Got1) and malate dehydrogenase (Mdh1).
 (B) AGC1 KD in C2C12 cells using different shRNA hairpins was assessed by western blot as shown. Also shown is the fold change in viable cell number (proliferation rate) of control (NTC) and cells expressing three of the five hairpins (KD1, KD2, and KD3) as doublings/day (n = 3).
 (C) Relative proliferation rate of control (NTC) and AGC1-KD1 C2C12 cells in the presence and absence of the indicated concentrations of pyruvate (Pyr) and aspartate (Asp) (n = 3).
 (D) NAD⁺/NADH ratio of control (NTC) and AGC1-KD1 C2C12 cells cultured in pyruvate-free DMEM (n = 5). Means ± SEM are shown.
 (E) Pyruvate to lactate ratio of control (NTC) and AGC1-KD1 C2C12 cells cultured in pyruvate-free media (n = 3).
 (F) Mitochondrial oxygen consumption rate of control (NTC) and AGC1-KD1 C2C12 cells cultured in serum-free, phenol-red free media containing 5 mM glucose, 1 mM sodium pyruvate, and 2 mM glutamine (n = 3, each including 7–8 technical replicates).
 (G) Relative cellular aspartate and asparagine levels of control (NTC) and AGC1-KD1 C2C12 cells cultured in standard DMEM without pyruvate (n = 3).
 All figures denote mean ± SD unless indicated otherwise. *p ≤ 0.05, **p ≤ 0.01, ***p ≤ 0.001. See also Figure S1.

low-glutamine conditions (Figure 2C). Glutamine depletion (0.1 mM) significantly increased the percent of dead and apoptotic cells as measured by Annexin V/promidium iodide (PI) staining in both control and AGC1-KD cells (Figure S1L). Interestingly, AGC1-KD also induced cell death in glutamine-replete media that is further exacerbated by glutamine starvation (Figure S1L). Furthermore, cleaved caspase 3 levels, a marker of apoptotic cells, were increased in low-glutamine conditions, suggesting that glutamine starvation promotes cell death in AGC1-KD cells (Figure S1M).

Glutamine has several fates in cells: it can serve as an exchange factor for import of other amino acids (Pochini et al., 2014), it provides nitrogen for nucleotide biosynthesis (Cory and Cory, 2006), or it can be converted to α-ketoglutarate (α-KG, also known as 2-oxoglutarate) via glutamate to provide carbon for TCA cycle intermediates (anaplerosis) (Wise and Thompson, 2010) (Figure 2D). To narrow down which fate of

glutamine is important for proliferation and viability of AGC1-KD cells, we used the glutaminase inhibitor CB-839 to limit glutamine to glutamate conversion. CB-839 treatment phenocopies the effects of culture in low glutamine on AGC1-KD cells (Figure 2C). These data argue that AGC1-KD cells require glutamine anaplerosis for survival, rather than for other downstream reactions that do not require glutaminase activity.

We next hypothesized that the increased vulnerability of AGC1-KD cells to glutaminase inhibition could be due to an inability to oxidize glucose. To test this, we treated C2C12 cells for 6 hr with CB-839 and measured oxygen consumption. Interestingly, CB-839 treatment reduces mitochondrial oxygen consumption by 50% in both AGC1-KD and control cells, arguing that AGC1-KD cells do not require more glutamine for mitochondrial respiration than control cells (Figure 3A). In addition, there is also no difference in the uptake or consumption rate of glucose and glutamine except that AGC1-KD C2C12 cells show slightly

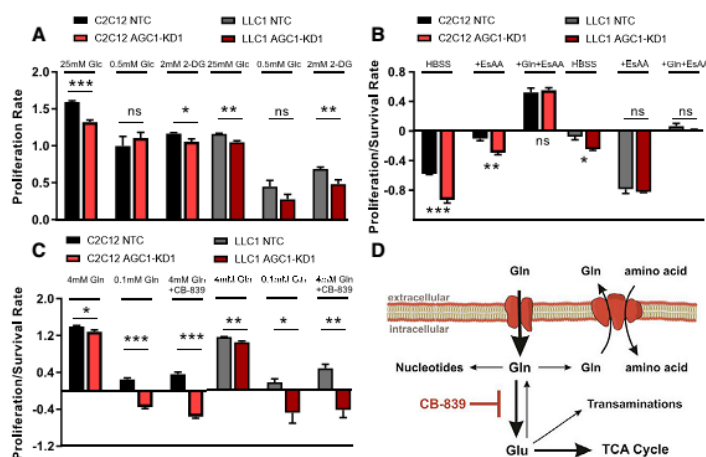


Figure 2. AGC1-KD Cells Are Sensitive to Glutamine Depletion

(A) Proliferation rate of control (NTC) and AGC1-KD (AGC1-KD1) C2C12 and LLC1 cells cultured in pyruvate-free DMEM containing 25 or 0.5 mM glucose (Glc), or 25 mM glucose and 2 mM 2-deoxyglucose (2-DG), as indicated (n = 5).

(B) Proliferation/survival rate of control (NTC) and AGC1-KD1 C2C12 and LLC1 cells cultured in pyruvate-free HBSS containing 5 mM glucose supplemented with 10% FBS and vitamins, with or without essential amino acids (EsAAs) and glutamine (Gln), as indicated (n = 3).

(C) Proliferation/survival rate of control (NTC) and AGC1-KD1 C2C12 and LLC1 cells cultured in pyruvate-free DMEM containing 4 or 0.1 mM glutamine (Gln), or 4 mM glutamine and 1 μ M CB-839 (glutaminase inhibitor), as indicated (n = 5).

(D) Schematic showing some potential fates of glutamine in a cell.

All panels show mean \pm SEM. *p \leq 0.05, **p \leq 0.01, ***p \leq 0.001. See also Figure S1.

elevated glutamate release (Figures 3B, 3C, and S2A–S2C). Of note, only a small fraction of the consumed glutamine could be accounted for by glutamate excretion in either group, suggesting that the elevated glutamate excretion could be a consequence of an increased cytosolic glutamate pool in AGC1-KD cells and is not the cause of glutamine dependency. Consistent with this interpretation, exposure to Erastin, which inhibits activity of the plasma membrane glutamate exporter xCT (*Slc7a11*) (Dixon et al., 2014), has no specific impact on glutaminase-inhibited AGC1-KD cells (Figures S2D and S2E).

Hypoxia and mitochondrial dysfunction both alter the cell NAD⁺/NADH ratio and promote reductive glutamine metabolism (Metallo et al., 2011; Mullen et al., 2011, 2014; Sullivan et al., 2015). To determine whether AGC1-KD cells metabolize nutrients differently, we traced [¹³C]glucose or [¹³C]glutamine fates using gas chromatography-mass spectrometry (GC-MS). We did not observe a major change in labeling from either nutrient such that glutamine remains the predominant source of aspartate and other TCA intermediates, and the relative contribution of glucose and glutamine to the TCA cycle is not drastically altered in AGC1-KD cells (Figures S2F and S2G). However, in alignment with a high mitochondrial NAD⁺/NADH ratio, AGC1-KD C2C12 cells display decreased M+3 aspartate and M+5 citrate from labeled glutamine, consistent with decreased reductive α -KG carboxylation (Figures 3D and 3E). Moreover, at steady state, M+3 species of glutamate and α -KG are increased while M+5 species are decreased in AGC1-KD C2C12 cells without any major differences observed in unlabeled (M+0) species (Figures 3F and 3G). These labeling patterns are consistent with a higher mitochondrial NAD⁺/NADH ratio promoting increased oxidative TCA cycling (Figure 3H). Also consistent with this interpretation, AGC1-KD C2C12 cells release more ¹⁴C-CO₂ from [¹⁴C]glutamine (Figures 3H and 3I). Interestingly, we did not observe the same decrease in reductive carboxylation in LLC1 cells with AGC1 KD (Figure S2G), suggesting that changes in reductive carboxylation are not why AGC-KD cells require glutamine. Together, these findings argue that, although changes are observed in the metabolism of AGC1-KD cells (Figures

S2H–S2M), glutamine utilization is not drastically altered in AGC1-KD cells, and glutamine remains the major precursor for aspartate independent of AGC1 expression (Figures S2F and S2G).

AGC1-KD Cells Are Unable to Sustain Cytosolic Aspartate Levels, Leading to Cell Death upon Glutamine Deprivation

Because cytosolic aspartate production is essential for survival of cells with mitochondrial dysfunction (Birsosy et al., 2015), we hypothesized that aspartate export from mitochondria might be important to survive glutamine limitation. In fact, AGC1 protein expression is higher following glutamine deprivation, suggesting a higher demand for mitochondrial aspartate export in such conditions (Figure 4A). We reasoned that glutamine withdrawal might deplete mitochondrial aspartate levels such that other mitochondrial transporters cannot export it efficiently (Figure 4B). To test whether cytosolic aspartate delivery can be limiting for AGC1-KD cells in low glutamine, we provided cells with exogenous aspartate and found that aspartate supplementation in low-glutamine media rescues AGC1-KD cell viability and proliferation (Figures S3A and 4C). Because aspartate is poorly permeable, non-physiological aspartate concentrations (5–20 mM) are needed to deliver aspartate into the cells (Sullivan et al., 2018). However, after expressing the aspartate transporter (SLC1A3), 150 μ M aspartate was sufficient to rescue proliferation/survival in low-glutamine conditions (Figure S3B), arguing that cytosolic aspartate delivery can be limiting for AGC1-KD cells.

A requirement for glutamine in cells with AGC1 loss was observed in other cell lines, as was the ability of aspartate to rescue AGC1 loss, despite the fact that the cell lines showed varying responses to glutamine deprivation and glutaminase inhibition (Figure 4C). In addition, CRISPR/Cas9-mediated knockout of AGC1 leads to comparable sensitivity to perturbations that limit glutamine metabolism in C2C12 cells (Figure S3C). Interestingly, total ablation of AGC1 also did not completely block proliferation in glutamine-replete media, suggesting that

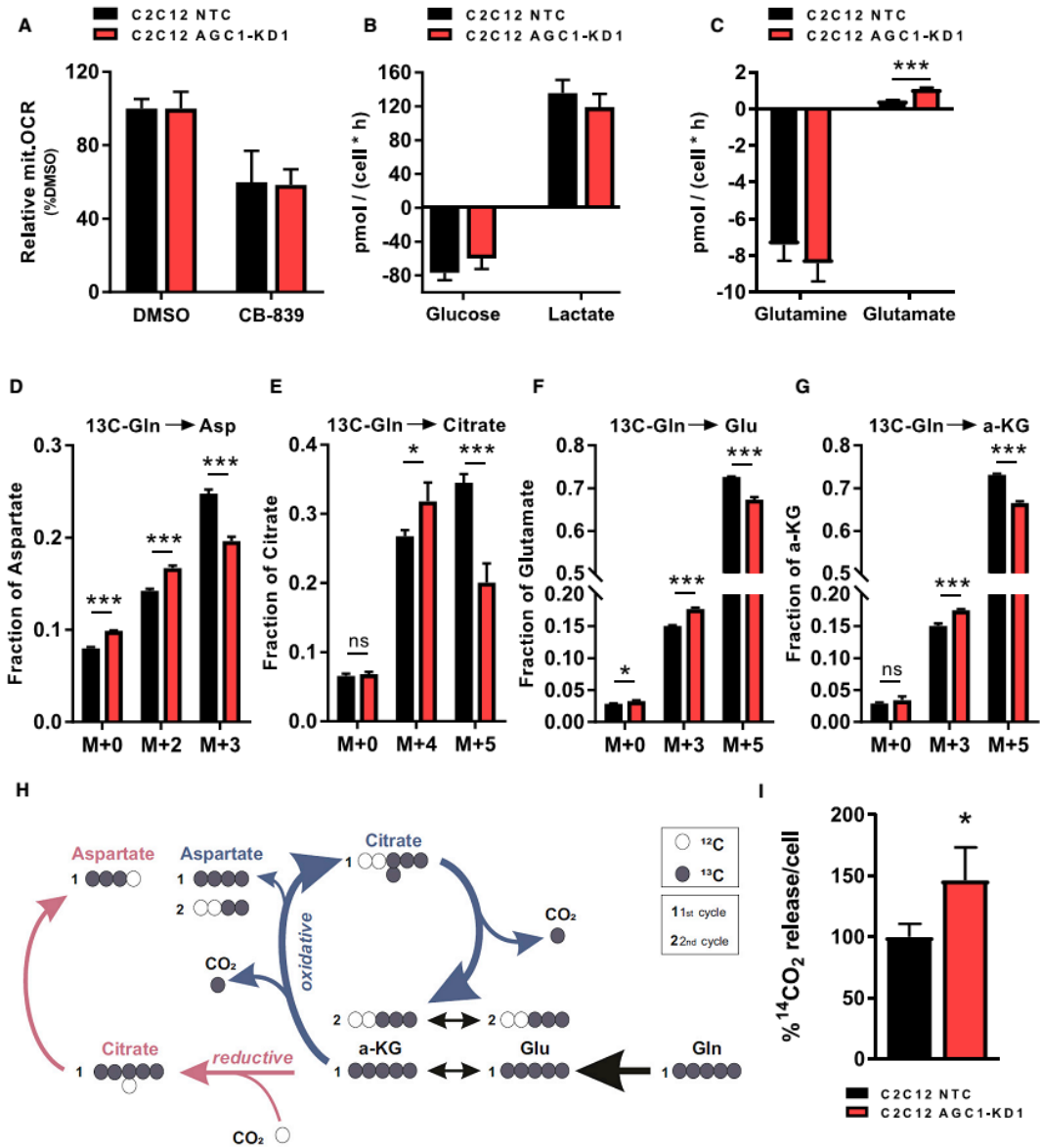


Figure 3. AGC1-KD Cells Exhibit Increased Oxidative TCA Cycle Metabolism

(A) Relative mitochondrial oxygen consumption rate (mit.OCR) of control (NTC) and AGC1-KD1 C2C12 cells cultured for 6 hr in pyruvate-free DMEM containing 4 mM glutamine with or without CB-839 (n = 5); data normalized to percent change compared to DMSO treatments of each group. Means ± SEM are shown. (B and C) Uptake/consumption rate of glucose and lactate (B), and glutamine and glutamate (C) are shown for control (NTC) and AGC1KD C2C12 cells cultured in pyruvate-free DMEM for 48 hr (n = 3). (D–G) Fractional labeling of aspartate (Asp) (D), citrate (E), glutamate (Glu) (F), and α-ketoglutarate (α-KG) (G) following culture of C2C12 control (black) or C2C12 AGC1-KD1 (red) cells (as in A–C) in media containing [¹³C]glutamine (Gln) for 24 hr (n = 3).

(legend continued on next page)

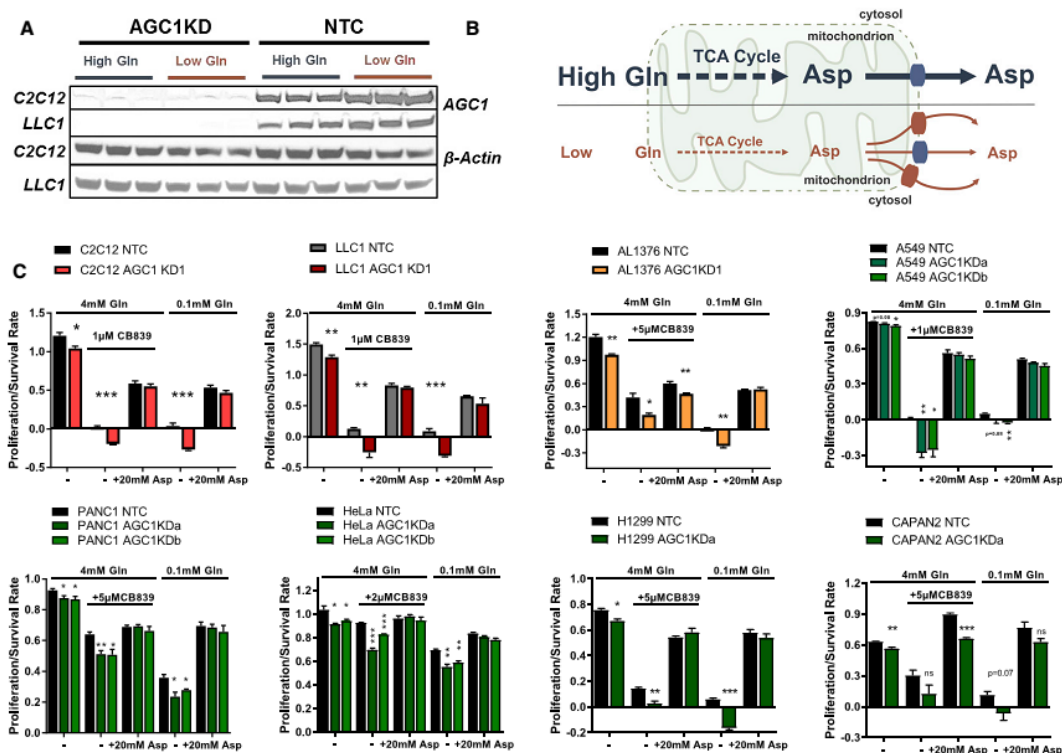


Figure 4. Cytosolic Aspartate Delivery Improves Proliferation/Survival Following Glutamine Limitation

(A) Western blot analysis of AGC1 protein expression in whole-cell lysates (40 μ g/lane) from AGC1 KD (AGC1KD) or control (NTC) C2C12 or LLC1 cultured in DMEM with 10% FBS and 4 mM glutamine (High Gln) or 0.1 mM glutamine (Low Gln) for 24 hr as indicated.

(B) Schematic depicting how low glutamine might lead to reduced cytosolic aspartate delivery and increased aspartate transporter expression.

(C) Proliferation/survival rate of control (NTC) and AGC1KD C2C12, LLC1, AL1376, A549, PANC1, HeLa, H1299, and CAPAN2 cells cultured in pyruvate-free DMEM containing 4 or 0.1 mM glutamine (Gln), or 4 mM glutamine with CB839 at the specified concentrations in the presence or absence of 20 mM aspartate (Asp), as indicated (n = 3). Mean \pm SEM.

*p \leq 0.05, **p \leq 0.01, ***p \leq 0.001. See also Figure S3.

some cytosolic aspartate delivery is sustained by AGC2 or other mitochondrial transporters when glutamine is present. Of note, glutamate supplementation failed to completely rescue AGC1-KD cells in low-glutamine conditions, suggesting that reduced mitochondrial glutamate uptake may be one factor exacerbating the dependence of AGC1-KD cells on glutamine anaplerosis (Figures S3D and S3E).

AGC1-KD Cells Require High Mitochondrial Aspartate Levels to Maintain Aspartate Export

We next hypothesized that AGC1-deficient cells require high mitochondrial aspartate levels to maintain sufficient aspartate

delivery to the cytosol. Therefore, we examined whether AGC1-KD cells are vulnerable to other perturbations that deplete mitochondrial aspartate. Metformin blocks mitochondrial aspartate production by inhibiting mitochondrial complex I and consequently disrupting the NAD⁺/NADH ratio (Sullivan et al., 2015) (Figure 5A), and AGC1-KD cells are more sensitive to metformin treatment than control cells (Figure 5B). Furthermore, other anaplerotic carbon sources might support mitochondrial aspartate production (Figure 5A), and both daKG and pyruvate supplementation improve proliferation/survival of AGC1-KD cells in glutamine limitation (Figure 5C) and increase aspartate levels (Figures 5D and S4A–S4D). These findings suggest that limiting

(H) Schematic overview of oxidative and reductive glutamine catabolism highlighting how labeled carbons from glutamine (Gln) label glutamate (Glu), α -ketoglutarate (α -KG), and the other indicated metabolites.

(I) Relative ¹⁴CO₂ release from control (NTC) and AGC1-KD C2C12 cells cultured in media containing [U-¹⁴C]-glutamine for 1 hr (n = 3).

All figures show mean \pm SD unless indicated otherwise. *p \leq 0.05, **p \leq 0.01, ***p \leq 0.001. See also Figure S2.

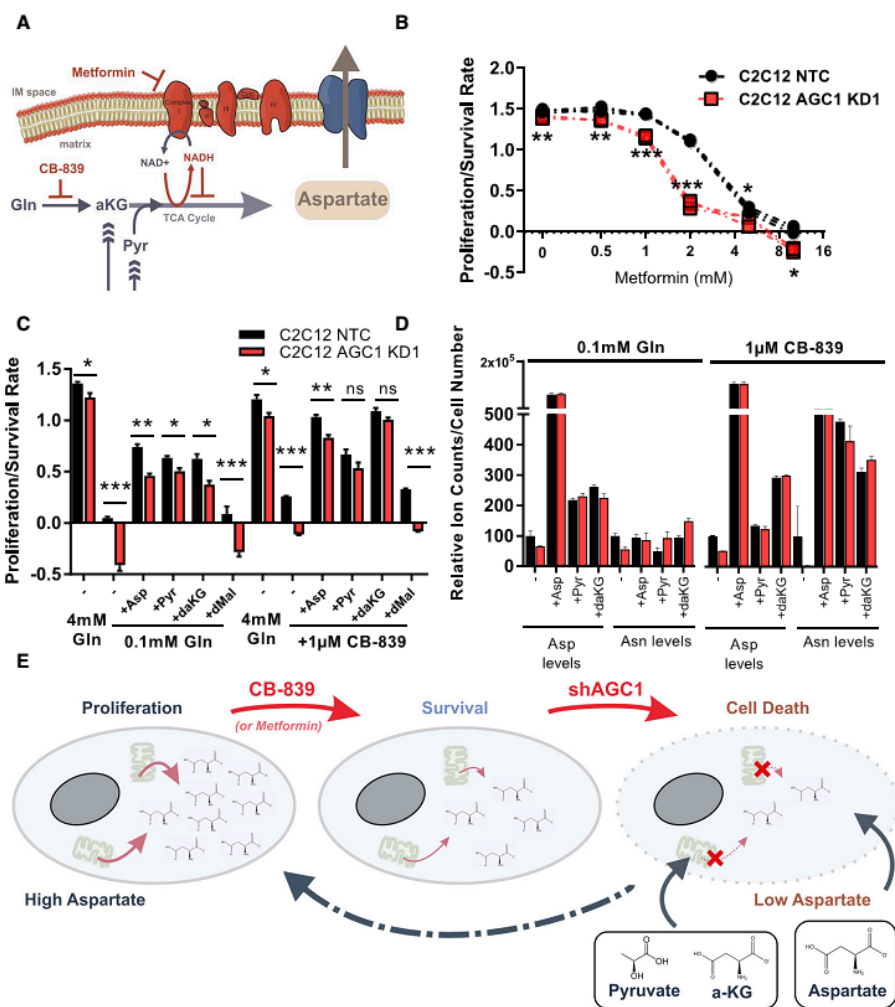


Figure 5. Sustaining Cytosolic Aspartate Levels Prevents Cell Death in Glutamine-Limiting Conditions

(A) Schematic showing how glutamine and alternative anaplerotic substrates can fuel the TCA cycle and support mitochondrial aspartate synthesis. How CB-839-mediated inhibition of glutaminase and metformin inhibition of NAD⁺ regeneration affect TCA cycling are also shown.

(B) Proliferation/survival rate of control (NTC) and AGC1-KD C2C12 cells treated with varying concentration of metformin in pyruvate-free DMEM (n = 3).

(C) Proliferation/survival rate of control (NTC) and AGC1-KD C2C12 cells cultured in 4 or 0.1 mM glutamine, or 4 mM glutamine with 1 µM CB-839, in the presence or absence of 20 mM aspartate (Asp), 2 mM sodium pyruvate (Pyr), 2 mM dimethyl- α -ketoglutarate (daKG), or 2 mM dimethylmalate (dMal), as indicated (n = 3).

(D) Relative cellular aspartate and asparagine levels in control (NTC) and AGC1-KD C2C12 cells cultured in 0.1 or 4 mM glutamine with 1 µM CB-839 in the presence or absence of 20 mM aspartate (Asp), 2 mM sodium pyruvate (Pyr), or 2 mM dimethyl- α -ketoglutarate (daKG), as indicated (n = 3).

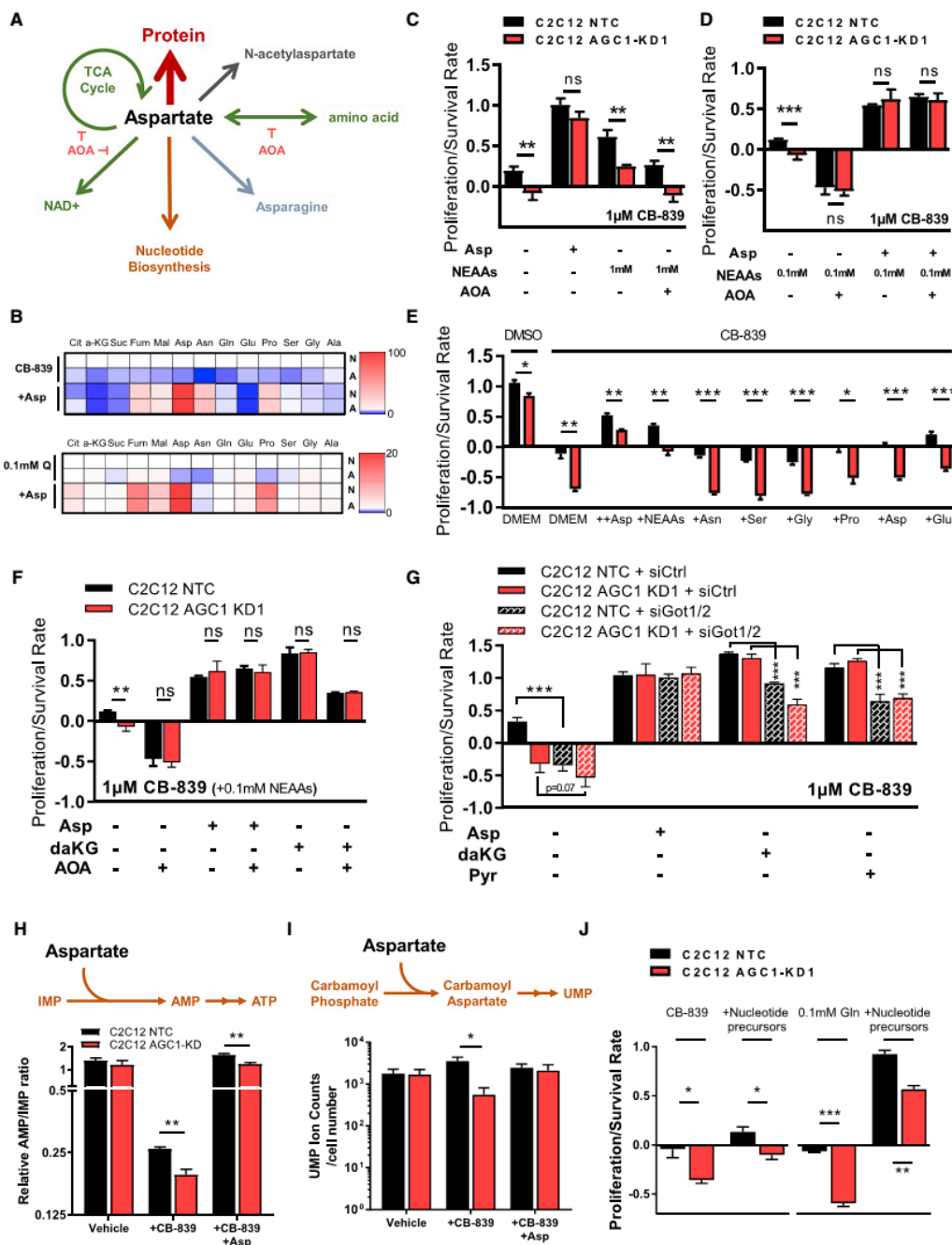
(E) Schematic depicting a model for how changes in cytosolic aspartate levels might correlate with cell survival.

All figures denote means \pm SEM unless indicated otherwise. *p \leq 0.05, **p \leq 0.01, ***p \leq 0.001. See also Figure S4.

glutamine anaplerosis for aspartate production decreases mitochondrial and cytosolic aspartate levels and inhibits cell proliferation. In AGC1-KD cells, however, the inability to export residual aspartate from mitochondria further reduces cytosolic aspartate and compromises cell proliferation and cell survival (Figure 5E).

Cytosolic Aspartate Is Essential for Nucleotide Biosynthesis, but Not for Non-essential Amino Acids or the TCA Cycle

Aspartate is a proteinogenic amino acid that is also involved in several metabolic pathways beyond its use for protein synthesis,



(legend on next page)

some of which have been reported to be associated with cell proliferation (Birsoy et al., 2015; Krall et al., 2016; Sullivan et al., 2015; Zand et al., 2016) (Figure 6A). Cytosolic aspartate could undergo transamination to support non-essential amino acid (NEAA) synthesis, deliver four carbon units to mitochondria for use in the TCA cycle, or recycle NAD⁺ through the cytosolic part of the MAS. In addition to fates involving transamination, aspartate can accept an amide nitrogen from glutamine for asparagine biosynthesis, is essential for both purine and pyrimidine biosynthesis, and is acetylated to produce N-acetylaspartate (NAA), a brain metabolite that may have roles outside of the central nervous system (Figure 6A). Although NAA was recently reported to have beneficial effects on survival of some cancer cells (Bogner-Strauss, 2017; Lou et al., 2016; Zand et al., 2016), we failed to detect endogenous NAA in either C2C12 or LLC1 cells, suggesting that production of NAA cannot explain why cytosolic aspartate is a limitation for the cells studied here (Figures S5A and S5B).

To explore the role of cytosolic aspartate in NEAA synthesis, we first checked mRNA expression of enzymes involved in amino acid metabolism in low-glutamine conditions. Glutamine starvation (0.1 mM) alters expression of many transaminases regulated by activating transcription factor 4 (*Atf4*), a component of the amino acid starvation response (Chen et al., 2014) (Figure S5C). Interestingly, the expression of genes encoding enzymes that would use aspartate in the cytosol (*Got1* and *Asns*), but not in the mitochondria (*Got2*), is upregulated in low-glutamine conditions (Figure S5C). Other cytosolic transaminase isoforms are also upregulated, while mitochondrial isoforms of the same transaminases remain unchanged or are downregulated (Figure S5C). This suggests that cytosolic transamination could be more important following glutamine limitation. In fact, levels of NEAAs (except for serine and glycine that are present in

DMEM) are reduced upon CB-839 treatment or in low glutamine (Figure S4A) and are lower in AGC1-KD cells compared to control cells, which is partially rescued by aspartate supplementation (Figure 6B). However, because transamination reactions are highly reversible and the transfer of nitrogen between amino acids is not uni-directional (Wiechert, 2007), NEAAs might also be consumed to make aspartate when aspartate levels drop upon glutamine withdrawal.

To test whether aspartate or other NEAAs are necessary to rescue cells in glutamine limitation, we provided cells with either a mixture of NEAAs or aspartate, in the presence or absence of the transaminase inhibitor aminooxyacetate (AOA) (Figure S5D). Similar to aspartate, high levels of NEAAs rescue AGC1-KD cells following glutaminase inhibition; however, this rescue is blunted by AOA, suggesting that NEAA rescue of glutaminase inhibition requires transamination (Figures 6C, 6D, S5E, and S5F). Of note, a 0.1 mM mixture of NEAAs was included when cells were treated with AOA as transaminase activity is needed to produce other NEAAs, and complete loss of NEAAs might impact proliferation/survival even when glutamine is not limiting (Figures 6D, S5E, and S5F). Notably, none of the amino acids, including asparagine, can rescue glutaminase inhibition individually, except for a partial rescue by glutamate, which is itself the product of glutaminase (Figures 6E and S5G). On the other hand, AOA treatment reduces the survival of control cells to the level of AGC1-KD cells upon CB-839 treatment (Figures 6D, S5E, and S5F). Importantly, AOA treatment did not affect proliferation/survival of cells rescued with aspartate, arguing that aspartate does not require transamination to rescue glutamine limitation. These data suggest that aspartate is an essential end product of transamination reactions and is not particularly limiting for NEAA synthesis when glutamine anaplerosis is inhibited.

Figure 6. Cytosolic Aspartate Is Limiting for Nucleotide Biosynthesis When Glutamine Metabolism Is Compromised

(A) Schematic showing the potential fates of cytosolic aspartate. Aspartate is a proteinogenic amino acid (red) that could undergo transaminations (green) to support NEAA biosynthesis, oxidize cytosolic NADH through MAS, and provide carbon for the mitochondrial TCA cycle. Aspartate can also be a precursor to produce asparagine (blue), be acetylated to produce N-acetylaspartate (gray), or support purine and pyrimidine biosynthesis (orange). Aspartate fates that are affected by transaminase inhibition by AOA are indicated.

(B) Relative intracellular levels of NEAAs and TCA cycle intermediates in control (N) and AGC1-KD (A) C2C12 cells cultured in 0.1 mM glutamine (0.1 mM Q) or 4 mM glutamine with CB-839 for 24 hr in the presence and absence of 20 mM aspartate; relative change compared to control with CB-839 or NTC with 0.1 mM Q is shown (n = 3). Cit, citrate; a-KG, alpha-ketoglutarate; Suc, succinate; Fum, fumarate; Mal, malate; Asp, aspartate; Asn, asparagine; Gln, glutamine; Glu, glutamate; Pro, proline; Ser, serine; Gly, glycine; Ala, alanine.

(C) Proliferation/survival rates of control (NTC) and AGC1-KD C2C12 cells cultured in pyruvate-free DMEM and treated with 1 μ M CB-839 in the presence or absence of 20 mM aspartate (Asp); 1 mM mixture of NEAAs containing serine, glycine, alanine, aspartate, asparagine, proline, and glutamate (NEAAs); and/or 0.3 mM AOA as indicated (n = 3).

(D) Proliferation/survival rates of control (NTC) and AGC1-KD C2C12 cells cultured in pyruvate-free DMEM and 0.1 mM mixture of NEAAs, and treated with 1 μ M CB-839 in the presence or absence of 20 mM aspartate (Asp) and/or 0.3 mM AOA as indicated (n = 3).

(E) Proliferation/survival rates of control (NTC) and AGC1-KD C2C12 cells cultured in 4 mM glutamine and treated with DMSO or with 1 μ M CB-839 in the presence of 10 mM aspartate (Asp); 1 mM of a mixture of NEAAs containing asparagine (Asn), serine (Ser), glycine (Gly), proline (Pro), alanine, aspartate (Asp), and glutamate (Glu) (NEAAs); or 1 mM of the individual specified free amino acid, as indicated (n = 3).

(F) Proliferation/survival rates of control (NTC) and AGC1-KD C2C12 cells cultured in 4 mM glutamine with 1 μ M CB-839 and 0.1 mM mixture of NEAAs in the presence or absence of 20 mM aspartate (Asp), 2 mM dimethyl- α -ketoglutarate (daKG), and/or 0.3 mM AOA, as indicated (n = 3).

(G) Proliferation/survival rates of control (NTC) and AGC1-KD C2C12 cells treated with 1 μ M CB-839 in the presence or absence of 20 mM aspartate (Asp), 2 mM dimethyl- α -ketoglutarate (daKG), and/or 2 mM sodium pyruvate (Pyr), without (siCtrl) or with (siGot1/2) siRNA KD of *Got1* and *Got2*, as indicated (n = 3).

(H) Top: schematic showing the need for aspartate to make AMP from IMP. Bottom: relative AMP to IMP ratio in control (NTC) and AGC1-KD C2C12 cells cultured with 4 mM glutamine for 24 hr in the absence (Vehicle) or presence of 1 μ M CB-839, without or with 20 mM aspartate (Asp), as indicated (n = 3).

(I) Top: schematic showing the role of aspartate in UMP synthesis. Bottom: relative intracellular UMP levels in control (NTC) and AGC1-KD C2C12 cells cultured in 4 mM glutamine for 24 hr in the absence (Vehicle) or presence of 1 μ M CB-839, without or with 20 mM aspartate (Asp), as indicated (n = 3).

(J) Proliferation/survival rates of control (NTC) and AGC1-KD C2C12 cells cultured in 0.1 or 4 mM glutamine with 1 μ M CB-839 in the presence or absence of a mix of nucleotide precursors containing 200 μ M hypoxanthine, 200 μ M adenine, 200 μ M guanine, 100 μ M thymine, and 400 μ M uridine, as indicated (n = 3).

All figures denote mean \pm SD unless indicated otherwise. *p \leq 0.05, **p \leq 0.01, ***p \leq 0.001. See also Figure S5.

The finding that aspartate rescues proliferation/survival in the presence of AOA argues that aspartate contribution to the TCA cycle or to cytosolic NAD⁺ regeneration is not essential to rescue proliferation/survival when glutamine is limiting, as these aspartate functions involve transamination reactions (Figure S5D). Similar to NEAAs, neither daKG nor pyruvate can completely rescue glutamine limitation when aspartate aminotransferases are inhibited using AOA or small interfering RNA (siRNA) (Figures 6F, 6G, S5E, and S5F), suggesting that conversion of aspartate to oxaloacetate by transamination reactions either to regenerate cytosolic NAD⁺ or to donate nitrogen is not limiting in AGC1-KD cells upon glutamine deprivation. These data also argue that a major role of TCA cycle anaplerosis is to produce aspartate. However, it is important to note that these findings do not argue that aspartate does not undergo transamination and/or fuel the TCA cycle, but only suggest that these pathways are not limiting in low-glutamine conditions. In fact, we observed that [¹³C] aspartate is incorporated into TCA cycle intermediates in low-glutamine conditions (Figure S5H). Similarly, aspartate supplementation modestly increases some TCA cycle intermediates (Figure 6B), although these changes are inconsistent across different cell lines (Figures S4C and S4D). Notably, [¹³C]glutamate labels TCA cycle intermediates more than [¹³C]aspartate (Figure S5I), suggesting that even when transaminases are active, glutamate is a better TCA cycle fuel than aspartate (Figures S5H and S5I).

Another downstream fate of cytosolic aspartate that is not blocked by AOA is the synthesis of asparagine. Asparagine availability can affect cell survival following glutamine deprivation (Zhang et al., 2014), and intracellular asparagine acts as an exchange factor to import other extracellular amino acids when glutamine metabolism is compromised (Krall et al., 2016). Levels of asparagine are also reduced in AGC1-KD cells upon glutamine starvation, and these levels are partially recovered by aspartate supplementation (Figure 6B). However, asparagine supplementation, even at concentrations up to 10 mM, failed to rescue CB-839-treated AGC1-KD cells (Figures 6E and S5G), indicating that asparagine production by itself is not limiting for AGC1-KD cell survival following CB-839 treatment.

Aspartate is required for proliferation partly because it supports nucleotide biosynthesis (Sullivan et al., 2015). Glutaminase inhibition suppresses pyrimidine biosynthesis in Von Hippel-Lindau (VHL)-deficient renal tumors (Okazaki et al., 2017), suggesting that these perturbations might converge on nucleotide metabolism. When aspartate is used for purine biosynthesis, fumarate is generated as a byproduct (Lane and Fan, 2015). We considered that this may account for a greater increase in fumarate levels compared to other TCA cycle intermediates after aspartate supplementation (Figure 6B). To test whether glutaminase inhibition affects nucleotide biosynthesis, we traced [¹⁵N-(amide)]glutamine into nucleotides following CB-839 treatment. Because aspartate donates its nitrogen to IMP for AMP production, AMP synthesis from IMP could be impaired when cytosolic aspartate is limiting (Figure S5J). Consistent with this, the relative AMP/IMP ratio is lower upon CB-839 treatment and is rescued by aspartate supplementation (Figure 6H), arguing that aspartate depletion slows nucleotide biosynthesis. Similarly, intracellular UMP levels are also lower in AGC1-KD cells upon CB-839 treatment compared to controls, suggesting that pyrimidine synthesis

is also affected by decreased cytosolic aspartate delivery (Figure 6I). To test whether nucleotides were indeed limiting for AGC1-KD cells, we supplemented AGC1-KD and control cells with thymine, uridine, hypoxanthine, adenine, and guanine. These nucleotide bases improved AGC1-KD cell proliferation/survival in low-glutamine conditions or following glutaminase inhibition (Figures 6J and S5K), although this rescue was less prominent than that observed with aspartate. These data suggest that nucleotide biosynthesis is one limitation caused by decreased cytosolic aspartate delivery.

AGC1 Knockdown Limits Tumor Growth and Sensitizes Tumors to CB-839 Treatment

We next examined whether AGC1 KD would affect tumor growth *in vivo*. We injected LLC1 cells with or without AGC1-KD into syngeneic C57BL/6 mice and monitored tumor progression. KD of AGC1 slowed tumor growth over the course of 16 days (Figures S6A and S6B).

CB-839 is ineffective in limiting tumor growth in some cancer models *in vivo* even when the cells derived from those tumors are sensitive to CB-839 in culture (Biancur et al., 2017; Davidson et al., 2016). To test whether AGC1-KD sensitizes tumors to CB-839 *in vivo*, we exposed mice with control and AGC1-KD LLC1 tumors to CB-839. CB-839 treatment further reduced the growth of AGC1-KD LLC1 tumors (Figures 7A and S6C) while having a minor effect on control tumors, despite causing comparable drops in glutamate/glutamine ratio in both (Figure 7B). Similar to *in vitro* culture, pyruvate/lactate ratio was lower in AGC1-KD tumors, highlighting that loss of AGC1 also affects the redox state of cells *in vivo* (Figure 7C). Interestingly, asparagine levels were increased in CB-839 treated tumors, yet were lower in AGC1-KD tumors compared to controls (Figures 7D and S6D). These findings are consistent with mitochondrial aspartate export being important in tumors when glutaminase is inhibited and consistent with an inability to maintain cytosolic aspartate levels, slowing the growth of AGC1-KD tumors upon CB-839 treatment. These findings also argue that AGC1-KD increases tumor vulnerability to glutaminase inhibition.

To test whether AGC1-KD would have similar effects on another cancer type, we allografted AL1376 pancreatic ductal adenocarcinoma cells that were derived from the LSL-KrasG12D, p53^{fllox/fllox}, Pdx1-Cre mouse model (Bardeesy et al., 2006). Consistently, AGC1-KD significantly impaired tumor growth (Figure S6E). In addition, unlike LLC1, AL1376 tumors were completely resistant to CB-839 treatment, yet AGC1-KD promoted CB-839 sensitivity (Figures S6E and S6F). These data suggest that targeting AGC1 may synergize with the glutaminase inhibitors to limit the growth of some tumors.

Because AGC1-KD impaired *in vivo* growth of mouse lung and pancreas cancer cell lines, we checked whether autochthonous tumors also express AGC1 protein. Although AGC1 protein levels are not increased in either Kras^{G12D}, p53^{-/-} mouse lung (Davidson et al., 2016) or pancreatic (Mayers et al., 2014) tumors that are resistant to CB-839 compared to corresponding healthy tissues, both tumor types had abundant AGC1 expression (Figure S7C). To explore the relevance of our findings in human cancer, we investigated AGC1 expression in several human solid tumors using immunohistochemistry with an antibody against AGC1. AGC1 is expressed in glioblastoma, as well as

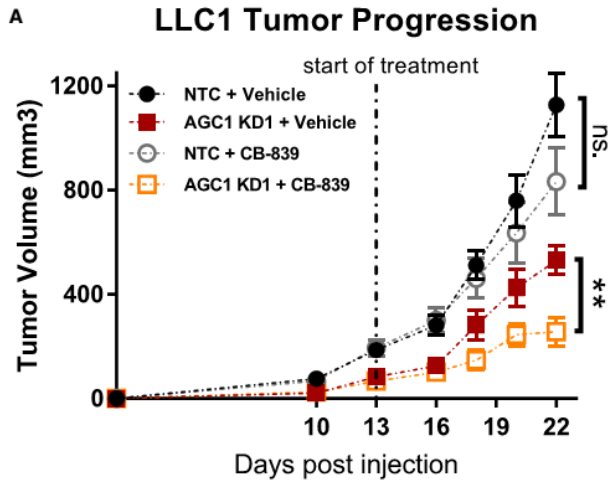


Figure 7. AGC1 Deficiency Sensitizes Tumors to CB-839 Treatment

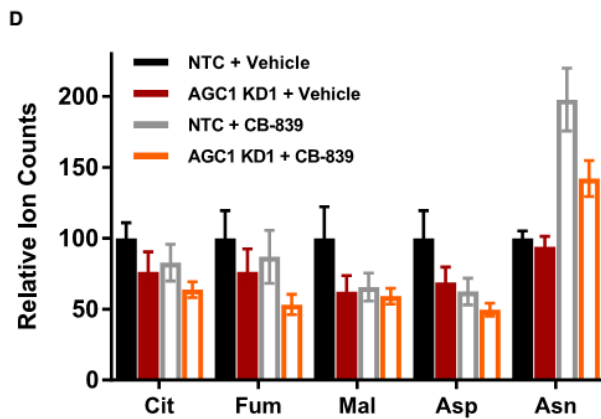
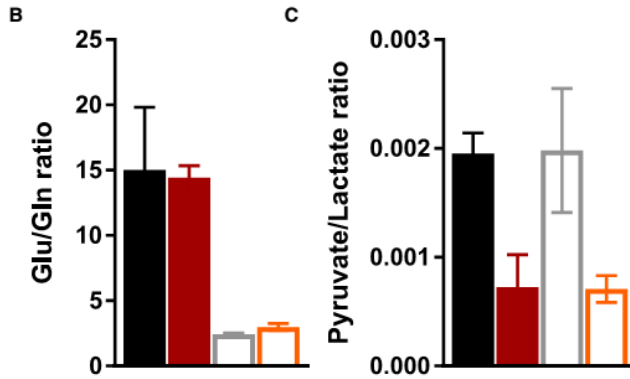
(A) Growth of tumors generated from control (NTC) or AGC1-KD LLC1 in C56BL/6 mice flanks that were treated without (Vehicle) or with CB-839 dosed at 200 mg/kg twice daily starting on day 13 as indicated ($n \geq 6$).

(B) Relative glutamate (Glu) to glutamine (Gln) ratio measured in metabolite extracts from the tumors shown in (A) at the experimental endpoint (day 22) ($n \geq 5$).

(C) Relative pyruvate to lactate ratio measured in metabolite extracts from the tumors shown in (A) at the experimental endpoint (day 22) ($n \geq 5$).

(D) Relative levels of the specified TCA intermediates and asparagine (normalized to valine) measured in metabolite extracts from the tumors shown in (A) at the experimental endpoint ($n \geq 5$). Cit, citrate; Fum, fumarate; Mal, malate; Asp, aspartate; Asn, asparagine.

All figures denote mean \pm SEM. * $p \leq 0.05$, ** $p \leq 0.01$, *** $p \leq 0.001$. See also Figures S6 and S7.



adenocarcinoma of ovary and pancreas (Figures S7A and S7B). While pancreatic ductal carcinoma (PDAC) cells have heterogeneous AGC1 expression, all healthy pancreatic duct cells are AGC1 negative, suggesting that AGC1 might be upregulated during tumorigenesis in this cancer type (Figure S7B). These observations argue that AGC1 could be a target to treat human cancers.

DISCUSSION

These findings argue that glutamine anaplerosis is important to produce aspartate, and that decreased cytosolic aspartate levels can lead to cell death. These findings are consistent with recent data showing AGC1-deficient neuroblastoma cells proliferate slower in low-glutamine media (Profilo et al., 2017). From a mechanistic standpoint, it appears that one function of AGC1 is to sustain proliferation/survival of glutamine-deprived cells by providing aspartate to the cytosol. While aspartate may become limiting for nucleotide biosynthesis following glutamine depletion, different aspartate fates could be more limiting in other circumstances. It is important to note that if one fate of aspartate is rescued, more aspartate will be available for other pathways, making it difficult to definitively conclude that nucleotide synthesis is the only critical fate of aspartate, particularly when levels of other NEAAs or TCA cycle intermediates are indirectly affected when cytosolic aspartate is depleted. It is also impossible to rescue aspartate use for protein synthesis in the same way that aspartate use for nucleotides can be rescued by providing exogenous bases, and a role in protein synthesis may be equally important even in the cells examined in this study. Furthermore, AGC2 is structurally and functionally similar to AGC1 (Thangaratnarajah et al., 2014) and expressed at different levels in various tissues (Begum et al., 2002). Therefore, AGC2 depletion could be more harmful for some cell types than AGC1 depletion, and complete loss of both isoforms could cause more severe limitations to impair cell survival, perhaps even under glutamine-replete conditions.

Glutamine metabolism in cancer can be influenced by the environment (Davidson et al., 2016). For instance, supraphysiological cystine levels in tissue culture media can promote both glutaminase activity and glutamine dependency (Muir et al., 2017). Consistent with these findings, glutamine contributes very little to the oxidative TCA cycle in some cancers *in vivo* (Davidson et al., 2016). Similar to high-cystine conditions, increased mitochondrial NAD⁺/NADH ratio could also enhance oxidative glutamine metabolism and drive glutamine flux into aspartate synthesis. We observed that AGC1-KD suppressed reductive glutamine metabolism in C2C12 cells, and this may also be the case for LLC1 cells *in vivo*, potentially explaining why AGC1-KD tumors are sensitive to glutaminase inhibition *in vivo*.

There are three glutaminase isoforms in mammalian cells: liver isoform (LGA), kidney isoform (KGA), and a splice variant of KGA (GAC, also known as glutaminase C) that localizes to mitochondria (Cassago et al., 2012). GAC is the enzymatically most efficient isoform and is often upregulated in cancers, and connected to glutamine anaplerosis (Cassago et al., 2012). Upon CB-839 treatment, which selectively inhibits GAC (Gross et al., 2014), cells may utilize cytosolic glutamate as an alternative source. Because AGC1 exports aspartate from mitochondria in exchange for cytosolic glutamate, decreased glutamate delivery to mitochondria might also contribute to CB-839 toxicity in AGC1-KD cells.

Decreased steady-state TCA cycle labeling from [U¹³C]glutamate in AGC1-KD cells (Figure S5I) could suggest that mitochondrial glutamate entry might indeed be impaired. However, two other glutamate importers are located in the inner mitochondrial membrane, Slc25a22 and Slc25a18 (Palmieri, 2013), and these transporters may maintain some mitochondrial glutamate delivery in AGC1-KD cells. In support of this, the inability of α -KG to fully rescue glutamine limitation when aspartate synthesis is blocked suggests that a potential deficiency in mitochondrial glutamate uptake might be a factor that exacerbates the drop in mitochondrial aspartate levels in AGC1-KD cells.

Although low glutamine and CB-839 treatment lead to similar phenotypes, these two conditions are not identical. Because low glutamine levels will affect more pathways than CB-839 treatment, cell proliferation/survival and the depletion of some NEAAs and TCA intermediates were more pronounced in low glutamine. However, CB-839 synergizes with AGC1-KD similarly to low glutamine, suggesting that decreased TCA cycle anaplerosis is one reason why AGC1-KD cells are sensitive to glutamine withdrawal. Mitochondrial transporters can be promiscuous and transport multiple metabolites across membranes with varying binding efficiencies (Fiermonte et al., 2009; Gutiérrez-Aguilar and Baines, 2013). For instance, uncoupling protein 2 (UCP2) can export four carbon metabolites from mitochondria, including aspartate (Voza et al., 2014). We speculate that various mitochondrial transporters, including AGC2, maintain some degree of cytosolic aspartate delivery in AGC1-KD cells as long as aspartate levels in mitochondria are sufficiently high. Interestingly, not all anaplerotic substrates rescue glutamine limitation in AGC1-KD cells. Dimethylmalate (dMal, a cell-permeable form of malate) failed to rescue low glutamine or CB-839 treatment (Figure 5C), was unable to increase aspartate levels (Figures S4A and S4B), and caused a reduction in TCA intermediates in some conditions. These data suggest that dMal might have potentially harmful effects on cells other than solely supplying four carbon units to the TCA cycle.

We used asparagine levels as a proxy for cytosolic aspartate in cell culture experiments; however, the fact that mouse plasma contains asparagine (Rivera et al., 1987) may explain why asparagine levels are unchanged in AGC1-KD tumors compared to controls *in vivo*. Interestingly, asparagine levels were increased with CB-839 treatment *in vivo* independently of AGC1 expression, in line with recent reports pointing out that asparagine synthase expression is upregulated in CB-839-resistant cells (Biancur et al., 2017). This may suggest an independent, anti-apoptotic function for asparagine as previously reported (Zhang et al., 2014). In our system, asparagine supplementation had no effect on CB-839-treated cells *in vitro*; however, this may change when cells are adapted to grow in the presence of glutaminase inhibitors (Krall et al., 2016). In addition, because asparagine is produced from both cytosolic aspartate and glutamine, in media where glutamine is limited, asparagine levels may not be a good proxy for cytosolic aspartate and could explain why aspartate supplementation did not increase asparagine levels in low glutamine.

Aspartate availability can be limiting for tumor growth *in vivo* (Gui et al., 2016; Sullivan et al., 2018) and we find that AGC1 deficiency leads to both reduced cytosolic aspartate and increased dependence on glutaminase. Adaptive programs downstream of

glutamine withdrawal can also promote the uptake of extracellular aspartate (Tajan et al., 2018). These findings suggest that combination therapies targeting both aspartate and glutamine metabolism may be synergistic. We found that AGC1 plays a central role in sustaining cytosolic aspartate levels, particularly when mitochondrial glutaminolysis is compromised. This implies that targeting AGC1 could sensitize some cancers to glutaminase inhibitors. It is worth noting that genetic background and tissue of origin are also important aspects to consider for targeting metabolism (Mayers et al., 2016; Yuneva et al., 2012), and additional studies are necessary to define the cancer subsets that are most likely to respond to these interventions.

Environmental nutrients can also impact cancer cell metabolism (Tardito et al., 2015; Cantor et al., 2017; Muir et al., 2017; Muir and Vander Heiden, 2018). Another caveat of our study in this respect is that the mechanistic analysis for why cells require mitochondrial aspartate export used cells in culture that rely on glutamine for TCA cycle anaplerosis. However, glutamine is not the major source of aspartate for all tumor cells *in vivo* (Davidson et al., 2016; Muir et al., 2017), and some tumors have been shown to synthesize glutamine from glucose in a series of reactions that consume TCA cycle intermediates (Tardito et al., 2015; Hensley et al., 2016). Thus, despite showing that AGC1 loss can sensitize some tumors to glutaminase inhibition, whether tumors that use the TCA cycle to make, rather than consume, glutamine exhibit a similar dependence on AGC1 remains unknown. Furthermore, potential toxicities of AGC inhibition in healthy cells could limit targeting of AGC1, as AGC1 deficiency in mice and humans leads to loss of motor coordination and neuronal defects (Falk et al., 2014; Jalil et al., 2005; Sakurai et al., 2010; Wibom et al., 2009), while loss-of-function mutations in AGC2 lead to the urea cycle-associated disorder type II citrullinemia (Saheki et al., 2002; Yasuda et al., 2000). Nevertheless, our data provide evidence that in some contexts tumor-specific inhibition of AGC1 can reduce tumor growth, and this effect can be exacerbated by glutaminase inhibition.

STAR★METHODS

Detailed methods are provided in the online version of this paper and include the following:

- KEY RESOURCES TABLE
- CONTACT FOR REAGENT AND RESOURCE SHARING
- EXPERIMENTAL MODEL AND SUBJECT DETAILS
 - Cell Lines
 - Animals
- METHOD DETAILS
 - Stable-knockdown of AGC1
 - Proliferation/Survival Rates
 - Cell Viability Assays
 - Determining Annexin V/Propidium Iodide staining using flow cytometry
 - Transient overexpression of mouse and human AGC1
 - CRISPR/Cas9-mediated knock-out of AGC1
 - siRNA-mediated knock-down of Got1/2
 - NAD⁺/NADH Measurements
 - Mitochondrial Oxygen Consumption
 - Isotope Tracing and GCMS Analysis

- Metabolic profiling using LCMS
- Metabolite Measurements using NMR
- Immunohistochemistry
- Radioactive CO₂ Release
- Extracellular Flux Analysis
- Western blot analysis
- Quantitative Real-Time PCR
- QUANTIFICATION AND STATISTICAL ANALYSIS

SUPPLEMENTAL INFORMATION

Supplemental Information includes seven figures and can be found with this article online at <https://doi.org/10.1016/j.cmet.2018.07.021>.

ACKNOWLEDGMENTS

This work was funded by the Austrian Science Fund FWF SFB LIPTOX F3018, P27108, P28854, W1226 DK “Metabolic and Cardiovascular Disease,” the Integrative Metabolism Research Center Graz, and the Austrian infrastructure program 2016/2017. M.G.V.H. acknowledges support from the Lustgarten Foundation, SU2C, the Ludwig Center at MIT, the MIT Center for Precision Cancer Medicine, and the NCI (P30 CA1405141 and R01 CA168653). M.G.V.H. is also an HHMI faculty scholar. H.F.A. was supported by Austrian Marshall Plan Scholarship. A.L. is supported by the Ludwig Center for Molecular Oncology Fund, NSF (GRFP DGE-1122374), and T32GM007287. S.S. was trained within frame of the PhD program Molecular Medicine. A.N.L. is a Robert Black Fellow of the Damon Runyon Cancer Research Foundation, DRG-2241-15. W.A.-Z. is supported by CBmed – Center for Biomarker Research in Medicine. We thank Thales Papagiannakopoulos for sharing CB-839. We are grateful for all the people in the Vander Heiden and Bogner-Strauss labs, especially Aaron Hosios, Lucas Sullivan, Zhaoqi Li, Laura Danai, Ariane Pessenteiner, and Daniel Schmidt, for constructive discussions, experimental advice, and critical reading of the manuscript. We acknowledge the support of NAWI Graz and the technical support of Thomas Schreiner, Wolfgang Krispel, Silvia Schauer, and Bena Chan.

AUTHOR CONTRIBUTIONS

H.F.A. designed and performed the majority of the experiments. K.E.W. and A.L. assisted with some *in vitro* and *in vivo* experiments, respectively. C.T.M.-S. and W.F.G. determined oxygen consumption. S.S. and T.M. performed NMR measurements and data analysis. A.N.L. assisted with flow cytometry experiments and generated the AL1376 cell line. W.A.-Z. and G.H. assessed immunohistochemistry slides. C.A.L. performed liquid chromatography-mass spectrometry measurements. C.J.T. supplied critical reagents. H.F.A. and J.G.B.-S. constructed the study and M.G.V.H. provided substantial guidance and shared lab space and equipment. H.F.A., M.G.V.H., and J.G.B.-S. wrote the manuscript.

DECLARATION OF INTERESTS

M.G.V.H. discloses that he is a consultant and scientific advisory board member for Agios Pharmaceuticals and Aeglea Biotherapeutics, and T.M. discloses that he is a consultant and scientific advisory board member of Cleara Biotech.

Received: August 17, 2017

Revised: May 29, 2018

Accepted: July 29, 2018

Published: August 16, 2018

REFERENCES

- Ahn, C.S., and Metallo, C.M. (2015). Mitochondria as biosynthetic factories for cancer proliferation. *Cancer Metab.* 3, 1.
- Amoedo, N.D., Punzi, G., Obre, E., Lacombe, D., De Grassi, A., Pierri, C.L., and Rossignol, R. (2016). AGC1/2, the mitochondrial aspartate-glutamate carriers. *Biochim. Biophys. Acta* 1863, 2394–2412.

- Bardeesy, N., Aguirre, A.J., Chu, G.C., Cheng, K.H., Lopez, L.V., Hezel, A.F., Feng, B., Brennan, C., Weissleder, R., Mahmood, U., et al. (2006). Both p16(Ink4a) and the p19(Arf)-p53 pathway constrain progression of pancreatic adenocarcinoma in the mouse. *Proc. Natl. Acad. Sci. USA* 103, 5947–5952.
- Begum, L., Jaill, M.A., Kobayashi, K., Iijima, M., Li, M.X., Yasuda, T., Horiuchi, M., del Arco, A., Satrústegui, J., and Saheki, T. (2002). Expression of three mitochondrial solute carriers, citrin, aralar1 and ornithine transporter, in relation to urea cycle in mice. *Biochim. Biophys. Acta* 1574, 283–292.
- Bianchr, D.E., Paulo, J.A., Małachowska, B., Quiles Del Rey, M., Sousa, C.M., Wang, X., Sohn, A.S.W., Chu, G.C., Gygi, S.P., Harper, J.W., et al. (2017). Compensatory metabolic networks in pancreatic cancers upon perturbation of glutamine metabolism. *Nat. Commun.* 8, 15965.
- Birsoy, K., Wang, T., Chen, W.W., Freinkman, E., Abu-Remaileh, M., and Sabatini, D.M. (2015). An essential role of the mitochondrial electron transport chain in cell proliferation is to enable aspartate synthesis. *Cell* 162, 540–551.
- Bogner-Strauss, J.G. (2017). N-Acetylaspartate metabolism outside the brain: lipogenesis, histone acetylation, and cancer. *Front. Endocrinol. (Lausanne)* 8, 240.
- Cantor, J.R., and Sabatini, D.M. (2012). Cancer cell metabolism: one hallmark, many faces. *Cancer Discov.* 2, 881–898.
- Cantor, J.R., Abu-Remaileh, M., Kanarek, N., Freinkman, E., Gao, X., Louissaint, A., Jr., Lewis, C.A., and Sabatini, D.M. (2017). Physiologic medium rewires cellular metabolism and reveals uric acid as an endogenous inhibitor of UMP synthase. *Cell* 169, 258–272.e17.
- Cassago, A., Ferreira, A.P., Ferreira, I.M., Fornezari, C., Gomes, E.R., Greene, K.S., Pereira, H.M., Garratt, R.C., Dias, S.M., and Ambrosio, A.L. (2012). Mitochondrial localization and structure-based phosphate activation mechanism of Glutaminase C with implications for cancer metabolism. *Proc. Natl. Acad. Sci. USA* 109, 1092–1097.
- Catalina-Rodríguez, O., Kolkulka, V.K., Tomita, Y., Preet, A., Palmieri, F., Wellstein, A., Byers, S., Giaccia, A.J., Glasgow, E., Albanese, C., and Avantaggiati, M.L. (2012). The mitochondrial citrate transporter, CIT, is essential for mitochondrial homeostasis. *Oncotarget* 3, 1220–1235.
- Chen, R., Zou, Y., Mao, D., Sun, D., Gao, G., Shi, J., Liu, X., Zhu, C., Yang, M., Ye, W., et al. (2014). The general amino acid control pathway regulates mTOR and autophagy during serum/glutamine starvation. *J. Cell Biol.* 206, 173–182.
- Christensen, C.E., Karlsson, M., Winther, J.R., Jensen, P.R., and Lerche, M.H. (2014). Non-invasive in-cell determination of free cytosolic [NAD⁺]/[NADH] ratios using hyperpolarized glucose show large variations in metabolic phenotypes. *J. Biol. Chem.* 289, 2344–2352.
- Cory, J.G., and Cory, A.H. (2006). Critical roles of glutamine as nitrogen donors in purine and pyrimidine nucleotide synthesis: asparaginase treatment in childhood acute lymphoblastic leukemia. *In Vivo* 20, 587–589.
- Davidson, S.M., Papagiannakopoulos, T., Olenchock, B.A., Heyman, J.E., Keibler, M.A., Luengo, A., Bauer, M.R., Jha, A.K., O'Brien, J.P., Pierce, K.A., et al. (2016). Environment impacts the metabolic dependencies of Ras-driven non-small cell lung cancer. *Cell Metab.* 23, 517–528.
- DeBerardinis, R.J., and Chandel, N.S. (2016). Fundamentals of cancer metabolism. *Sci. Adv.* 2, e1600200.
- del Arco, A., Morcillo, J., Martínez-Morales, J.R., Galián, C., Martos, V., Bovolenta, P., and Satrústegui, J. (2002). Expression of the aspartate/glutamate mitochondrial carriers aralar1 and citrin during development and in adult rat tissues. *Eur. J. Biochem.* 269, 3313–3320.
- Dixon, S.J., Patel, D.N., Welsch, M., Skouta, R., Lee, E.D., Hayano, M., Thomas, A.G., Gleason, C.E., Tatonetti, N.P., Slusher, B.S., and Stockwell, B.R. (2014). Pharmacological inhibition of cystine-glutamate exchange induces endoplasmic reticulum stress and ferroptosis. *eLife* 3, e02523.
- Falk, M.J., Li, D., Gai, X., McCormick, E., Place, E., Lasorsa, F.M., Otieno, F.G., Hou, C., Kim, C.E., Abdel-Magid, N., et al. (2014). AGC1 deficiency causes infantile epilepsy, abnormal myelination, and reduced N-acetylaspartate. *JIMD Rep.* 14, 77–85.
- Fernandez, C.A., Des Rosiers, C., Previs, S.F., David, F., and Brunengraber, H. (1996). Correction of ¹³C mass isotope distributions for natural stable isotope abundance. *J. Mass Spectrom.* 31, 255–262.
- Fiermonte, G., Paradies, E., Todisco, S., Marobbio, C.M., and Palmieri, F. (2009). A novel member of solute carrier family 25 (SLC25A42) is a transporter of coenzyme A and adenosine 3',5'-diphosphate in human mitochondria. *J. Biol. Chem.* 284, 18152–18159.
- Greenhouse, W.V., and Lehninger, A.L. (1976). Occurrence of the malate-aspartate shuttle in various tumor types. *Cancer Res.* 36, 1392–1396.
- Gross, M.I., Demo, S.D., Dennison, J.B., Chen, L., Chernov-Rogan, T., Goyal, B., Janes, J.R., Laidig, G.J., Lewis, E.R., Li, J., et al. (2014). Antitumor activity of the glutaminase inhibitor CB-839 in triple-negative breast cancer. *Mol. Cancer Ther.* 13, 890–901.
- Gui, D.Y., Sullivan, L.B., Luengo, A., Hosios, A.M., Bush, L.N., Gitego, N., Davidson, S.M., Freinkman, E., Thomas, C.J., and Vander Heiden, M.G. (2016). Environment dictates dependence on mitochondrial complex I for NAD⁺ and aspartate production and determines cancer cell sensitivity to metformin. *Cell Metab.* 24, 716–727.
- Gutiérrez-Aguilar, M., and Baines, C.P. (2013). Physiological and pathological roles of mitochondrial SLC25 carriers. *Biochem. J.* 454, 371–386.
- Hensley, C.T., Faubert, B., Yuan, Q., Lev-Cohain, N., Jin, E., Kim, J., Jiang, L., Ko, B., Skelton, R., Loudat, L., et al. (2016). Metabolic heterogeneity in human lung tumors. *Cell* 164, 681–694.
- Hosios, A.M., Hecht, V.C., Danaei, L.V., Johnson, M.O., Rathmell, J.C., Steinhilber, M.L., Manalis, S.R., and Vander Heiden, M.G. (2016). Amino acids rather than glucose account for the majority of cell mass in proliferating mammalian cells. *Dev. Cell* 36, 540–549.
- Jaill, M.A., Begum, L., Contreras, L., Pardo, B., Iijima, M., Li, M.X., Ramos, M., Marmol, P., Horiuchi, M., Shimotsu, K., et al. (2005). Reduced N-acetylaspartate levels in mice lacking aralar, a brain- and muscle-type mitochondrial aspartate-glutamate carrier. *J. Biol. Chem.* 280, 31333–31339.
- Jiang, L., Boufersaoui, A., Yang, C., Ko, B., Rakheja, D., Guevara, G., Hu, Z., and DeBerardinis, R.J. (2017). Quantitative metabolic flux analysis reveals an unconventional pathway of fatty acid synthesis in cancer cells deficient for the mitochondrial citrate transport protein. *Metab. Eng.* 43 (Pt B), 198–207.
- Krall, A.S., Xu, S., Graeber, T.G., Braas, D., and Christoff, H.R. (2016). Asparagine promotes cancer cell proliferation through use as an amino acid exchange factor. *Nat. Commun.* 7, 11457.
- Lane, A.N., and Fan, T.W. (2015). Regulation of mammalian nucleotide metabolism and biosynthesis. *Nucleic Acids Res.* 43, 2466–2485.
- Lewis, C.A., Parker, S.J., Fiske, B.P., McCloskey, D., Gui, D.Y., Green, C.R., Vokes, N.I., Feist, A.M., Vander Heiden, M.G., and Metallo, C.M. (2014). Tracing compartmentalized NADPH metabolism in the cytosol and mitochondria of mammalian cells. *Mol. Cell* 55, 253–263.
- Lou, T.F., Sethuraman, D., Dospoy, P., Srivastava, P., Kim, H.S., Kim, J., Ma, X., Chen, P.H., Huffman, K.E., Frink, R.E., et al. (2016). Cancer-specific production of N-acetylaspartate via NAT8L overexpression in non-small cell lung cancer and its potential as a circulating biomarker. *Cancer Prev. Res. (Phila.)* 9, 43–52.
- Lunt, S.Y., and Vander Heiden, M.G. (2011). Aerobic glycolysis: meeting the metabolic requirements of cell proliferation. *Annu. Rev. Cell Dev. Biol.* 27, 441–464.
- Mayers, J.R., Wu, C., Clish, C.B., Kraft, P., Torrence, M.E., Fiske, B.P., Yuan, C., Bao, Y., Townsend, M.K., Tworoger, S.S., et al. (2014). Elevation of circulating branched-chain amino acids is an early event in human pancreatic adenocarcinoma development. *Nat. Med.* 20, 1193–1198.
- Mayers, J.R., Torrence, M.E., Danaei, L.V., Papagiannakopoulos, T., Davidson, S.M., Bauer, M.R., Lau, A.N., Ji, B.W., Dixit, P.D., Hosios, A.M., et al. (2016). Tissue of origin dictates branched-chain amino acid metabolism in mutant Kras-driven cancers. *Science* 353, 1161–1165.
- Metallo, C.M., Gameiro, P.A., Bell, E.L., Mattaini, K.R., Yang, J., Hiller, K., Jewell, C.M., Johnson, Z.R., Irvine, D.J., Guarente, L., et al. (2011). Reductive glutamine metabolism by IDH1 mediates lipogenesis under hypoxia. *Nature* 481, 380–384.
- Muir, A., and Vander Heiden, M.G. (2018). The nutrient environment affects therapy. *Science* 360, 962–963.
- Muir, A., Danaei, L.V., Gui, D.Y., Waingarten, C.Y., Lewis, C.A., and Vander Heiden, M.G. (2017). Environmental cystine drives glutamine anaplerosis

- and sensitizes cancer cells to glutaminase inhibition. *eLife* 6, e27713, <https://doi.org/10.7554/eLife.27713>.
- Mullen, A.R., Wheaton, W.W., Jin, E.S., Chen, P.H., Sullivan, L.B., Cheng, T., Yang, Y., Linehan, W.M., Chandel, N.S., and DeBerardinis, R.J. (2011). Reductive carboxylation supports growth in tumour cells with defective mitochondria. *Nature* 481, 385–388.
- Mullen, A.R., Hu, Z., Shi, X., Jiang, L., Boroughs, L.K., Kovacs, Z., Boriack, R., Rakheja, D., Sullivan, L.B., Linehan, W.M., et al. (2014). Oxidation of alpha-ketoglutarate is required for reductive carboxylation in cancer cells with mitochondrial defects. *Cell Rep.* 7, 1679–1690.
- Okazaki, A., Gameiro, P.A., Christodoulou, D., Laviollette, L., Schneider, M., Chaves, F., Stemmer-Rachamimov, A., Yazinski, S.A., Lee, R., Stephanopoulos, G., et al. (2017). Glutaminase and poly(ADP-ribose) polymerase inhibitors suppress pyrimidine synthesis and VHL-deficient renal cancers. *J. Clin. Invest.* 127, 1631–1645.
- Palmieri, F. (2013). The mitochondrial transporter family SLC25: identification, properties and physiopathology. *Mol. Aspects Med.* 34, 465–484.
- Palmieri, L., Pardo, B., Lasorsa, F.M., del Arco, A., Kobayashi, K., Iijima, M., Runswick, M.J., Walker, J.E., Saheki, T., Satrustegui, J., and Palmieri, F. (2001). Citrin and aralar1 are Ca²⁺-stimulated aspartate/glutamate transporters in mitochondria. *EMBO J.* 20, 5060–5069.
- Pochini, L., Scalise, M., Galluccio, M., and Indiveri, C. (2014). Membrane transporters for the special amino acid glutamine: structure/function relationships and relevance to human health. *Front Chem.* 2, 61.
- Profilo, E., Peña-Altamira, L.E., Corricelli, M., Castegna, A., Danese, A., Agrimi, G., Petralla, S., Giannuzzi, G., Porcelli, V., Sbrano, L., et al. (2017). Down-regulation of the mitochondrial aspartate-glutamate carrier isoform 1 AGC1 inhibits proliferation and N-acetylaspartate synthesis in Neuro2A cells. *Biochim. Biophys. Acta* 1863, 1422–1435.
- Prokesch, A., Graef, F.A., Madl, T., Kahlhofer, J., Heidenreich, S., Schumann, A., Moyschewitz, E., Pristoynik, P., Blaschitz, A., Knauer, M., et al. (2017). Liver p53 is stabilized upon starvation and required for amino acid catabolism and gluconeogenesis. *FASEB J.* 31, 732–742.
- Radović, B., Vujić, N., Leopold, C., Schlager, S., Goeritzer, M., Patankar, J.V., Korbellus, M., Kolb, D., Reindl, J., Wegscheider, M., et al. (2016). Lysosomal acid lipase regulates VLDL synthesis and insulin sensitivity in mice. *Diabetologia* 59, 1743–1752.
- Rivera, S., López-Soriano, F.J., Azcón-Bieto, J., and Argilés, J.M. (1987). Blood amino acid compartmentation in mice bearing Lewis lung carcinoma. *Cancer Res.* 47, 5644–5646.
- Rubi, B., del Arco, A., Bartley, C., Satrustegui, J., and Maechler, P. (2004). The malate-aspartate NADH shuttle member Aralar1 determines glucose metabolic fate, mitochondrial activity, and insulin secretion in beta cells. *J. Biol. Chem.* 279, 55659–55666.
- Saheki, T., Kobayashi, K., Iijima, M., Nishi, I., Yasuda, T., Yamaguchi, N., Gao, H.Z., Jalil, M.A., Begum, L., and Li, M.X. (2002). Pathogenesis and pathophysiology of citrin (a mitochondrial aspartate glutamate carrier) deficiency. *Metab. Brain Dis.* 17, 335–346.
- Sakurai, T., Ramoz, N., Barreto, M., Gazdoul, M., Takahashi, N., Gertner, M., Dorr, N., Gama Sosa, M.A., De Gasperi, R., Perez, G., et al. (2010). Slc25a12 disruption alters myelination and neurofilaments: a model for a hypomyelination syndrome and childhood neurodevelopmental disorders. *Biol. Psychiatry* 67, 887–894.
- Sanjana, N.E., Shalem, O., and Zhang, F. (2014). Improved vectors and genome-wide libraries for CRISPR screening. *Nat. Methods* 11, 783–784.
- Shalem, O., Sanjana, N.E., Hartenian, E., Shi, X., Scott, D.A., Mikkelsen, T., Heckl, D., Ebert, B.L., Root, D.E., Doench, J.G., and Zhang, F. (2014). Genome-scale CRISPR-Cas9 knockout screening in human cells. *Science* 343, 84–87.
- Sullivan, L.B., Gui, D.Y., Hosios, A.M., Bush, L.N., Freinkman, E., and Vander Heiden, M.G. (2015). Supporting aspartate biosynthesis is an essential function of respiration in proliferating cells. *Cell* 162, 552–563.
- Sullivan, L.B., Luengo, A., Danai, L.V., Bush, L.N., Diehl, F.F., Hosios, A.M., Lau, A.N., Elmiligy, S., Malstrom, S., Lewis, C.A., and Vander Heiden, M.G. (2018). Aspartate is an endogenous metabolic limitation for tumour growth. *Nat. Cell Biol.* 20, 782–788.
- Tajan, M., Hock, A.K., Blagih, J., Robertson, N.A., Labuschagne, C.F., Kruijswijk, F., Humpton, T.J., Adams, P.D., and Vousden, K.H. (2018). A role for p53 in the adaptation to glutamine starvation through the expression of SLC1A3. *Cell Metab.* Published online August 16, 2018. <https://doi.org/10.1016/j.cmet.2018.07.005>.
- Tardito, S., Oudin, A., Ahmed, S.U., Fack, F., Keunen, O., Zheng, L., Miletic, H., Sakariassen, P.O., Weinstock, A., Wagner, A., et al. (2015). Glutamine synthetase activity fuels nucleotide biosynthesis and supports growth of glutamine-restricted glioblastoma. *Nat. Cell Biol.* 17, 1556–1568.
- Thangaratnarajah, C., Ruprecht, J.J., and Kunji, E.R. (2014). Calcium-induced conformational changes of the regulatory domain of human mitochondrial aspartate/glutamate carriers. *Nat. Commun.* 5, 5491.
- Vander Heiden, M.G., and DeBerardinis, R.J. (2017). Understanding the intersections between metabolism and cancer biology. *Cell* 168, 657–669.
- Vander Heiden, M.G., Cantley, L.C., and Thompson, C.B. (2009). Understanding the Warburg effect: the metabolic requirements of cell proliferation. *Science* 324, 1029–1033.
- Voza, A., Parisi, G., De Leonadis, F., Lasorsa, F.M., Castegna, A., Amorese, D., Marmo, R., Calcagnile, V.M., Palmieri, L., Ricquier, D., et al. (2014). UCP2 transports C4 metabolites out of mitochondria, regulating glucose and glutamine oxidation. *Proc. Natl. Acad. Sci. USA* 111, 960–965.
- Vyas, S., Zaganjor, E., and Haigis, M.C. (2016). Mitochondria and Cancer. *Cell* 166, 555–566.
- Warburg, O. (1956). On the origin of cancer cells. *Science* 123, 309–314.
- Wibom, R., Lasorsa, F.M., Töhönen, V., Barbaro, M., Sterky, F.H., Kucinski, T., Naess, K., Jonsson, M., Pierri, C.L., Palmieri, F., and Wedell, A. (2009). AGC1 deficiency associated with global cerebral hypomyelination. *N. Engl. J. Med.* 361, 489–495.
- Wiechert, W. (2007). The thermodynamic meaning of metabolic exchange fluxes. *Biophys. J.* 93, 2255–2264.
- Williamson, D.H., Lund, P., and Krebs, H.A. (1967). The redox state of free nicotinamide-adenine dinucleotide in the cytoplasm and mitochondria of rat liver. *Biochem. J.* 103, 514–527.
- Wise, D.R., and Thompson, C.B. (2010). Glutamine addiction: a new therapeutic target in cancer. *Trends Biochem. Sci.* 35, 427–433.
- Yasuda, T., Yamaguchi, N., Kobayashi, K., Nishi, I., Horinouchi, H., Jalil, M.A., Li, M.X., Ushikai, M., Iijima, M., Kondo, I., and Saheki, T. (2000). Identification of two novel mutations in the SLC25A13 gene and detection of seven mutations in 102 patients with adult-onset type II citrullinemia. *Hum. Genet.* 107, 537–545.
- Yuneva, M., Zamboni, N., Oefner, P., Sachidanandam, R., and Lazebnik, Y. (2007). Deficiency in glutamine but not glucose induces MYC-dependent apoptosis in human cells. *J. Cell Biol.* 178, 93–105.
- Yuneva, M.O., Fan, T.W., Allen, T.D., Higashi, R.M., Ferraris, D.V., Tsukamoto, T., Matés, J.M., Alonso, F.J., Wang, C., Seo, Y., et al. (2012). The metabolic profile of tumors depends on both the responsible genetic lesion and tissue type. *Cell Metab.* 15, 157–170.
- Zand, B., Previs, R.A., Zacharias, N.M., Rupaimoole, R., Mitamura, T., Nagaraja, A.S., Guindani, M., Dalton, H.J., Yang, L., Baddour, J., et al. (2016). Role of increased n-acetylaspartate levels in cancer. *J. Natl. Cancer Inst.* 108, djv426.
- Zhang, J., Fan, J., Venneti, S., Cross, J.R., Takagi, T., Bhinder, B., Djaballah, H., Kanai, M., Cheng, E.H., Judkins, A.R., et al. (2014). Asparagine plays a critical role in regulating cellular adaptation to glutamine depletion. *Mol. Cell* 56, 205–218.
- Zong, W.X., Rabinowitz, J.D., and White, E. (2016). Mitochondria and Cancer. *Mol. Cell* 61, 667–676.

8.2 Published Commentary: Maintaining cytosolic aspartate levels is a major function of the TCA cycle in proliferating cells.

Alkan, H. F., & Bogner-Strauss, J. G. (2019). Maintaining cytosolic aspartate levels is a major function of the TCA cycle in proliferating cells. **Molecular & Cellular Oncology**, 6(5). doi: 10.1080/23723556.2018.1536843

Maintaining cytosolic aspartate levels is a major function of the TCA cycle in proliferating cells

H. Furkan Alkan  and Juliane G. Bogner-Strauss

Institute of Biochemistry, Graz University of Technology, Graz, Austria

ABSTRACT

Cancer cells rely on glutamine to fuel mitochondria, however it remains unclear whether this is needed for bioenergetic or biosynthetic pathways. Our study suggests that an essential function of mitochondrial glutamine metabolism is to provide aspartate to the cytosol where it can be used for nucleotide and protein synthesis.

ARTICLE HISTORY

Received 11 September 2018
Revised 12 October 2018
Accepted 13 October 2018

KEYWORDS

Glutamine; CB-839; TCA cycle; aspartate; AGC1; aspartate-glutamate carrier; Aralar; Slc25a12; cancer metabolism; targeting metabolism; mitochondrial transporters

Background

Cancer cells acquire certain bioenergetic and biosynthetic demands. As the production of new proteins and organelles consumes great amounts of ATP, energetic needs of cancer cells are increased compared to non-proliferating cells. In addition to energy, cancer cells require building blocks such as nucleotides and amino acids to construct new cells.¹ A deficit of certain micromolecules could be a limitation for cell growth as much as the lack of energy. Therefore, the two major metabolic requirements for maintaining cell proliferation are production of sufficient energy and *de novo* synthesis or salvaging of micromolecules. Consequently, most cancer cells utilize glucose and glutamine as their main carbon sources.² Cancer cells commonly take up excessive amounts of glucose however convert almost every glucose molecule into lactate, even under normoxic conditions (Figure 1).² Due to this glycolytic phenotype, cancer cells were ascribed to have defective mitochondria and/or that mitochondrial dysfunctions may cause cancer. However, recent findings provide more evidence that despite prominent lactate secretion, mitochondria are still active in cancer cells and that mitochondrial function is essential for proliferation.²⁻⁴ Along this line, cultured cancer cells use glutamine as the predominant carbon source to fuel mitochondrial tricarboxylic acid (TCA) cycle, known as glutamine anaplerosis (Figure 1).^{2,5}

Glutamine replenishes the TCA cycle by being converted to glutamate via glutaminase enzyme and subsequently to alpha-ketoglutarate (α -KG). Several studies suggested that a decline in extracellular glutamine levels impairs cell proliferation and survival which led to development of glutaminase inhibitors with therapeutic potential.^{5,6} Furthermore, pyruvate anaplerosis is known to improve the ability of cancer cells to tolerate glutamine starvation, suggesting that TCA cycle anaplerosis is essential for proliferation.⁶ However, is it the

bioenergetic or the biosynthetic reactions following glutamine anaplerosis are more limiting for proliferation remains unraveled. In our recent study, we found that an essential function of TCA cycle and glutamine anaplerosis in proliferating cells is to provide aspartate to the cytosol where it can be used for nucleotide and protein synthesis (Figure 1).⁷

Findings

Besides harboring bioenergetic pathways, mitochondria are also biosynthetic hubs for cancer cells by supporting *de novo* lipogenesis and nucleotide biosynthesis.² In addition, recent studies showed that mitochondrial redox homeostasis is crucial for maintaining cellular aspartate levels^{3,4} which is described as one of the limiting metabolites for tumor growth, *in vivo*.^{8,9} Hence, movements of *de novo* synthesized metabolites across mitochondrial membrane could impact cell proliferation.

To investigate the importance of mitochondrial aspartate export for proliferation, we first knocked-down mitochondrial aspartate-glutamate carrier 1 (AGC1; also known as ARALAR; gene name: Solute Carrier Family 25 Member 12 “*SLC25A12*”).⁷ AGC1 knockdown led to a significant drop in cytosolic aspartate levels and proliferation rate in several cell lines, suggesting that exporting aspartate from mitochondria is one of the requirements for cell proliferation.⁷ More importantly, the proliferation defect of AGC1 knockdown (AGC1-KD) cells was strongly exacerbated when cells were cultured in a low-glutamine environment or when glutamine anaplerosis was inhibited using glutaminase inhibitor CB-839; arguing that inhibition of glutamine anaplerosis and mitochondrial aspartate export are synergistic.⁷ Levels of cytosolic aspartate and the nucleotides downstream of aspartate were drastically declined upon glutaminase inhibition or during low-glutamine treatment and these levels, as well as the

CONTACT Juliane G. Bogner-Strauss  juliane.bogner-strauss@tugraz.at  Institute of Biochemistry, Graz University of Technology, Humboldtstrasse 46/III, Graz 8010, Austria

© 2019 The Author(s). Published with license by Taylor & Francis Group, LLC.
This is an Open Access article distributed under the terms of the Creative Commons Attribution-NonCommercial-NoDerivatives License (<http://creativecommons.org/licenses/by-nc-nd/4.0/>), which permits non-commercial re-use, distribution, and reproduction in any medium, provided the original work is properly cited, and is not altered, transformed, or built upon in any way.

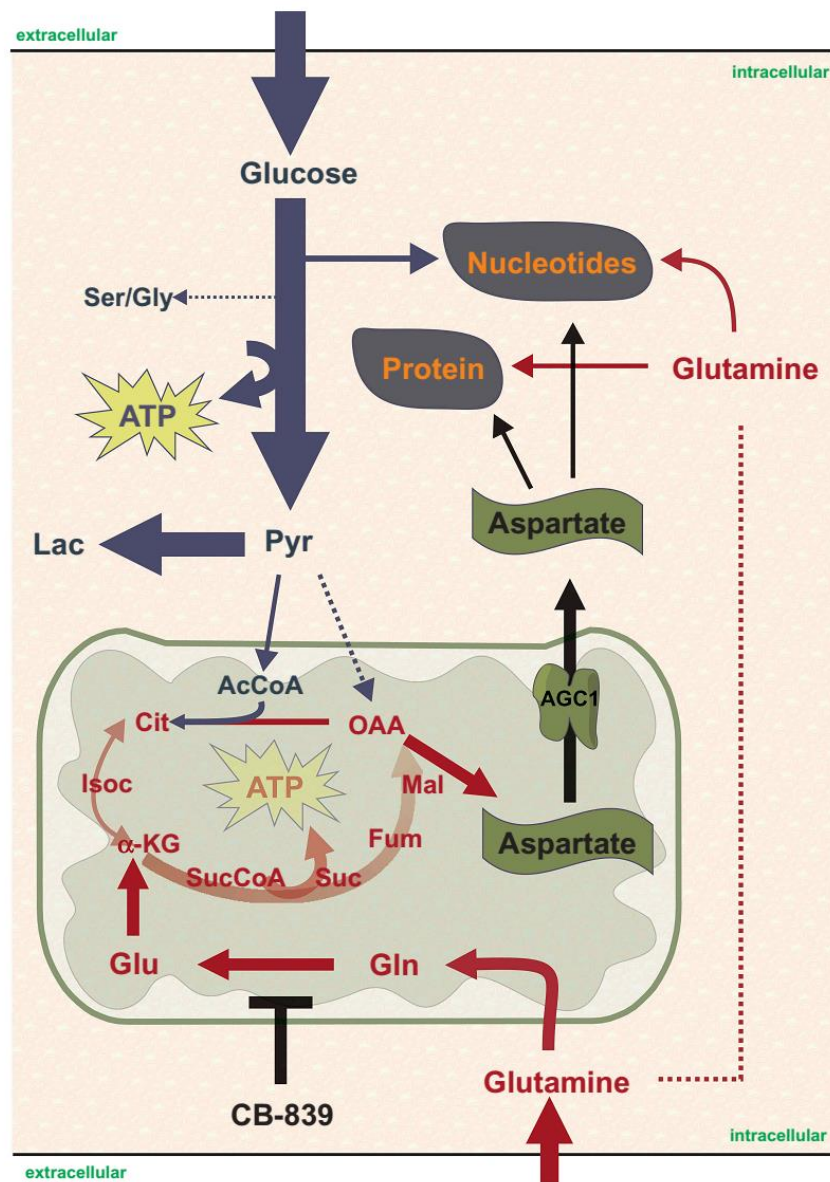


Figure 1. Pathways downstream of glucose and glutamine metabolism in proliferating cells.

While glucose is mostly converted to lactate, glutamine replenishes the TCA cycle to support aspartate biosynthesis. Aspartate delivery to cytosol becomes limiting for biosynthetic pathways and for cell proliferation/survival especially upon glutaminase inhibition with CB-839. Ser/Gly: serine/glycine; Pyr: pyruvate; Lac: lactate; AcCoA: acetyl-CoA; Cit: citrate; Isoc: isocitrate; α -KG: alpha-ketoglutarate; SucCoA: succinylCoA; Suc: succinate; Fum: fumarate; Mal: malate; OAA: oxaloacetate; Glu: glutamate; Gln: glutamine; ATP: adenosine triphosphate; AGC1: aspartate-glutamate carrier 1.

proliferation/survival rate of AGC1-KD cells were recovered by supplementation of exogenous aspartate.⁷ Interestingly, inhibiting aspartate aminotransferases, which blocks aspartate anaplerosis, had no considerable impact on the ability of exogenous aspartate to rescue low-glutamine or CB-839 treatment, providing evidence

that aspartate is not required to replenish TCA cycle for restoring proliferation.⁷ These findings suggest that AGC1-KD cells suffer from a shortage of cytosolic aspartate in the absence of sufficient anaplerotic substrate, however could by-pass the need of TCA cycle function when sufficient exogenous aspartate is provided.⁷

Based on previous works,¹⁰ we hypothesized that high levels of aspartate produced in mitochondria, subsequent to the TCA cycle, could potentially be exported by mitochondrial carriers other than AGC1 and some degree of proliferation could be maintained in the presence of sufficient glutamine anaplerosis. However, because the unspecific transporters may require higher K_m for aspartate, AGC1-KD cells cannot retain efficient cytosolic aspartate delivery when mitochondrial aspartate levels are declined after removal of glutamine, the major anaplerosis substrate. Confirming this, proliferation of AGC1-KD cells could also be rescued by supplementation of other anaplerosis sources such as pyruvate or dimethylalpha-ketoglutarate (a cell permeable form of α -KG) however only when aspartate aminotransferases are active. This suggests that TCA cycle function alone is insufficient to fully restore the proliferation when it is uncoupled from aspartate biosynthesis. Furthermore, because inhibition of mitochondrial respiration would also impair TCA cycle activity and reduce mitochondrial aspartate levels,^{3,4} we investigated whether Complex I inhibition has similar impact on AGC1-KD cells as CB-839. Importantly, AGC1-KD cells were also more sensitive to Complex I inhibition compared to control cells, providing another evidence that the decline in mitochondrial aspartate levels was responsible for impaired cell growth and survival in AGC1-KD cells under glutamine limitations.

Finally, we reported that knocking down AGC1 in subcutaneously growing tumors significantly slowed-down tumor growth and increased their sensitivity to glutaminase inhibitor treatment. Because intracellular aspartate levels could limit tumor growth,^{8,9} blocking cytosolic aspartate delivery (by inhibiting AGC1 or by mitochondrial respiration) could provide a novel strategy to sensitize CB-839-resistant tumors to the treatment in clinics.

Conclusions

In conclusion, our work provides evidence that a major function of TCA cycle in proliferating cells is to provide aspartate to cytosol which could be used for further biosynthetic pathways. Because aspartate supplementation is sufficient to maintain cell growth when TCA cycle is blocked, we argue that energy derived from mitochondrial respiration is not essential for proliferation and/or could be compensated through other pathways such as glycolysis. In addition, our work also underlines that local concentration (mitochondria) of a metabolite (aspartate) or abundance of its transporter (AGC1) could be a key determining factor for cell proliferation or survival under certain nutrient limitations (glutamine) which can be exploited for dual therapeutic possibilities to combat fast growing cancers.

Acknowledgments

We acknowledge Matthew Vander Heiden and his lab members for their generous helps during the creation of the original paper which this

commentary is based on. We are also thankful for many other great research papers on this topic that we were unable to cite due to space limitations.

Funding

Bogner-Strauss lab is funded by the Austrian Science Fund FWF [SFB LIPTOX F3018 and P27108]; H.F.A trained within the doctoral program [W1226 DK] "Metabolic and Cardiovascular Disease" and was supported by Austrian Marshall Plan Scholarship 2017.

ORCID

H. Furkan Alkan  <http://orcid.org/0000-0003-0078-248X>

References

1. Cantor JR, Sabatini DM. Cancer cell metabolism: one hallmark, many faces. *Cancer Discov.* 2012;2:881–898. doi:10.1158/2159-8290.CD-12-0345.
2. Vander Heiden MG, DeBerardinis RJ. Understanding the intersections between metabolism and cancer biology. *Cell.* 2017;168:657–669. doi:10.1016/j.cell.2016.12.039.
3. Sullivan LB, Gui DY, Hosios AM, Bush LN, Freinkman E, Vander Heiden MG. Supporting aspartate biosynthesis is an essential function of respiration in proliferating cells. *Cell.* 2015;162:552–563. doi:10.1016/j.cell.2015.07.017.
4. Birsoy K, Wang T, Chen WW, Freinkman E, Abu-Remaileh M, Sabatini DM. An essential role of the mitochondrial electron transport chain in cell proliferation is to enable aspartate synthesis. *Cell.* 2015;162:540–551. doi:10.1016/j.cell.2015.07.016.
5. Gross MI, Demo SD, Dennison JB, Chen L, Chernov-Rogan T, Goyal B, Janes JR, Laidig GJ, Lewis ER, Li J, et al. Antitumor activity of the glutaminase inhibitor CB-839 in triple-negative breast cancer. *Mol Cancer Ther.* 2014;13:890–901. doi:10.1158/1535-7163.MCT-13-0870.
6. Cheng T, Sudderth J, Yang C, Mullen A, Jin E, Mates J, DeBerardinis R. Pyruvate carboxylase is required for glutamine-independent growth of tumor cells. *Proc Natl Acad Sci.* 2011;108:8674–8679. doi:10.1073/pnas.1016627108.
7. Alkan H, Walter K, Luengo A, Madreiter-Sokolowski C, Strycek S, Lau A, Al-Zoughbi W, Lewis C, Thomas C, Hoefler G, et al. Cytosolic aspartate availability determines cell survival when glutamine is limiting. *Cell Metab.* 2018;(2018):28. doi:10.1016/j.cmet.2018.07.021.
8. Sullivan LB, Luengo A, Danai LV, Bush LN, Diehl FF, Hosios AM, Lau AN, Elmiligy S, Malstrom S, Lewis CA, et al. Aspartate is an endogenous metabolic limitation for tumour growth. *Nat Cell Biol.* 2018;20:782–788. doi:10.1038/s41556-018-0125-0.
9. Garcia-Bermudez J, Baudrier L, La K, Zhu X, Fidelin J, Sviderskiy V, Papagiannakopoulos T, Molina H, Snuderl M, Lewis C, et al. Aspartate is a limiting metabolite for cancer cell proliferation under hypoxia and in tumours. *Nat Cell Biol.* 2018;20:775–781. doi:10.1038/s41556-018-0118-z.
10. Vozza A, Parisi G, De Leonardi F, Lasorsa FM, Castegna A, Amorese D, Marmo R, Calcagnile VM, Palmieri L, Ricquier D, et al. UCP2 transports C4 metabolites out of mitochondria, regulating glucose and glutamine oxidation. *Proc Natl Acad Sci U S A.* 2014;111:960–965. doi:10.1073/pnas.1317400111.